This is to certify that the
thesis entitled

PORPHYRIN AGGREGATES AS REPORTERS OF CHIRALITY USING EXCITON COUPLED CIRCULAR DICHROISM

presented by

MERCY ANYIKA

has been accepted towards fulfillment
of the requirements for the

M.S. degree in CHEMISTRY

Babak Borhan
Major Professor's Signature

2/9/2009
Date

PORPHYRIN AGGREGATES AS REPORTERS OF CHIRALITY USING EXCITON COUPLED CIRCULAR DICHROISM

By

Mercy Anyika

A THESIS

Submitted to
Michigan State University
in partial fulfillment of the requirements
for the degree of

MASTERS OF SCIENCE

Chemistry

2009

ABSTRACT

PORPHYRIN AGGREGATES AS REPORTERS OF CHIRALITY, USING EXCITON COUPLED CIRCULAR DICHROISM.

By

Mercy Anyika

Many important molecules required for life exist in two forms. These two forms are non-superimposable mirror images of each other, i.e. they are related like our left and right hands, a property called chirality. Despite the abundance of chiral molecules, there is still much to be learned about about chirality. We are interested in using Exciton Coupled Circular Dichroism to probe chirality in organic molecules.

Chiral compounds with only one site of attachment usually require derivatization with carrier molecules before using ECCD method. The research presented herein is focused on the absolute stereochemical determination of such compounds but without requiring derivatization. To develop this method, we will design porphyrin systems capable of undergoing self assembly into stable aggregates via non-covalent interactions.

Upon addition of the chiral molecule of interest, the molecule binds to the zinc incorporated within the porphyrin core, upon which there is a transfer of chirality from the molecule to the porphyrin aggregate. This induced chirality is then observed as an ECCD curve.

A number of porphyrins have been designed, synthesized and employed as reporters of chirality.

Dedicated to my mother, for her love and support.

ACKNOWLEDGEMENTS

I would like to first express my gratitude to my research advisor, Professor Babak Borhan. I have sincerely appreciated his encouragement and strong support for my graduate career. I am grateful for the excellent education I received, and continue to receive under his guidance.

I also appreciate the Borhan research group members from whom I learned a lot. I want to give special thanks to Dr. Chrysoula Vasileiou, Dr. Marina Tanasova, Xiaoyong Li and Dan Whitehead for their help and patience in reading and correcting my thesis, and all their great suggestions.

I would like to thank the people who worked with me on the ECCD project: Marina, Xiaoyong and Carmin. Through our discussions, I was able to learn a lot and also obtain a greater understanding of my research, especially during my first years. I also wish to thank everyone that I had the opportunity of working with in the Borhan lab. Calvin, Camille and Wenjing deserve special thanks for making sure I retained some sense of sanity during the writing of my thesis.

I wish to thank Dr. Rui-Huang for his assistance in running solid probe Mass Spectroscopy.

Finally, I would like to thank my family for their love and support.

TABLE OF CONTENTS

List of Tables

List of Figures

Images in this thesis are presented in color.

List of Schemes

Key to Symbols and Abbreviations

α	angle of rotation
$[\alpha]$	specific rotation
Å	angstrom
A	CD amplitude
Ar	aromatic
$BF_3 \bullet Et_2O$	boron trifluoride diethyl ether
BINOL	1,1'-Bi-2-naphthol
Bn	Benzyl
BnBr	benzylbromide
CD	circular dichroism
CE	cotton effect
p-chloranil	tetrachloro-1,4-benzoquinine
cm	centimeter
d	doublet
DCM	dichloromethane
DDQ	2,3-dichloro-5,6-dicyano-1,4-benzoquinone
DMAP	4-diaminopyridine
DMF	N,N-dimethylformamide
DNA	deoxyribonucleic acid
Et_3N	triethylamine
EtOH	ethanol

ε	molar absorption coefficient
ECCD	Exciton Coupled Circular Dichroism
EDCI	N-(3-Dimethylaminopropyl)-N'-ethyl-carbodiimide
EtMgBr	ethyl magnesium bromide
EtOAc	ethyl acetate
equiv	equivalents
g	gram
HPLC	high pressure liquid chromatography
HRMS	high resolution mass spectrometry
h	hour
IR	infrared
J	NMR coupling constant
KI	potassium iodide
K_2CO_3	potassium carbonate
LDA	lithium diisopropylamine
LAH	lithim aluminum hydride
m	magnetic dipole transition moment
m	multiplet
MeOH	methanol
min	minute
mg	milligram
MHz	megahertz
M	molar

M	molar
μM	micromolar
MS	mass spectrometry
n	refractive index
$NaBH_4$	sodium borohydride
NaOH	sodium hydroxide
NaH	sodium hydride
nm	nanometer
NMR	nuclear magnetic resonance
ORD	optical rotatory dispersion
$POCl_3$	phosphorous chloride oxide
PCC	pydidinium chlorochromate
Ph	phenyl
$^{n}PrNH_2$	propyl amine
q	quartet
s	singlet
R	rotational strength
Rt	room temperature
t	triplet
TFA	trifluoroacetic acid
THF	tetrahydrofuran
TBP-tz	5-(4-carboxyphenyl)-10,15,20-tri-3,5-di-*t*-butylphenylporphyrin tweezer

TPP-tz	5-(4-carboxyphenyl)-10,15,20-triphenylporphyrin tweezer
UV-vis	ultraviolet-visible spectroscopy
Zn-TPP	zinc tetraphenylporphyrin
ZnTPP-tz	zinc 5-(4-carboxyphenyl)-10,15,20-tri-3,5-di-t- butylphenylporphyrin tweezer
$Zn(OAc)_2$	zinc acetate

Chapter 1

Introduction.

1-1. The Exciton Coupled Circular Dichroic Method

1-1.1 Introduction to Chirality

Ever since Van't Hoff and LeBel suggested in 1874 that individual molecules possess a three-dimensional structure that may gives rise to dissymmetry,[1,2] the exact orientation of the atoms in space, i.e. the absolute configuration, has been an intriguing problem to be solved.

Chirality refers to non-superimposable mirror images and comes from the Greek word *cheir*, meaning "hand".[3] Examples of chiral molecules can range from the simplest, a single atom with four different substituents, such as 2-methylbutyric acid, to large natural products with multiple chiral centers, such as Taxol®.

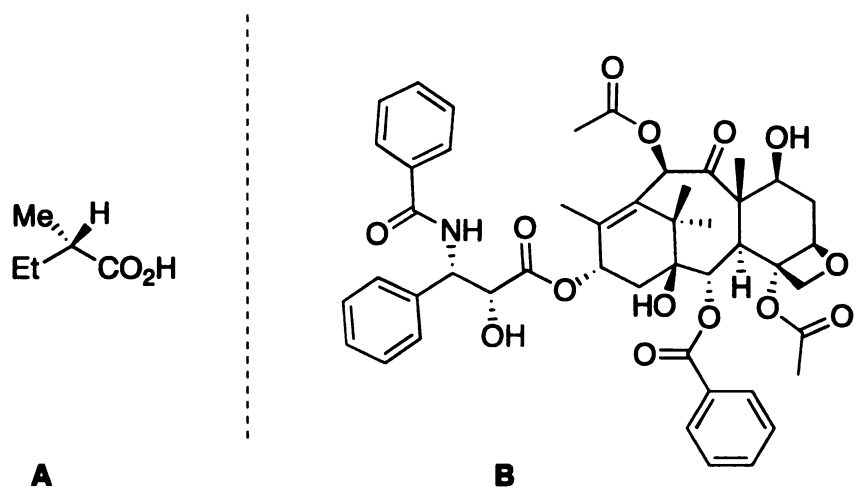

Figure 1-1. Example of chiral molecules, (*S*)-2-methylbutyric acid (**A**) and Taxol® (**B**)

The letters *R* (from Latin "*rectus*") and *S* (from Latin "*sinister*") are used to indicate the configuration (arrangement of groups) on the chiral center, based on priorities set in place by Cahn, Ingold and Prelog.[4] However, molecules do not have to have a chiral center to be chiral; non-superimposability on the mirror image is the only necessary requirement for chirality. Any molecule that lacks an element of symmetry is considered chiral. Some examples of chiral molecules lacking a chiral center are shown in Figure 1-2.

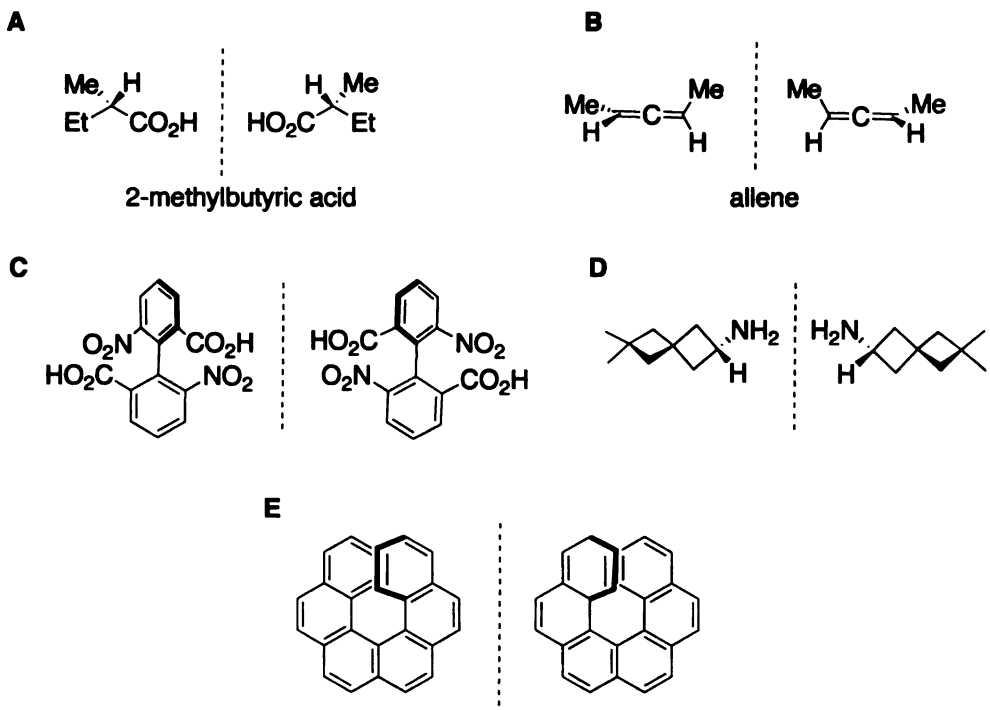

Figure 1-2. Examples of some chiral molecules and their mirror images

Figure 1-2A shows a classic example of chirality, 2-methylbutyric acid, which contains a chiral carbon center. Figure 1-2B shows an allene[5] where the overall molecule is not planar, but rather the two π bonds are perpendicular to each other causing the molecule to lack any plane of symmetry when both sides are unsymmetrically

substituted. Figure 1-2C shows a biphenyl molecule, bearing large groups on each side of the C-C single bond. This molecule is chiral because of restricted rotation around the single bond hence, it is "locked" into a chiral conformation since steric hindrance between the *ortho*-substituents prevents bond rotation. This restriction of rotation is the source of geometric isomerism (atropisomerism). Restricted rotation can also be found in spiranes, which are compounds that have two rings with a common carbon atom, as shown in Figure 1-2D. Because of this, the rings are perpendicular to each other giving rise to axial chirality.[6] Figure 1-2E shows a classic example of an inherently chiral chromophore,[7] hexahelicene. Despite the fact that this molecule does not have any asymmetric carbons, it is not planar, but rather lacks a plane of symmetry as it traces a helix when one side of the molecule lies above the other due to crowding of the rings. The defined helix can be either right-handed, (+)-hexahelicene, or left-handed, (-)-hexahelicene and, therefore, non-superimposable on its mirror image.[8]

Chirality affects all of life, from the very simplest amino acids to pharmaceuticals used to treat diseases. Living organisms use exclusively one chiral molecular form (homochirality): virtually all active forms of amino acids are of the L-form (D-serine being a notable exception) while most biologically relevant sugars are of the D-form. Enzymes, which are chiral, often distinguish between two enantiomers of a chiral substrate, and only one enantiomer can fit inside an enzyme's binding cavity, while the other cannot. Despite its ubiquity, the origin of chirality on earth is still not completely understood.[9-18] Nonetheless, whatever its origin, chirality has been, and still remains one

of the most fundamental aspects of life on earth. The stereochemistry of molecules affects their chemical and biological properties.

For example, while the (*S*) enantiomer of Carvone has the odor of caraway seeds, its (*R*) enantiomer has the odor of spearmint; also, (*S*)-mercaptohexanal has a pleasant, fruity odour, while its (*R*) enantiomer has the pungent sulfur smell. Chiral organic molecules are currently of widespread interest to organic and pharmaceutical chemists, and currently, chirality plays a major role in the development of new pharmaceuticals. This is because the two enantiomers of many natural products used as drugs have different actions in the body, hence the resolution and clinical testing of both enantiomers is prerequisite to the development of the optimum drug. Drugs generally work by interacting with receptors on cell surfaces, or enzymes within cells. Receptors have a specific three-dimensional structure, which will allow only the isomer that fits precisely to bind preferentially while the other has little or no activity.

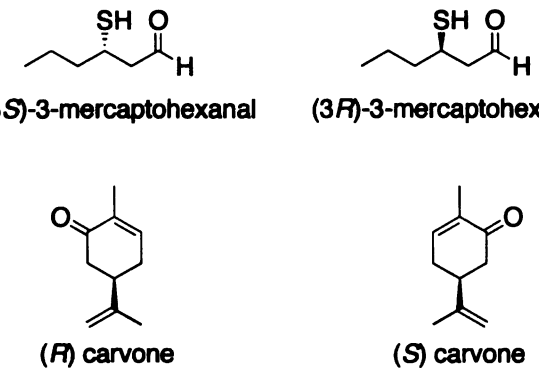

(3*S*)-3-mercaptohexanal (3*R*)-3-mercaptohexanal

(*R*) carvone (*S*) carvone

Figure 1-3. Enantiomeric forms of 3-mercaptohexanal and carvone

Most of the pharmaceuticals sold commercially are chiral compounds. Drugs obtained from natural sources, or those prepared from natural materials are produced as pure enantiomers, because chiral compounds from nature usually occur as the pure form of one of the enantomers. However, until recently (1970s) most chiral drugs produced

synthetically from achiral starting materials were produced and sold in their racemic forms, even though their therapeutic effect was mainly due to only one isomer. In most cases, the unwanted isomer was physiologically inactive, and did not cause any serious side effects. However, that was not always the case. One tragic example of historical note is thalidomide. Thalidomide was developed and sold from 1957 – 1961 in almost 50 countries. It was mainly prescribed to pregnant women as an antiemetic to treat morning sickness and as a sleep aid.

(*S*)-Thalidomide (*R*)-Thalidomide

Figure 1-4. Structures of (*R*)- and (*S*)-Thalidomide

As shown in Figure 1-4, thalidomide contains a stereocenter and so exists in its two enantiomeric forms.[4] Tragically, while the (*S*)-isomer had the desired anti-nausea effects, the (*R*)-form was teratogenic and caused fetal abnormalities, such as severely deformed limbs.

Most new drugs today and those under development consist of a single optically active isomer. Chirality is not only becoming an important issue in the pharmaceutical industry, but also in the agrochemical and other industries as well.[19] As a result of this, there is an increasing interest in determining molecular chirality,[1] and the need for simple and effective ways for the determination of absolute configuration is more prominent than ever. The stereochemical assignment of chiral compounds is a challenging task.

There are several methods that are used to establish the absolute stereochemistry of chiral molecules, including chemical correlation with known chiral compounds,[3] the NMR Mosher ester method[13] as well as X-ray crystallography. The Mosher ester method and its modified versions have been the most widely applied approach for configurational assignments of chiral compounds. This method involves derivatization of the compound of interest into two diastereomers containing an aryl ring. The ^{1}H NMR spectra of the two diastereomeric derivatives are compared, and the shielding effect values ($\Delta\delta^{RS}$) for the protons neighboring the chiral center are measured. The scope of the Mosher ester method has been extended further,[3] but generally, milligram quantities of the substrate are needed, and derivatization of the substrate is necessary, hence limiting the use of this method.

X-ray crystallography is the most unambiguous method for absolute stereochemical determination. Although X-ray crystallography provides full stereochemical analysis of chiral compounds in a single experiment, there are some shortcomings associated with the method. The most common are the difficulty in crystallizing many molecules, the need for multi milligram amounts of compound, and also the fact that suitable single crystals can be hard to obtain. These problems limit the application of X-ray crystallography for absolute stereochemical determination. That is why development of a general and more accessible protocol that allows for easy stereochemical determination is key. In the past few years chiroptical methods based on optical rotatory dispersion (ORD) and circular dichroism (CD) spectroscopy have been

developed. Their advantage is that they are easy to use and are very sensitive, generally requiring only μM concentrations of the compound of interest.

The goal of our research is to expand the use of CD-based spectroscopic techniques by designing general and sensitive circular dichroic (CD) methods for the absolute stereochemical determination of chirality.

1-1.2 Optical Rotatory Dispersion (ORD) and Circular Dichroism (CD) spectrosopy

Optical Rotatory Dispersion and Circular Dichroism are both methods that make use of the different chiroptical properties of enantiomers. In these methods, light is used to distinguish between enantiomers. Light is a transverse wave, consisting of both an electric and a magnetic field, which oscillate perpendicular to one another and to the direction of propagation of light forming a right handed coordinate system.[18] The polarization of light is defined by the direction of its electric field vector.[18]

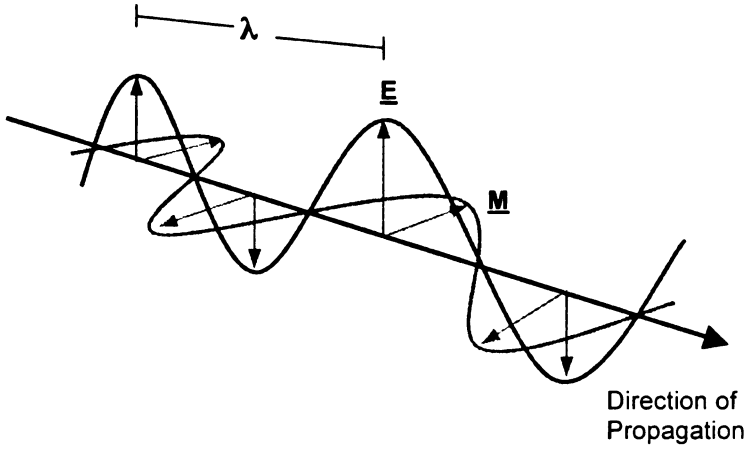

Figure 1-5. Light as an electromagnetic radiation

Light from ordinary light sources, such as the sun or a light bulb, is unpolarized, since it consists of light waves propagating in all directions. On the other hand, when unpolarized light passes through a polarizing filter, only the light waves with oscillation parallel to the direction of the filter pass through. The light passing through the filter is now aligned in one plane of oscillation, and is defined as linearly polarized light. Linearly polarized light only oscillates in one specific direction, where the electric field (E) remains constant in magnitude, but traces out a helix as a function of time,[20] and can be resolved into two circularly polarized light beams: a left circular component (L) and a right circular component (R) as shown in Figure 1-6.

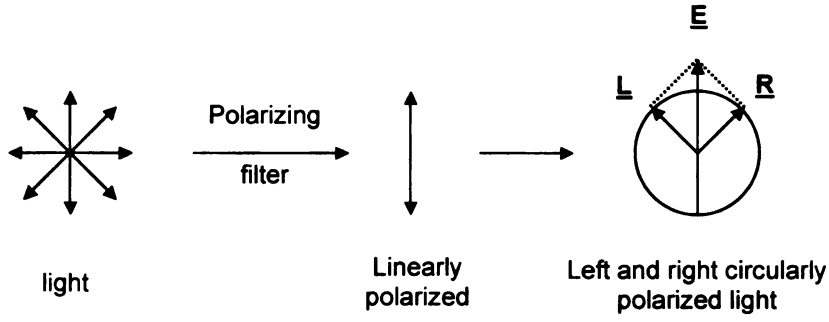

Figure 1-6. Linearly and circularly polarized light

When circularly polarized light passes through an achiral or racemic compound, the velocity and absorbance of the left and right circularly polarized light is equally affected.

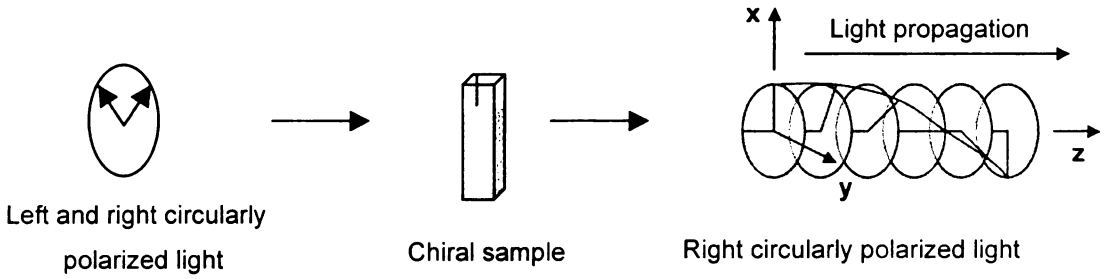

Figure 1-7. Circularly polarized light passing through a chiral medium, which absorbs the left circularly polarized component more than the right.

On the other hand, if it passes through an optically active medium, (Figure 1-7) the velocity and absorbance of either one of the circularly polarized components is altered to a greater extent as compared to the other component.[21] This is referred to as the Cotton effect (CE, in honor of French physicist Aimé Cotton, who observed both ORD and CD phenomena).

ORD results from the difference in velocity of the left and right components of circularly polarized light. This difference correlates to the differences in the respective refractive indices, as can be shown in equation 1-1.[18]

$$\Delta n = n_L - n_R \neq 0 \qquad (1\text{-}1)$$

Where n_L and n_R are the refractive indices for left and right circularly polarized light respectively. Because the left and right circularly polarized light travels through the optically active medium at different velocities, the two components are no longer in phase, and the resultant vector has been rotated by an angle α relative to the original plane of polarization. ORD spectroscopy is the measurement of specific rotation $[\alpha]$, as a

function of wavelength, and can be calculated from the observed angle of rotation, α, as expressed by equation 1-2.[18]

$$[\alpha] = \alpha/cl \qquad (1\text{-}2)$$

Where α is the angle of rotation (degree units), c is the concentration of the sample (g mL^{-1}), and l is the path length (decimeters). Because ORD is only based on the difference in the refractive indices, and all chiral molecules exhibit a molecular refraction at almost any wavelength of irradiation, theoretically, ORD can be detected over all wavelengths. Typically, the sodium D-line (589 nm) is used to detect and quantitate optical activity.

When circularly polarized light passes through an optically active medium, there is both a difference in the velocity of the left and right circularly polarized light, as well as a difference in the absorbance of these two components (equation 1-4).[18] The difference in molar absorptivity, $\Delta\varepsilon$, is Circular Dichroism (CD).

$$\Delta\varepsilon = \varepsilon_L - \varepsilon_R \neq 0 \qquad (1\text{-}4)$$

ε_L and ε_R are the molar absorption coefficients for left and right circularly polarized light.

CD is an absorptive process and therefore, CD only occurs in the vicinity of an absorption band. Therefore, chiral compounds need to contain a chromophore in order for a CD spectrum to be observed. The shape and appearance of a CD curve is very similar to that of the ordinary UV-vis absorption curve of the electronic transition to which it corresponds. The only difference is that, unlike the ordinary UV-vis absorption curves, CD curves may be positive or negative as shown in Figure 1-8.

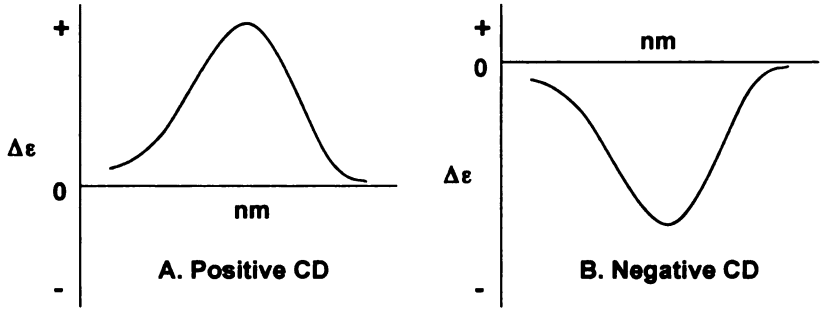

Figure 1-8. Positive (A) and negative (B) Cotton effects

CD curves plot Δε vs. wavelength.[18] CD and ORD are both manifestations of the same phenomenon. The molar amplitude *A* of an ORD can be related to the intensity of the CD curve, Δε, by equation 1-5:[22]

$$A \approx 40.28\Delta\varepsilon \qquad (1\text{-}5)$$

When a molecule absorbs light, an electron is promoted from its ground state to an excited state. This creates a momentary dipole, referred to as the electric dipole transition moment, denoted by the vector μ. The direction in which μ points is the direction in which the electrons move during the transition.

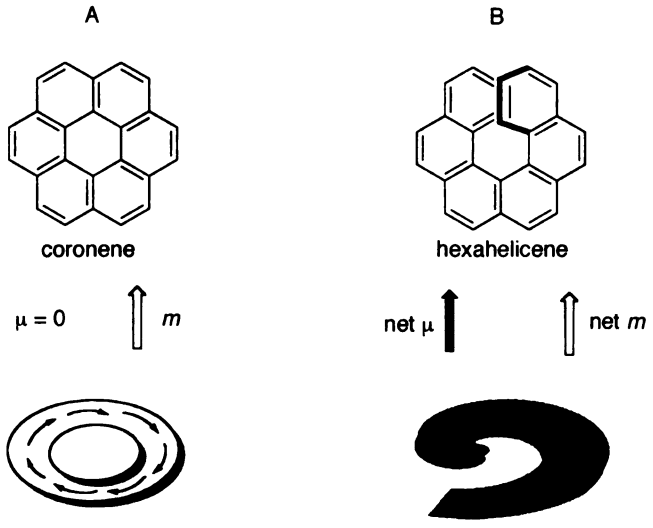

Figure 1-9. Electron redistribution upon light excitation for a transition of (a) achiral and (b) chiral molecule.

In an achiral molecule, the net electron redistribution during the process is always planar, while in a chiral molecule the electron rearrangement is always helical.[23] In the latter case, not only does the charge displacement take place during the electronic transition, which generates the electric transition dipole moment, but also the rotation of electric charge creates a magnetic field, the strength and direction of which may be described by the magnetic transition dipole moment denoted by the vector m.[3] The direction of magnetic transition moment (m), can be determined by application of the "right hand rule" (Figure 1-10[24]) to the rotation of the charge (circular electric current). Instructively, the outstretched thumb points to the direction of the magnetic transition dipole moment when the right hand fingers are curved in the direction of electron flow.[25]

The rotational strength, R, which is a theoretical parameter representing the sign and strength of a CD Cotton effect (CE), is given by the scalar product of the electric and magnetic transition moments (equation 1-6):[3]

$$R = \mu \cdot m = |\mu| \, |m| \cos\beta \qquad (1\text{-}6)$$

Where μ and m are the electric and magnetic transition dipole moments, respectively, and β is the angle between the two transition moments. The sign of the CE is positive when the angle is acute ($0<\beta<90^{\circ}$) or, in the limiting case, parallel, and it is negative when the angle is obtuse ($90^{\circ}<\beta<180^{\circ}$) or, in the

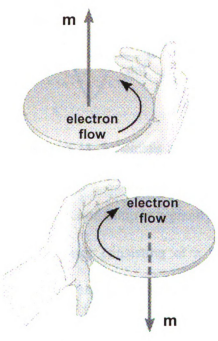

Figure 1-10. The right hand rule to determine the direction of magnetic dipole transition moment (m)

limiting case, antiparallel. Dextrorotation results when $R > 0$, together with positive CD, and levorotation is generated when $R < 0$, together with negative CD curve. There is no CE when the electric and magnetic transition dipole moments are perpendicular to each other.

1-1.3 A brief introduction to Circular Dichrometers (spectropolarimeter)

Circular dichrometers are used to record both ORD and CD spectroscopy. The essential features of a spectropolarimeter are shown in Figure 1-11.

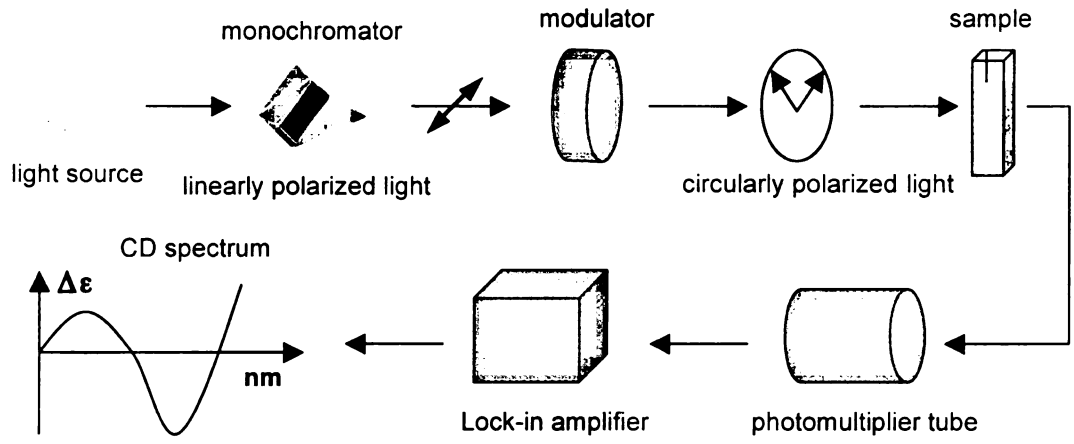

Figure 1-11 Schematic representation of a CD spectropolarimeter

A zenon lamp is typically used as the source of light. This light passes through a monochromator consisting of a series of crystal prisms to produce linearly polarized light. In the CD spectropolarimeter, the optical system comprises of two monochromators (a double monochromator), which helps in reducing stray light. The linearly polarized light is then modulated into left and right circularly polarized light.

The modulator consists of a thin crystalline plate known as a wave plate. When

linearly polarized light is incident on a wave plate at 45°, the light is divided into two equal electric field components, one of which is retarded by a quarter wavelength by the plate. This throws the two components 90° out of phase with each other such that upon emerging, one is always maximum, while the other is always zero and vice versa. The effect is to produce circularly polarized light. The 90° phase shift is produced by a precise thickness *d* of the birefringent crystal, which, because of the 90° shift, is referred to as a quarter wave plate. This then passes through the sample chamber. The light transmitted through the sample is measured by a photomultiplier tube, which produces a current whose magnitude depends on the number of incident photons. This current is then detected by a lock-in amplifier and recorded.

Most CD spectropolarimeters measure differential absorbance, ΔA, between the left and right circularly polarized light, which can then be converted to $\Delta\varepsilon$ based on the Beer-Lambert law, using equation 1-7.[3]

$$\Delta A = \Delta\varepsilon\, c\, l \qquad (1\text{-}7)$$

Where ΔA is the difference in absorbance and $\Delta\varepsilon$ is the difference in molar extinction coefficients ($M^{-1}L^{-1}$). Since Optical Rotatory Dispersion (ORD) and Circular Dichroism (CD) are manifestations of chiral substances and are not observed for achiral compounds or racemic mixtures, they can be used to detect and quantitate optical activity. However, ORD and CD by themselves do not allow the configuration of a given product to be defined.

1.2 Exciton Coupled Circular Dichroism (ECCD)

1.2-1 Theoretical background of ECCD

The ECCD method is a non-empirical method to establish the absolute configuration of chiral compounds. This method is developed from the simple dibenzoate chirality method[26] that was first applied to organic compounds by Mason to determine the absolute sense of twist between two adjacent hydroxyl groups. The dibenzoate chirality method is based on the nonempirical coupled oscillator theory[27] and group polarizability theory.[28]

ECCD is based on the through space exciton coupling between two or more chirally oriented non-conjugated chromophores. The coupling of the chromophores' electric transition dipole moment leads to the observed bisignate CD spectrum and the nonempirical determination of their orientation. Figure 1-12 shows the exciton coupling between two benzoates in steroidal 2,3-bisbenzoate.[26]

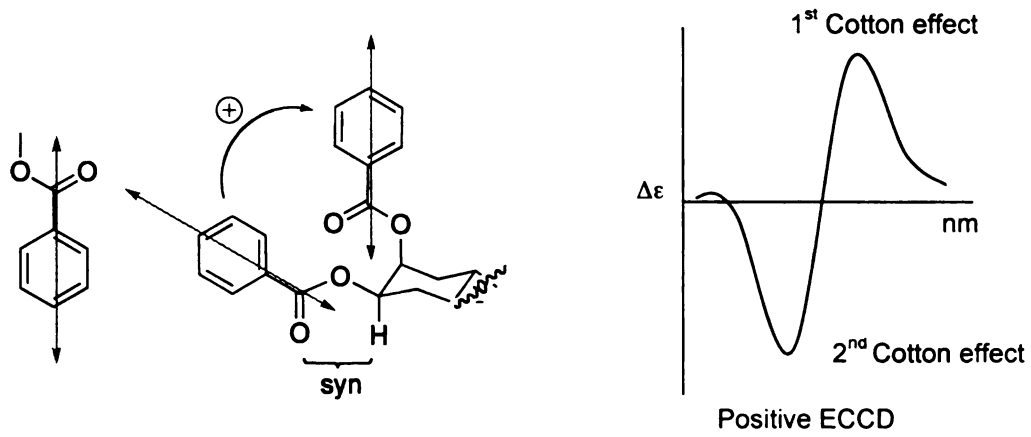

Figure 1-12. Exciton Coupled Circular Dichroism (ECCD) of steroidal 2,3-bisbenzoate.

Upon excitation, the through space interaction causes the energy level of the excited state (exciton)[31] to split into two states (α and β) by resonance interaction of the local excitation. The transitions from the ground state to either the α state or β state, are responsible for the two different UV-vis absorbances as shown in Figure 1-13. The transitions from the ground state to either the α state or β state, are responsible for the two different UV-vis absorbances as shown in Figure 1-13.

The difference in the λ_{max} of the two UV-vis peaks is due to the energy gap, $2vij$, and is called the Davydov splitting,[29] after the Russian physicist who developed the theory of exciton coupling in the electronic spectra of molecular crystals.

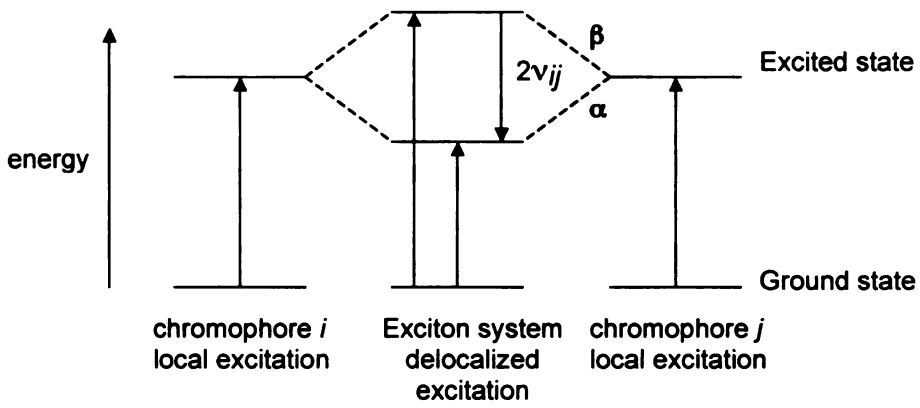

Figure 1-13. Splitting of the excited states of isolated chromophores *i* and *j* by exciton interaction. The energy gap 2v*ij* is called Davydov splitting.

If this energy gap is small, the two separate peaks overlap and appear as one in the spectral trace. Because the two Cotton effects in a CD spectra are not in phase, the Davydov splitting is also present in a CD spectrum (Figure 1-14).

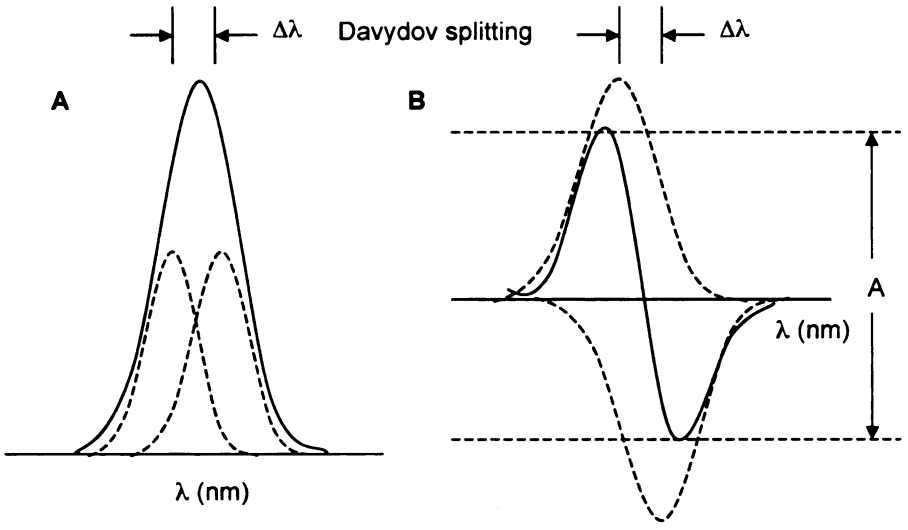

Figure 1-14. The UV spectrum (A) and ECCD spectrum (B) upon through space interaction of two degenerate chromophores. The two observed Cotton effects are shown using dashed lines, while the observed, summation curves are in solid lines.

As mentioned before, upon light absorption by a chromophore, an electron gets promoted from its ground state to an excited state. In a chiral molecule, this results in the interaction between the electric dipole transition moments (edtm) of each chromophore in a chiral, helical fashion, generating one of the two helices. Depending upon whether the electric dipole transition moments are in phase (symmetric) or out of phase (anti symmetric), a Cotton effect of different sign is produced, and so we expect to see a CD spectrum with two peaks (bisignate curve), since the two Cotton effects, one positive and one negative, are not in phase. This phenomenon is known as Exciton Coupled Circular Dichroism, and can be further explained by examining its application to a specific molecule, bearing two identical benzoate groups.[25]

The coupling of two identical chromophores is shown in Figure 1-15, where benzoate esters of a vicinal cyclohexanediol are interacting. Benzoate esters have a

strong UV-Vis absorption band at around 230 nm, arising from the $\pi \rightarrow \pi^*$ transition involving the benzene ring and the ester group.[30] The large electric dipole transition moment μ of each benzoate group is oriented colinearly with the long axis of the molecule, almost parallel to the direction of the C-O bond and oscillates in both directions (Figure 1-15A). Determination of absolute configuration means determination of the absolute sense of chirality between the C(2)-O and C(3)-O bonds, by looking down the C-C bonds from front to back, the orientation of the two benzoate groups is set in a clockwise manner, which leads to positive chirality. The absolute sense of twist is the same regardless of whether it is viewed from C(3) to C(2) or *vice versa*.

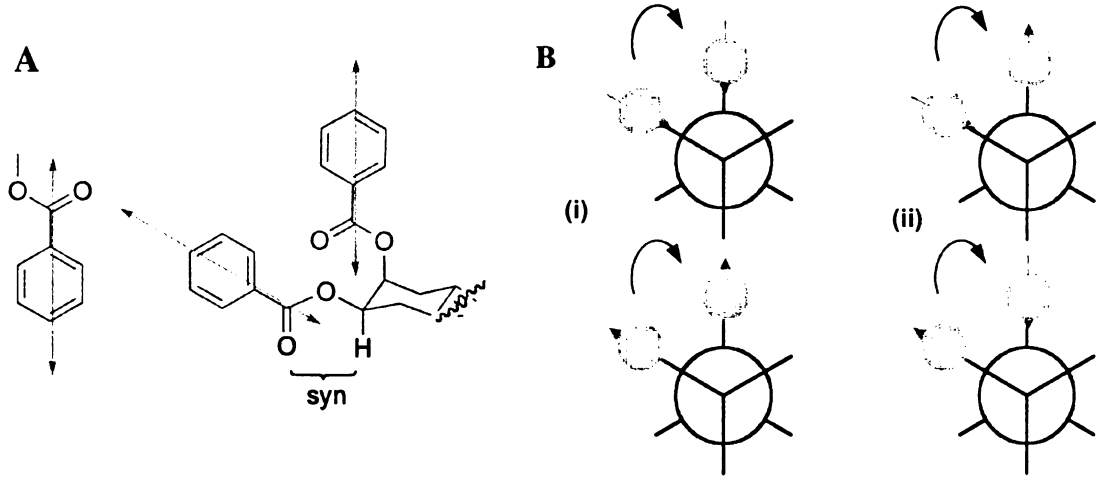

Figure 1-15. A qualitative explanation of ECCD. **A**. Structures of benzoate and dibenzoate esters. edtm's are shown in red; **B**. Possible in phase (i) and out of phase (ii) interactions of the edtm's of the degenerate chromophores (shown in blue)

Despite the free rotation about the two C-O bonds, ester bonds are known to be *s*-trans,[23] placing the axial hydrogen on the ring *syn* to the carbonyl of the ester.

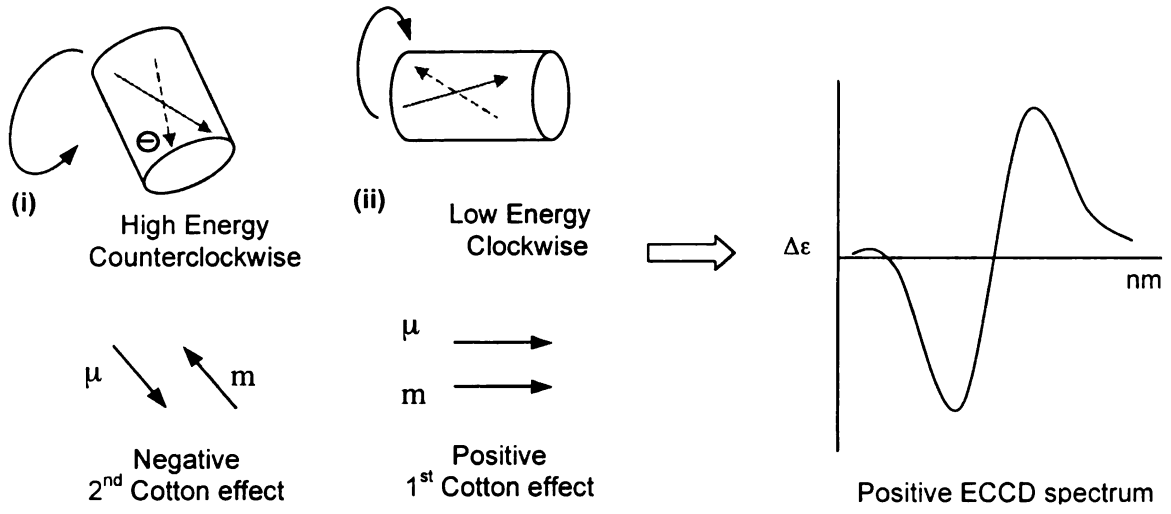

Figure 1-16. The expected ECCD spectrum of dibenzoate, and its rationalization.

The individual edtm μ of an electric transition, for each chromophore, couples to the other in phase (symmetric) or out of phase (asymmetric), Figure 1-16 i and ii respectively. In the case i, where the two electric transition dipole moments couple in phase, the "total" electric transition dipole moments are oriented along the chromophoric C_2 axis, and in case B, where they couple out of phase, the "total" electric transition moments are oriented perpendicular to the chromophoric C_2 axis.

The helix associated with the charge rotation generated from the transition can be visualized by placing the partial edtm in a cylinder, aligned along the axis of the "total" edtm, μ. As shown, in Figure 1-16 (i), the symmetric coupling results in a counterclockwise helical movement and, therefore, according to the right hand rule, the magnetic transition dipole moment (m) is anti-parallel to μ. As expected, the out of phase

interaction causes the opposite effect, leading to parallel m and μ vectors (Figure 1-16 ii); and that leads to a negative Cotton effect (negative CD band), and positive Cotton effect (positive CD band) respectively. According to Equation 1-6, $R = \mu.m = |\mu||m|\cos\beta$, the sign of a Cotton effect depends exclusively on the angle between the electric and the magnetic transition dipole moment. Therefore, the symmetric coupling of the edtm will result in a negative peak ($\beta = 180°$, $\cos\beta = -1$), while the anti-symmetric will result in a positive one ($\beta = 0°$, $\cos\beta = 1$), both of equal magnitude. The positions of these two Cotton effects relative to each other (which defines whether the overall ECCD spectrum is positive or negative) depends on the relative energies of the two occurring transitions. The in phase coupling is of higher energy because of the repulsion between like charges, and so the corresponding negative Cotton effect will appear at a lower wavelength. Because nomenclature dictates that the bisignate ECCD curve be named after the lower energy 1st Cotton effect, the spectrum of the dibenzoate discussed above (Figures 1-15 and 1-16) will be referred to as a positive ECCD curve.

1.2-2 The Quantum Mechanics explanation of ECCD

The ECCD theory can also be explained by Quantum Mechanical theories. As mentioned previously, when a molecule contains two identical chromophores, because of the through space interactions, excitation is delocalized between the two chromophores, and the excited state[31] is split into two states α and β (Figure 1-10).

$$R_{\alpha.\beta} = \pm\frac{1}{2}\pi\sigma_0\vec{R}_{ij}\bullet(\vec{\mu}_{i\alpha}\times\vec{\mu}_{j\alpha}) \qquad 1\text{-}8$$

Based on theoretical calculations on the binary system, the rotational strength, R, which represents the sign and the strength of a CD Cotton effect, can be defined by Equation 1-8,[26] where the positive and negative signs correspond to α- and β- state, respectively, R_{ij} is the distance vector between two chromophores, μ_{ioa} and μ_{joa} are the etdm of excitations, and σ_o is the excitation number of transition from 0 to α state.

Table 1-1. Definition of Exciton Chirality for a Binary System

	Qualitative Definition	Quantitative Definition	Cotton effects
positive chirality	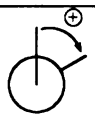	$\vec{R}ij \bullet (\vec{\mu}ioa \times \vec{\mu}joa)Vij > 0$	positive first, then negative Cotton effects
negative chirality	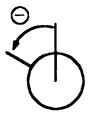	$\vec{R}ij \bullet (\vec{\mu}ioa \times \vec{\mu}joa)Vij < 0$	negative first, then positive Cotton effects

If Equation 1-8 is positive, the observed ECCD spectrum is positive, and if it is negative, then the observed ECCD spectrum is negative. From the equation above, the sign of the bisignate curve completely depends on the spatial orientation of the two chromophores.[32] As shown in Table1-1,[33] if the electric transition dipole moments of the two chromophores from front to back constitutes a clockwise orientation, then according to Equation 1-8 above, a positive bisignate spectrum will be observed, which refers to a

positive 1st and negative 2nd Cotton effects, while an opposite but otherwise identical spectrum is produced by the counterclockwise orientation.[34,35]

Therefore, the sign of an ECCD spectrum for a chiral molecule can be predicted as long as the spartial orientation of two chromophores is known. Moreover, the sign of a bisignate ECCD spectrum can enable the determination of the relative orientation of two chromophores in space in a non-empirical manner.

The difference in $\Delta\varepsilon$ between the 1st and 2nd Cotton effects is called the amplitude, A, of the ECCD couplet (Figure 1-14). This amplitude depends on several factors:[36]

a. *Molar absorption coefficient (ε) of the interacting chromophores.* The amplitude is proportional to ε^2. Therefore, in order to have increased sensitivity in the ECCD methods, chromophores with strong absorptions are preferred. These highly active chromophores enable CD measurements to be performed at micro molar concentrations, which make it an extremely useful property when only limited amount of chiral compound is available.

b. *Interchromophoric distance (R).* The amplitude is inversely proportional to the distance *R*, between the interacting chromophores.[37,38] To achieve enhanced interaction, the coupling chromophores should be oriented close to each other in space. This tendency is exemplified by a series of dibenzoates as shown by Nakanishi,[29] (Figure 1-17) where remote dibenzoates generally exhibit weaker amplitudes.

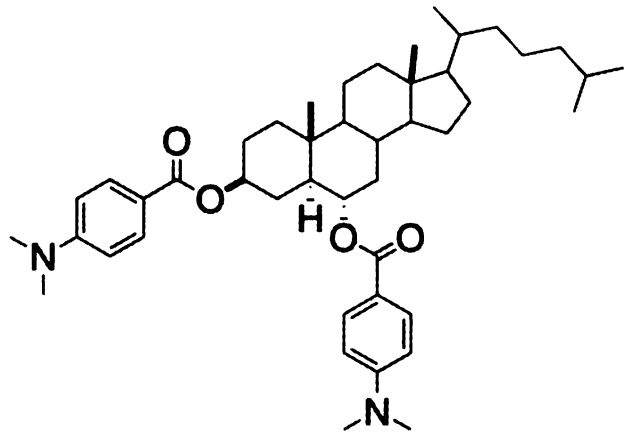

1,4- dibenzoate

+89.4

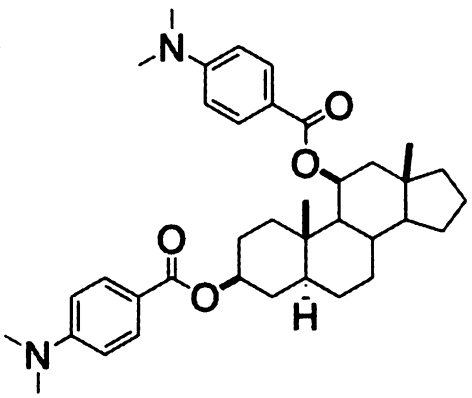

1,6- dibenzoate

+27.5

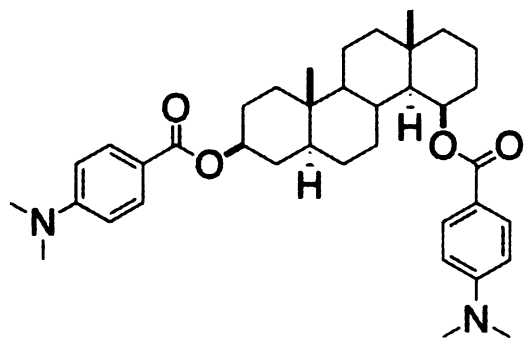

1,8- dibenzoate

-26.4

Figure 1-17. Dibenzoate chirality method – Distance effect

Although the 1,8-dibenzoate has an interchromophoric distance of 12.8 Å, a relatively strong ECCD is still observed. Generally, a distance of about 13 Å is enough to observe ECCD for most organic molecules. However, strong chromophores such as porphyrins (Soret band λ_{max} at 415 nm, ε = 350,000 M^{-1} cm^{-1}) are known to couple at distances of up to 50 Å.[39-41]

c. *Projection angle between the interacting chromophores.* The *A* value is maximal at a chromophoric projection angle of around 70°. There is no exciton coupling when the chromophores are either parallel or perpendicular to each other.

d. *Number of interacting chromophores (X, Y, Z).* The *A* value of the whole molecule is the summation of the *A* value of each pair of interacting chromophores, i.e. the principle of pair-wise additivity holds in systems comprising of three or more chromophores: $A_{total} = A_{xy}+A_{xz}+A_{yz}$. This observation has been proven by experiments and theoretical calculations.[42-44]

Not only can exciton coupling take place between identical chromophores, but it can also occur between different chromophores, but the UV-vis absorption λ_{max} values for the interacting chromophores need to be close for the coupling to be effective.

In systems containing two different chromophores, two opposite Cotton effects appear, slightly red- and blue-shifted from the respective maxima of the interacting chromophores.[26] The interacting chromophores do not have to be within the same molecule, as long as they are in close proximity in space. In particular, supramolecular compounds, like stacking of anthocyanins[45] and porphyrin containing brevetoxins[41] have been reported to give rise to exciton coupled CD bands.

1.2-3 The application of the ECCD method to determine the absolute stereochemistry of chiral molecules

The Exciton Coupled Circular Dichroic (ECCD) method is a method based on sound theoretical calculations as seen in the previous section, therefore, the absolute

stereochemistry of chiral organic compounds exhibiting typical bisignate ECCD spectrum is assignable in a non-empirical manner. The ECCD method is a versatile and sensitive method requiring only microgram amounts of sample. Because the ECCD spectrum originates as a direct result of the relative orientation of two interacting chromophores, nonempirical applications have been developed for the absolute stereochemical determination of both chemical and biological interest, including polyols,[46] carbohydrates,[47] quinuclidines,[48] hydroxy acids,[49] and others.[29] Figure 1-18 is an example of determining the absolute stereochemistry of (+)-abscisic acid by the ECCD method.[50,51] Abscisic acid, a plant hormone, contains two non-conjugated chromophores, an enone and a dienoic acid, separated by the only chiral center, a tertiary alcohol.

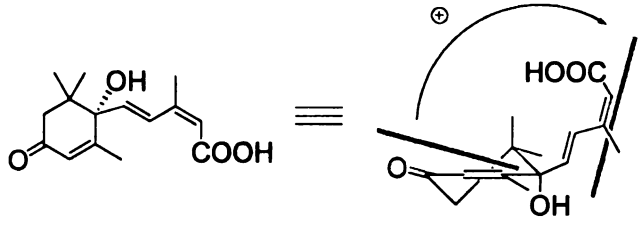

Figure 1-18. ECCD active abscisic acid

The enone and the dienoic acid moieties interact through space, resulting in a positive ECCD couplet. Based on the sign of the spectrum, the two chromophores must be oriented in a oriented in a clockwise manner, which directly indicates the β-configuration of the hydroxyl group.

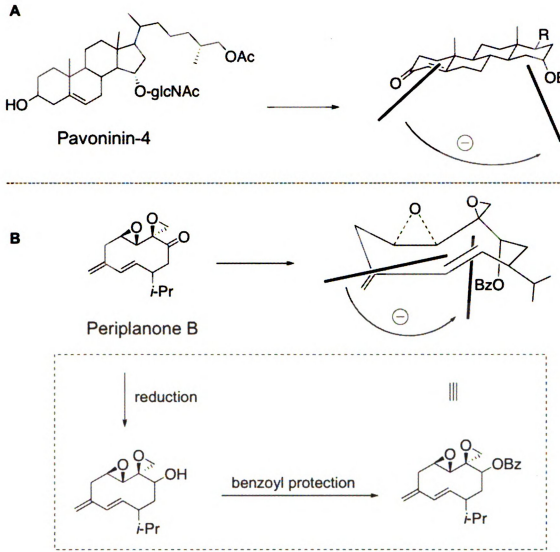

Figure 1-19. Application of the ECCD method in absolute configurational assignment of natural products.

Figure 1-19 shows some additional examples of chiral molecules, whose absolute stereochemistry has been determined using the ECCD method.

In A, the configuration of the 15-glcNAc group in Pavoninin-4, which is a shark repellant, has been determined according to the ECCD couplet between the enone and the bromobenzoate moiety.[52]

In order to use ECCD, there has to be spatial interaction between two chromophores. Therefore, in order to determine the absolute configuration of the potent cockroach sex excitant periplanone B, that has only one chromophore (the diene), derivatization of the molecule had to be carried out first, so as to install the second requisite chromophore. After stereoselective reduction of the carbonyl and benzoylation of the resulting alcohol, the observed ECCD defines the absolute stereochemistry.[53]

1.2-4 Use of chromophoric hosts such as porphyrins for ECCD studies

As mentioned earlier, the ECCD method requires the presence of at least two interacting chromophores in the molecule. This requirement can significantly limit its use, since the majority of chiral compounds do not fulfill this requirement. One way to overcome this problem is by introducing a second chromophore, usually in the form of a benzoyl group, as in the Periplanone B case discussed above. However, that is not always feasible, since a great number of chemically and biologically important compounds do not include any chromophoric moiety within their structures and the opportunity for derivatization is not always present. In order to address this issue, chromophoric receptors have been designed to act as hosts for non-chromophoric, chiral molecules. Once the chiral substrate binds to the host receptor either covalently or non-covalently, it will induce the host to adopt a preferred chiral conformation, which can then be observed as an ECCD couplet. This chiral induction was first demonstrated on dyes bound to polypeptides in their helical conformations.[54] This binding induced a helical orientation within the chromophoric molecule producing an ECCD-active species. The process for transmission of configurational information comprises of at least two elementary

processes: (1) complex formation between the chiral molecule (guest) and the chromophoric receptor (host) and (2) some dynamic processes associated with it, usually a conformational change of interacting molecules[55,56] that can induce the signal. If the interactions between the two molecules are strong enough, this will lead to efficient transmission of information. In order to simplify the observed ECCD signal, the chromophoric hosts used for ECCD studies are either achiral or in the form of racemates. When an achiral host is used, it can adopt the dictated chirality of the chiral substrate that binds to it through chiral induction. This induction leads to the formation of a preferred helical conformer, the orientation of which can be determined by ECCD.

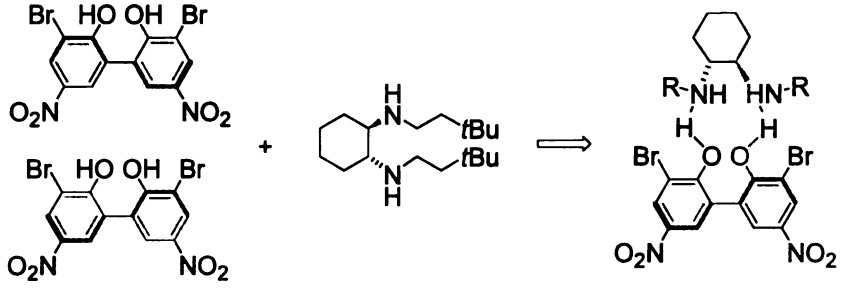

Figure 1-20. The induced chirality of biphenol upon binding to chiral amine

Binding between the host and guest molecules can either be covalent or non-covalent, depending on the complex being formed. One example of induced chirality on a prochiral host, upon interaction with a chiral guest, is shown in Figure 1-20.[57]

The biphenol shown is an ECCD active molecule (atropisomeric molecule); due to steric interactions between the two hydroxyl groups the molecule is not planar but exists as a mixture of the two enantiomeric forms.

When the chiral *trans*-1,2-cyclohexane diamine is added, a preferred complex is formed as shown, due to the hydrogen bonding between the phenols and the amine

groups.[58-60] The observed ECCD spectrum is determined by the induced complex and is dictated by the absolute stereochemistry of the chiral diamine.[57] This is an example of non-covalent complex formation. In a similar manner, covalent bonding has been used to form chiral complexes of binapthalenes to determine the absolute stereochemistry of chiral secondary alcohols.[61] As shown in Figure 1-21, the chromophoric reagent, 3-cyanocarbonyl-3'-methoxycarbonyl-2,2'-binapthalene, can be esterified with chiral secondary alcohols and the resultant complex exhibits induced ECCD as a result of favoring one atropisomer, due to restricted rotation about the C-C phenyl bonds.

The chirality has been transferred from the chiral alcohols to the binaphthylene

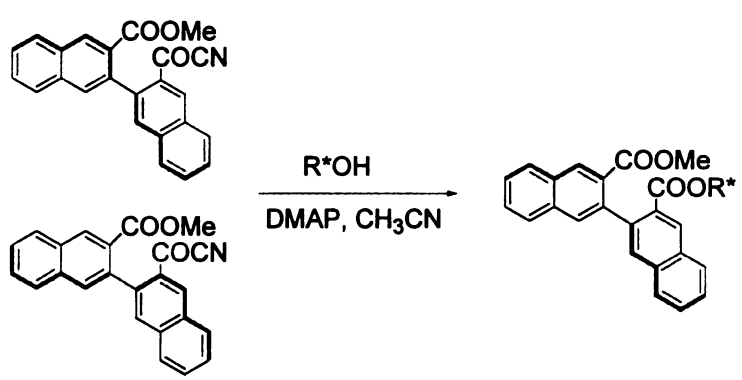

Figure 1-21. Determination of stereochemistry of chiral alcohols by ECCD.

system by minimizing the steric interaction between the substituents on the chiral alcohols with the methyl ester group in the binaphthylene.

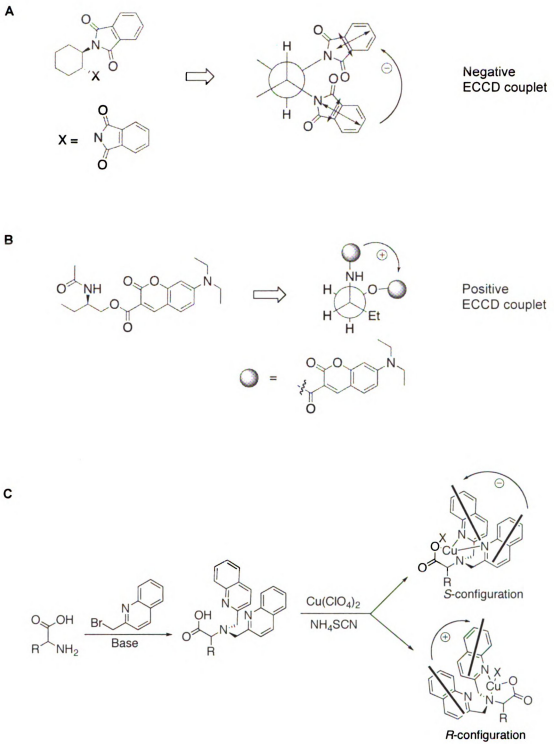

Figure 1-22. Derivatization methods for analysis of absolute configurations with various chromophores.

In recent years, several methods for the determination of absolute stereochemistry of difunctional amines have been developed and widely studied by ECCD, after derivatization of the functional groups to introduce the required chromophores. Figure 1-22 shows a few examples of chromophores that have been applied.

In A, Gawronski et. al.[62] used pthalimide to study the absolute stereochemistry of diamines. Their study also included the use of benzoate as the chromophore for hydroxyl and carboxyl groups to include the study of absolute stereochemistry of amino acids and amino alcohols. Lo et al.[63] have used 7-diethylaminocoumarin-3-carboxylate shown in B for amines, hydroxyl and carboxyl functional groups.

Canary and coworkers have published a number of systems,[64-66] one of which is shown in C, where they make use of quinoline chromophores for the formation of chiral propellers. In these systems, a tripodal system bearing a chiral group on one of the arms is synthesized. Upon complexation of Cu(II) or Zn one of the two possible propeller conformations is formed, depending on the chirality of the original molecule, giving rise to the corresponding characteristic ECCD couplet.

1.2-5 Use of zinc porphyrin as chromophoric host

Throughout literature, there is a predominance of porphyrin-based systems as chromophoric hosts for application in the ECCD method of stereochemical determination. The study of porphyrins has received increased interest in recent years since they have been utilized for the development of various projects, both of chemical and biochemical interest.[67] Especially in the case of chromophoric receptors for the

determination of stereochemistry using ECCD, the unique features of these highly conjugated rings have made them extremely attractive targets:[68]

(1) Their planar structures provide a well-defined binding pocket that is accentuated by substitutions on the ring. There are many sites that can be derivatized, such as the meso and β-positions, the central metal and the inner nitrogen atoms. By varying the substituents on the periphery of porphyrins, the solubility of the porphyrin containing compounds can be easily modified, for use in both polar and non-polar solvents.

(2) Porphyrins are excellent chromophores, with an average molar absorption coefficient of around 400,000 M^{-1} cm^{-1}; the amplitude (A) of the ECCD couplet is proportional to ε^2, so that the method's sensitivity is greatly enhanced in the presence of a strong chromophore.

(3) UV-vis absorption maximum of porphyrins rests around 418 nm for the main absorption band (Soret band), located in a region of the spectrum far red shifted than most chromophores that likely preexist in the analyte (typically carbonyls and olefins). This prevents the unwanted interaction between the introduced chromophore and the chiral substrate that can potentially complicate the spectral analysis.

(4) Metal incorporation into the porphyrin ring can be easily achieved, providing a coordination center for the binding of the chiral molecule. Metalloporphyrins, such as zinc porphyrins and magnesium porphyrins, can provide extra stereodifferentiation with their Lewis base binding sites. Therefore, porphyrins have been recognized as the ideal chromophores for detecting subtle changes in their close environment, including chirality induction.

Porphyrins have been widely utilized in stereochemical studies by CD. These include absolute configurational assignments,[40,69,70] stereochemical differentiations of sugars and amino acids,[71,72] and interactions with bio-macromolecules.[73,74]

Porphyrins, as the alkyl connected bis-metalloporphyrins shown in Figure 1-23, can be used as chromophoric host systems for stereochemical determination of chiral compounds because of their ability to bind to the chiral compounds at the metal centers, and report the chirality of bound guests based on Exciton Coupled Circular Dichroic Spectroscopy (ECCD).[67,75-78]

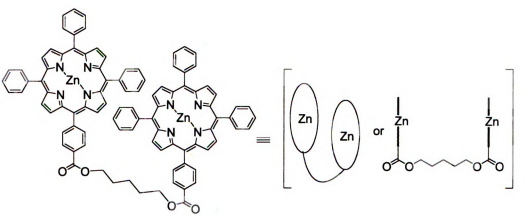

Figure 1-23. Structure and schematic representation of a porphyrin tweezer

Binding of chiral diamines forces the complex to adopt a helical conformation that results in an observable ECCD spectrum. In turn, the helicity of the receptor reflects the chirality of the bound compound.

As shown in Figure 1-25, when zinc tweezer is added to the solution of chiral diamine (*S*)-methyl-2,6-diaminohexanoate, the porphyrin tweezer binds to the chiral diamine via Zn-N coordination to form a "sandwich" structure.[77]

The interaction between the porphyrin coordinated to the end closer to the chiral center and the chiral groups is such that the steric interactions between them are kept at minimum. In order to achieve that, the porphyrin ring 'slides away' from the large group on the chiral center and covers the small group. This conformation is more stable than the alternative (Figure 1-24), in which the porphyrin ring 'slides away' from the large group and interacts with the small group instead. The more stable conformation leads to the two porphyrin planes adopting a counterclockwise orientation and a negative ECCD couplet is predicted. This prediction matches the CD observation.

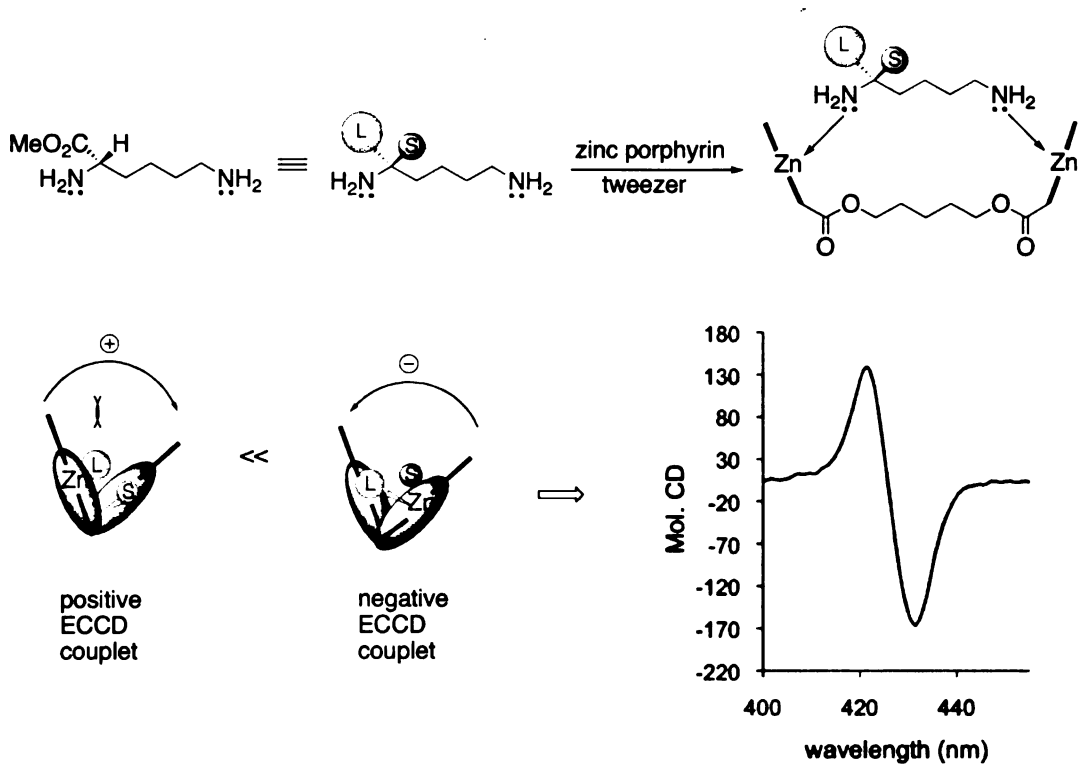

Figure 1-24. Assignment of absolute configuration of acyclic chiral diamines using ECCD

This tweezer approach has been extended for the determination of the absolute stereochemistry of chiral amino acids and amino alcohols which have a primary amino group directly attached to the stereogenic center. After simple chemical modifications, amino acids or amino alcohols can be converted to diamines (derivatization of amino acids with ethylene diamine, derivatization of amino alcohols with glycine) and the above rationalization is followed.[77]

As previously mentioned, zinc porphyrin tweezers cannot be used directly to determine the absolute stereochemistry of chiral compounds that have only one site of attachment. In order to overcome this problem, carrier molecules have been designed to convert compounds with only one site of attachment to molecules possessing two sites of attachment. Carriers are achiral molecules, which can be derivatized with the chiral substrates to provide the requisite two sites of attachment for binding to zinc porphyrin tweezer.

The carrier, upon derivatization with chiral compounds, should exhibit a rigid and predictable conformation about the free rotating single bonds. Rotation along any of the single bonds can dramatically alter the position of the large, medium, and small group with respect to the porphyrins. An ideal carrier molecule needs to possess the following characteristics:[79]

1) They should have a functional group that can be derivatized with the chiral molecules. For example, a carboxylic acid will serve well when a chiral amine is to be analyzed;
2) The derivatized carriers should be able to bind to the porphyrin tweezer at 1:1 ratio;

3) The carrier derivatized conjugates should be rigid, since flexible structures will give multiple conformations leading to weak or even complex CD spectra;

4) The carriers should be achiral, since the introduction of an extra chiral center into the system will result in diastereomers, which will complicate interpretation of the ECCD spectrum.

Ultimately, the success of this carrier method relies on identifying the most energetically favored conformation of the derivatized carrier. This is imperative because the conformation of the derivatized carrier dictates the position of the substituents at the chiral center in space relative to the porphyrins, and therefore will dictate the spatial orientation adopted by the two porphyrin planes.

Utilizing this method, a series of systems have been designed and successfully applied for the stereochemical assignment of derivatized chiral secondary monoamines,[76] and α-chiral carboxylic acids.[78-80]

As mentioned above, the use of porphyrin tweezers requires the use of a chiral molecule bearing two sites of attachment. An exception to this rule is the work by Inoue and coworkers.[81,82] They have developed a methodology for the assignment of the stereochemistry of monoamines and monoalcohols, without the need for derivatization, using a porphyrin tweezer with a very short linkage. The major drawback of this method, believed to be based on induced supramolecular chirality, involves the need for a great excess of chiral molecule (mM concentration), and low amplitudes, $< 50\ M^{-1}cm^{-1}$ for most substrates.

Our research has focused on exploring and expanding this latter approach. We are interested in designing a porphyrin-based system that can be used for the assignment of

the stereochemistry of compounds with only one site of attachment, without the need for derivatization, in μM scale. In particular, we wish to employ the use of porphyrin aggregate systems as reporters of chirality for monoamines.

The controlled organization of molecules into self-assemblies has seen an explosion of interest in the recent past because of the ability to create novel supramolecular architectures with useful properties. Porphyrins are known[83-88] to align into one-dimensional aggregates by π-π interaction, electrostatic forces, or Van-der-Waals forces. The control of chirality in porphyrin-based self-assemblies is of increasing interest both in biological applications, for the construction of systems mimicking biological functions, for example Cytochrome P-450 activity, as well as in material science and chemistry, for example creating nanowires, or new molecules.

This research will focus on taking advantage to the π-π stacking ability of porphyrins in order to form aggregate systems. Once the aggregates are formed, we wish to use chiral monoamines to induce chirality into the aggregate system, which will then be studied by CD spectroscopy.

References:

(1) Allenmark, S.; Gawronski, J. "Determination of absolute configuration - an overview related to this special issue" *Chirality* **2008**, *20*, 606-608.

(2) Stephens, P. J.; Devlin, F. J.; Pan, J. J. "The determination of the absolute configurations of chiral molecules using vibrational circular dichroism (VCD) spectroscopy" *Chirality* **2008**, *20*, 643-663.

(3) Eliel, E. L. W., S. W. "stereochemistry of organic compounds" *wiley: New York* **1994**.

(4) Bruice, P. Y. "Organic Chemistry 3rd ed." *Prentice-Hall, Inc.: Upper Saddle Rivevr, New Jersey* **2001**.

(5) Rossi, R.; Diversi, P. "SYNTHESIS, ABSOLUTE CONFIGURATION, AND OPTICAL PURITY OF CHIRAL ALLENES" *Synthesis-Stuttgart* **1973**, 25-36.

(6) Oki, M. "In Topics in Stereochemistry (Eds.: Allinger, N. L.; Eliel, E. L.; Wilen, S. W. " *Interscience Publication, New York* **1983**.

(7) Laarhoven, W. H.; Prinsen, W. J. C. "CARBOHELICENES AND HETEROHELICENES" *Topics in Current Chemistry* **1984**, *125*, 63-130.

(8) Prinsen, W. J. C.; Laarhoven, W. H. "DETERMINATION OF THE ENANTIOMERIC EXCESS OF HEXAHELICENE AND ITS METHYL-SUBSTITUTED DERIVATIVES BY HIGH-PERFORMANCE LIQUID-CHROMATOGRAPHY" *Journal of Chromatography* **1987**, *393*, 377-390.

(9) Bada, J. L. "Meteoritics - Extraterrestrial handedness?" *Science* **1997**, *275*, 942-943.

(10) Bonner, W. A.; Kavasmaneck, P. R. "ASYMMETRIC ADSORPTION OF DL-ALANINE HYDROCHLORIDE BY QUARTZ" *Journal of Organic Chemistry* **1976**, *41*, 2225-2226.

(11) Bonner, W. A.; Kavasmaneck, P. R.; Martin, F. S.; Flores, J. J. "ASYMMETRIC ADSORPTION BY QUARTZ - MODEL FOR PREBIOTIC ORIGIN OF OPTICAL-ACTIVITY" *Origins of Life and Evolution of the Biosphere* **1975**, *6*, 367-376.

(12) Cronin, J. R.; Pizzarello, S. "Enantiomeric excesses in meteoritic amino acids" *Science* **1997**, *275*, 951-955.

(13) Dale, J. A.; Mosher, H. S. "NUCLEAR MAGNETIC-RESONANCE ENANTIOMER REAGENTS - CONFIGURATIONAL CORRELATIONS VIA

NUCLEAR MAGNETIC-RESONANCE CHEMICAL-SHIFTS OF DIASTEREOMERIC MANDELATE, O-METHYLMANDELATE, AND ALPHA-METHOXY-ALPHA-TRIFLUOROMETHYLPHENYLACETATE (MTPA) ESTERS" *Journal of the American Chemical Society* **1973**, *95*, 512-519.

(14) Feringa, B. L.; van Delden, R. A. "Absolute asymmetric synthesis: The origin, control, and amplification of chirality" *Angewandte Chemie-International Edition* **1999**, *38*, 3419-3438.

(15) Freire, F.; Seco, J. M.; Quinoa, E.; Riguera, R. "The assignment of the absolute configuration of 1,2-diols by low-temperature NMR of a single MPA derivative" *Organic Letters* **2005**, *7*, 4855-4858.

(16) Hazen, R. M.; Filley, T. R.; Goodfriend, G. A. "Selective adsorption of L- and D-amino acids on calcite: Implications for biochemical homochirality" *Proceedings of the National Academy of Sciences of the United States of America* **2001**, *98*, 5487-5490.

(17) Kavasmaneck, P. R.; Bonner, W. A. "ADSORPTION OF AMINO-ACID DERIVATIVES BY D-QUARTZ AND L-QUARTZ" *Journal of the American Chemical Society* **1977**, *99*, 44-50.

(18) Lambert, J. B. S., J. F.; Lightner, D. A.; Cooks,R. G. "Organic Structural Spectroscopy" *Prentice Hall, Upper Saddle River* **1998**.

(19) Stinson, S. C. "Chiral chemistry" *Chemical & Engineering News* **2001**, *79*, 45-+.

(20) Solomons, T. W. "*Organic Chemistry*" *John Wiley & Sons Inc., New York* **1978**.

(21) Velluz, L. L., M.; Grosjean, M. "*Optical Circular Dichroism*" *Academic Press, New York* **1965**.

(22) Mislow, K.; Glass, M. A. W.; Obrien, R. E.; Rutkin, P.; Djerassi, C.; Weiss, J.; Steinber.Dh "CONFIGURATION CONFORMATION AND ROTATORY DISPERSION OF OPTICALLY ACTIVE BIARYLS" *Journal of the American Chemical Society* **1962**, *84*, 1455-&.

(23) Snatzke, G. "SEMI-EMPIRICAL RULES IN CIRCULAR-DICHROISM OF NATURAL-PRODUCTS" *Pure and Applied Chemistry* **1979**, *51*, 769-785.

(24) Vasileiou, C. *PhD Thesis* **2006**.

(25) Snatzke, G. "CIRCULAR-DICHROISM AND ABSOLUTE CONFORMATION - APPLICATION OF QUALITATIVE MO THEORY TO CHIROPTICAL PHENOMENA" *Angewandte Chemie-International Edition in English* **1979**, *18*, 363-377.

(26) Harada, N. N., K. "Circular Dichroic Spectroscopy: Exciton Coupling in Organic Stereochemistry" *University Science Books: Mill Valley* **1983**.

(27) Kuhn, W. "The physical significance of optical rotatory power" *Transactions of the Faraday Society* **1930**, *26*, 0293-0307.

(28) Kirkwood, J. G. "On the theory of optical rotatory power" *Journal of Chemical Physics* **1937**, *5*, 479-491.

(29) Nakanishi, K. "Circular Dichroism Principles and Applications" **1994**.

(30) Wiesler, W. T.; Vazquez, J. T.; Nakanishi, K. "PAIRWISE ADDITIVITY IN EXCITON-COUPLED CD CURVES OF MULTICHROMOPHORIC SYSTEMS" *Journal of the American Chemical Society* **1987**, *109*, 5586-5592.

(31) Chen, S. M. L.; Harada, N.; Nakanish.K "LONG-RANGE EFFECT IN EXCITON CHIRALITY METHOD" *Journal of the American Chemical Society* **1974**, *96*, 7352-7354.

(32) Harada, N.; Nakanish.K "EXCITON CHIRALITY METHOD AND ITS APPLICATION TO CONFIGURATIONAL AND CONFORMATIONAL STUDIES OF NATURAL-PRODUCTS" *Accounts of Chemical Research* **1972**, *5*, 257-&.

(33) Harada, N.; Chen, S. L.; Nakanishi, K. "QUANTITATIVE DEFINITION OF EXCITON CHIRALITY AND DISTANT EFFECT IN EXCITON CHIRALITY METHOD" *Journal of the American Chemical Society* **1975**, *97*, 5345-5352.

(34) Hug, W.; Wagniere, G. "OPTICAL-ACTIVITY OF CHROMOPHORES OF SYMMETRY C2" *Tetrahedron* **1972**, *28*, 1241-&.

(35) Wagniere, G.; Hug, W. "POLARIZATION AND SIGN OF LONG-WAVELENGTH COTTON-EFFECTS IN CHROMOPHORES OF SYMMETRY C2" *Tetrahedron Letters* **1970**, 4765-&.

(36) Weckerle, B.; Schreier, P.; Humpf, H. U. "A new one-step strategy for the stereochemical assignment of acyclic 2-and 3-sulfanyl-1-alkanols using the CD exciton chirality method" *Journal of Organic Chemistry* **2001**, *66*, 8160-8164.

(37) Oancea, S.; Formaggio, F.; Campestrini, S.; Broxterman, Q. B.; Kaptein, B.; Toniolo, C. "Distance dependency of exciton coupled circular dichroism using turn and helical peptide spacers" *Biopolymers* **2003**, *72*, 105-115.

(38) Pescitelli, G.; Gabriel, S.; Wang, Y. K.; Fleischhauer, J.; Woody, R. W.; Berova, N. "Theoretical analysis of the porphyrin-porphyrin exciton interaction in circular

dichroism spectra of dimeric tetraarylporphyrins" *Journal of the American Chemical Society* **2003**, *125*, 7613-7628.

(39) Matile, S.; Berova, N.; Nakanishi, K. "Intramolecular porphyrin pi,pi-stacking: Absolute configurational assignment of acyclic compounds with single chiral centers by exciton coupled circular dichroism" *Enantiomer* **1996**, *1*, 1-12.

(40) Matile, S.; Berova, N.; Nakanishi, K. "Exciton coupled circular dichroic studies of self-assembled brevetoxin-porphyrin conjugates in lipid bilayers and polar solvents" *Chemistry & Biology* **1996**, *3*, 379-392.

(41) Matile, S.; Berova, N.; Nakanishi, K.; Fleischhauer, J.; Woody, R. W. "Structural studies by exciton coupled circular dichroism over a large distance: Porphyrin derivatives of steroids, dimeric steroids, and brevetoxin B" *Journal of the American Chemical Society* **1996**, *118*, 5198-5206.

(42) Dong, J. G.; Akritopoulou-Zanze, I.; Guo, J. S.; Berova, N.; Nakanishi, K.; Harada, N. "Theoretical calculation of circular dichroic exciton-split spectra in presence of three interacting 2-naphthoate chromophores" *Enantiomer* **1997**, *2*, 397-409.

(43) Lichtenthaler, F. W.; Sakakibara, T.; Oeser, E. "SUGAR ENOLONES .6. "TETRA-O-BENZOYL-2-HALOHEXOPYRANOSYL HALIDES - PREPARATION, ASSIGNMENT OF CONFIGURATION, AND HYDROLYSIS TO ENOLONES" *Carbohydrate Research* **1977**, *59*, 47-61.

(44) Liu, H. W.; Nakanishi, K. "A MICROMETHOD FOR DETERMINING THE BRANCHING POINTS IN OLIGOSACCHARIDES BASED ON CIRCULAR-DICHROISM" *Journal of the American Chemical Society* **1981**, *103*, 7005-7006.

(45) Goto, T.; Kondo, T. "STRUCTURE AND MOLECULAR STACKING OF ANTHOCYANINS - FLOWER COLOR VARIATION" *Angewandte Chemie-International Edition in English* **1991**, *30*, 17-33.

(46) Rele, D.; Zhao, N.; Nakanishi, K.; Berova, N. "Acyclic 1,2-/1,3-mixed pentols. Synthesis and general trends in bichromophoric exciton coupled circular dichroic spectra" *Tetrahedron* **1996**, *52*, 2759-2776.

(47) Wiesler, W. T.; Nakanishi, K. "RELATIVE AND ABSOLUTE CONFIGURATIONAL ASSIGNMENTS OF ACYCLIC POLYOLS BY CIRCULAR-DICHROISM .1. RATIONALE FOR A SIMPLE PROCEDURE BASED ON THE EXCITON CHIRALITY METHOD" *Journal of the American Chemical Society* **1989**, *111*, 9205-9213.

(48) Zhao, N.; Berova, N.; Nakanishi, K.; Rohmer, M.; Mougenot, P.; Jurgens, U. J. "Structures of two bacteriohopanoids with acyclic pentol side-chains from the cyanobacterium Nostoc PCC 6720" *Tetrahedron* **1996**, *52*, 2777-2788.

(49) Gimple, O.; Schreier, P.; Humpf, H. U. "A new exciton-coupled circular dichroism method for assigning the absolute configuration in acyclic alpha- and beta-hydroxy carboxylic acids" *Tetrahedron-Asymmetry* **1997**, *8*, 11-14.

(50) Harada, N. "ABSOLUTE CONFIGURATION OF (+)-TRANS-ABSCISIC ACID AS DETERMINED BY A QUANTITATIVE APPLICATION OF EXCITON CHIRALITY METHOD" *Journal of the American Chemical Society* **1973**, *95*, 240-242.

(51) Koreeda, M.; Weiss, G.; Nakanish.K "ABSOLUTE CONFIGURATION OF NATURAL (+)-ABSCISIC ACID" *Journal of the American Chemical Society* **1973**, *95*, 239-240.

(52) Tachibana, K.; Sakaitani, M.; Nakanishi, K. "PAVONININS, SHARK-REPELLING AND ICHTHYOTOXIC STEROID N-ACETYLGLUCOSAMINIDES FROM THE DEFENSE SECRETION OF THE SOLE PARADACHIRUS-PAVONINUS (SOLEIDAE)" *Tetrahedron* **1985**, *41*, 1027-1037.

(53) Adams, M. A.; Nakanishi, K.; Still, W. C.; Arnold, E. V.; Clardy, J.; Persoons, C. J. "SEX-PHEROMONE OF THE AMERICAN COCKROACH - ABSOLUTE-CONFIGURATION OF PERIPLANONE-B" *Journal of the American Chemical Society* **1979**, *101*, 2495-2498.

(54) Blout, E. R.; Stryer, L. "ANOMALOUS OPTICAL ROTATORY DISPERSION OF DYE - POLYPEPTIDE COMPLEXES" *Proceedings of the National Academy of Sciences of the United States of America* **1959**, *45*, 1591-1593.

(55) Beer, P. D.; Rothin, A. S. "A NEW ALLOSTERIC BIS CROWN ETHER LIGAND THAT DISPLAYS NEGATIVE BINDING CO-OPERATIVITY OF THE DIQUAT DICATION BY THE COMPLEXATION OF A TRANSITION-METAL GUEST" *Journal of the Chemical Society-Chemical Communications* **1988**, 52-54.

(56) Mizutani, T.; Yagi, S.; Honmaru, A.; Ogoshi, H. "Interconversion between point chirality and helical chirality driven by shape-sensitive interactions" *Journal of the American Chemical Society* **1996**, *118*, 5318-5319.

(57) Mizutani, T.; Takagi, H.; Hara, O.; Horiguchi, T.; Ogoshi, H. "Axial chirality induction in flexible biphenols by hydrogen bonding and steric interactions" *Tetrahedron Letters* **1997**, *38*, 1991-1994.

(58) Bell, C. L.; Barrow, G. M. "EVIDENCE FOR A LOW-LYING 2ND POTENTIAL MINIMUM IN HYDROGEN-BONDED SYSTEMS" *Journal of Chemical Physics* **1959**, *31*, 1158-1163.

(59) Hanessian, S.; Simard, M.; Roelens, S. "MOLECULAR RECOGNITION AND SELF-ASSEMBLY BY NON-AMIDIC HYDROGEN-BONDING - AN EXCEPTIONAL ASSEMBLER OF NEUTRAL AND CHARGED SUPRAMOLECULAR STRUCTURES" *Journal of the American Chemical Society* **1995**, *117*, 7630-7645.

(60) Kramer, R.; Lang, R.; Brzezinski, B.; Zundel, G. "PROTON-TRANSFER IN INTRAMOLECULAR HYDROGEN-BONDS WITH LARGE PROTON POLARIZABILITY IN 1-PIPERIDINECARBOXYLIC ACIDS - TEMPERATURE, SOLVENT AND CONCENTRATION-DEPENDENCE" *Journal of the Chemical Society-Faraday Transactions* **1990**, *86*, 627-630.

(61) Hosoi, S.; Kamiya, M.; Ohta, T. "Novel development of exciton-coupled circular dichroism based on induced axial chirality" *Organic Letters* **2001**, *3*, 3659-3662.

(62) Skowronek, P.; Gawronski, J. "A simple circular dichroism method for the determination of the absolute configuration of allylic amines" *Tetrahedron Letters* **2000**, *41*, 2975-2977.

(63) Lo, L. Y., C.; Tsai, C. "A CD Exciton Chirality Method for Determination of the Absolute Configuration of *threo*-beta-Aryl-beta-hydroxy-alpha-aminoAcid Derivatives" *J. Org. Chem.* **2002**, *4*, 1368 - 1371.

(64) Canary, J. W.; Allen, C. S.; Castagnetto, J. M.; Chiu, Y. H.; Toscano, P. J.; Wang, Y. H. "Solid state and solution characterization of chiral, conformationally mobile tripodal ligands" *Inorganic Chemistry* **1998**, *37*, 6255-6262.

(65) Canary, J. W.; Allen, C. S.; Castagnetto, J. M.; Wang, Y. H. "CONFORMATIONALLY DRIVEN, PROPELLER-LIKE CHIRALITY IN LABILE COORDINATION-COMPLEXES" *Journal of the American Chemical Society* **1995**, *117*, 8484-8485.

(66) Holmes, A. E.; Zahn, S.; Canary, J. W. "Synthesis and circular dichroism studies of N,N-bis(2-quinolylmethyl)amino acid Cu(II) complexes: Determination of absolute configuration and enantiomeric excess by the exciton coupling method" *Chirality* **2002**, *14*, 471-477.

(67) Huang, X. F.; Nakanishi, K.; Berova, N. "Porphyrins and metalloporphyrins: Versatile circular dichroic reporter groups for structural studies" *Chirality* **2000**, *12*, 237-255.

(68) Ogoshi, H.; Mizutani, T. "Multifunctional and chiral porphyrins: Model receptors for chiral recognition" *Accounts of Chemical Research* **1998**, *31*, 81-89.

(69) Arimori, S.; Takeuchi, M.; Shinkai, S. "Sugar-controlled aggregate formation in boronic acid-appended porphyrin amphiphiles" *Journal of the American Chemical Society* **1996**, *118*, 245-246.

(70) Matile, S.; Berova, N.; Nakanishi, K.; Novkova, S.; Philipova, I.; Blagoev, B. "PORPHYRINS - POWERFUL CHROMOPHORES FOR STRUCTURAL STUDIES BY EXCITON-COUPLED CIRCULAR-DICHROISM" *Journal of the American Chemical Society* **1995**, *117*, 7021-7022.

(71) Crossley, M. J.; Hambley, T. W.; Mackay, L. G.; Try, A. C.; Walton, R. "PORPHYRIN ANALOGS OF TROGERS BASE - LARGE CHIRAL CAVITIES WITH A BIMETALLIC BINDING-SITE" *Journal of the Chemical Society-Chemical Communications* **1995**, 1077-1079.

(72) Crossley, M. J.; Mackay, L. G.; Try, A. C. "ENANTIOSELECTIVE RECOGNITION OF HISTIDINE AND LYSINE ESTERS BY PORPHYRIN CHIRAL CLEFTS AND DETECTION OF AMINO-ACID CONFORMATIONS IN THE BOUND-STATE" *Journal of the Chemical Society-Chemical Communications* **1995**, 1925-1927.

(73) Foster, N.; Singhal, A. K.; Smith, M. W.; Marcos, N. G.; Schray, K. J. "INTERACTIONS OF PORPHYRINS AND TRANSFER-RNA" *Biochimica Et Biophysica Acta* **1988**, *950*, 118-131.

(74) Suenaga, H.; Arimori, S.; Shinkai, S. "Sugar-controlled association dissociation equilibria between DNA and boronic acid-appended porphyrin" *Journal of the Chemical Society-Perkin Transactions 2* **1996**, 607-612.

(75) Huang, X. F.; Borhan, B.; Rickman, B. H.; Nakanishi, K.; Berova, N. "Zinc porphyrin tweezer in host-guest complexation: Determination of absolute configurations of primary monoamines by circular dichroism" *Chemistry-a European Journal* **2000**, *6*, 216-224.

(76) Huang, X. F.; Fujioka, N.; Pescitelli, G.; Koehn, F. E.; Williamson, R. T.; Nakanishi, K.; Berova, N. "Absolute configurational assignments of secondary amines by CD-sensitive dimeric zinc porphyrin host" *Journal of the American Chemical Society* **2002**, *124*, 10320-10335.

(77) Huang, X. F.; Rickman, B. H.; Borhan, B.; Berova, N.; Nakanishi, K. "Zinc porphyrin tweezer in host-guest complexation: Determination of absolute configurations of diamines, amino acids, and amino alcohols by circular dichroism" *Journal of the American Chemical Society* **1998**, *120*, 6185-6186.

(78) Proni, G.; Pescitelli, G.; Huang, X. F.; Quraishi, N. Q.; Nakanishi,K.;Berova, N. "Configurational assignment of alpha-chiral carboxylic acids by complexation to dimeric Zn-porphyrin: host-guest structure, chiral recognition and circular dichroism" *Chemical Communications* **2002**, 1590-1591.

(79) Yang, Q.; Olmsted, C.; Borham, B. "Absolute stereochemical determination of chiral carboxylic acids" *Organic Letters* **2002**, *4*, 3423-3426.

(80) Proni, G.; Pescitelli, G.; Huang, X. F.; Nakanishi, K.; Berova, N. "Magnesium tetraarylporphyrin tweezer: A CD-sensitive host for absolute configurational assignments of alpha-chiral carboxylic acids" *Journal of the American Chemical Society* **2003**, *125*, 12914-12927.

(81) Borovkov, V. V.; Lintuluoto, J. M.; Inoue, Y. "Supramolecular chirogenesis in zinc porphyrins: Mechanism, role of guest structure, and application for the absolute configuration determination" *Journal of the American Chemical Society* **2001**, *123*, 2979-2989.

(82) Borovkov, V. V.; Yamamoto, N.; Lintuluoto, J. M.; Tanaka, T.; Inoue, Y. "Supramolecular chirality induction in bis(zinc porphyrin) by amino acid derivatives: Rationalization and applications of the ligand bulkiness effect" *Chirality* **2001**, *13*, 329-335.

(83) Kano, K.; Fukuda, K.; Wakami, H.; Nishiyabu, R.; Pasternack, R. F. "Factors influencing self-aggregation tendencies of cationic porphyrins in aqueous solution" *Journal of the American Chemical Society* **2000**, *122*, 7494-7502.

(84) Kano, K.; Minamizono, H.; Kitae, T.; Negi, S. "Self-aggregation of cationic porphyrins in water. Can pi-pi stacking interaction overcome electrostatic repulsive force?" *Journal of Physical Chemistry A* **1997**, *101*, 6118-6124.

(85) Koti, A. S. R.; Periasamy, N. "Cyanine induced aggregation in meso-tetrakis(4-sulfonatophenyl)porphyrin anions" *Journal of Materials Chemistry* **2002**, *12*, 2312-2317.

(86) Kubat, P.; Lang, K.; Prochakova, K.; Anzenbacher, P. "Self-aggregates of cationic meso-tetratolylporphyrins in aqueous solutions" *Langmuir* **2003**, *19*, 422-428.

(87) Wang, Y. T.; Jin, W. J. "H-aggregation of cationic palladium-porphyrin as a function of anionic surfactant studied using phosphorescence, absorption and RLS spectra" *Spectrochimica Acta Part a-Molecular and Biomolecular Spectroscopy* **2008**, *70*, 871-877.

(88) Yu, W.; Li, Z. S.; Wang, T. Y.; Liu, M. H. "Aggregation and supramolecular chirality of achiral amphiphilic metalloporphyrins" *Journal of Colloid and Interface Science* **2008**, *326*, 460-464.

CHAPTER 2

PORPHYRIN AGGREGATES AS HOSTS FOR CHIRAL DISCRIMINATION

2-1. Introduction to Porphyrin Aggregation

Figure 1-24 shows the use of the bis-zinc porphyrin dimer (porphyrin tweezer) for stereochemical determination of chiral molecules bearing two sites of attachment (diamines, diols, amino alcohols). However, as discussed previously, this method cannot be directly applied for the stereochemical determination of compounds with one site of attachment, (carboxylic acids, monoamines and alcohols) since the two porphyrins cannot be oriented relative to each other. Nakanishi, Berova, and co-workers, developed a method that enables the stereochemical determination of such compounds that lack a second site of coordination. This method requires derivatization of the chiral compound with a carrier molecule which functions to provide the second binding site (Figure 2-1).[1]

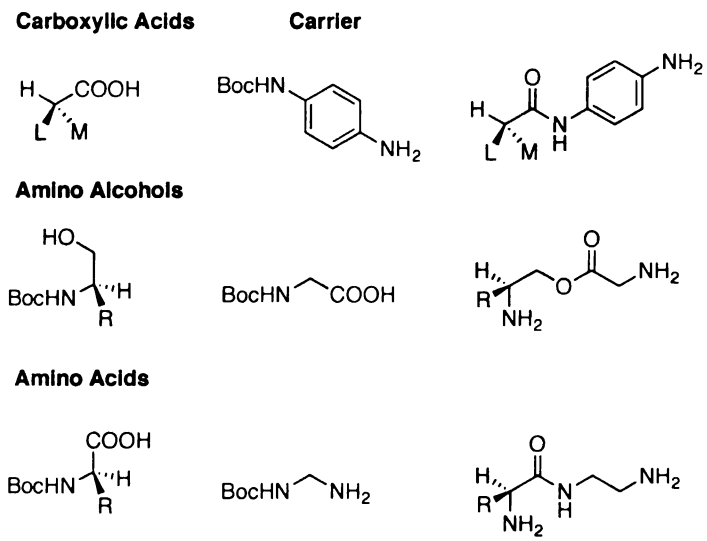

Figure 2-1. Application of carrier molecules to the stereochemical determination of molecules with one site of attachment: carboxylic acids, amino alcohols, amino acids.

This method has been extended to the determination of stereochemistry of chiral carboxylic acids,[2] amino acids and alcohols,[1] which have an amino group directly attached to the stereogenic centre.

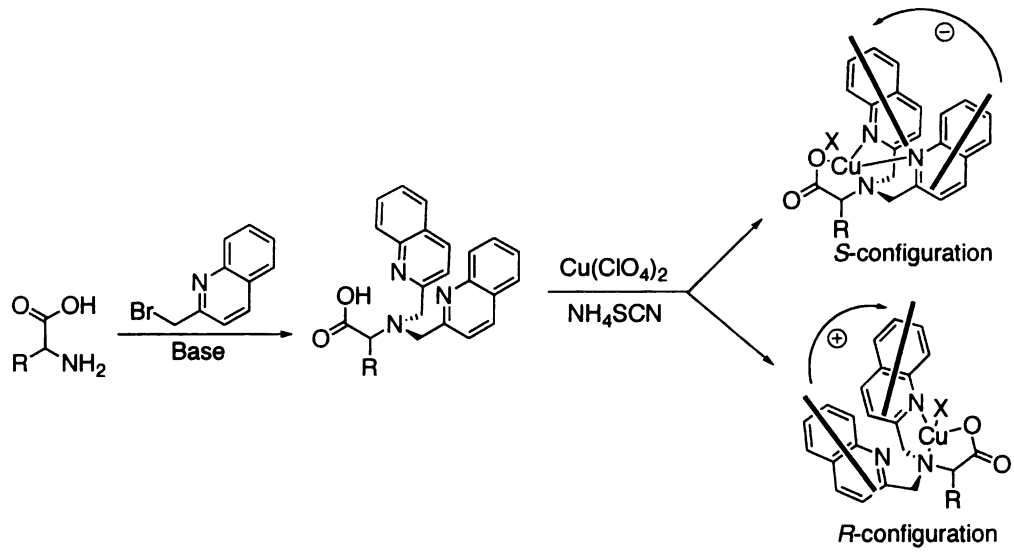

Figure 2-2. Derivatization method for analysis of absolute configurations of amino acids

Canary and co-workers have developed several modifications to the tweezer system, where instead of using a carrier for derivatization, they make use of quinoline chromophores for the formation of chiral propellers.[3-5] As shown in Figure 2-2, the chiral molecule is derivatized onto a tripodal system as one of the arms. Upon complexation of Cu(II), depending on the chirality of the molecule, one of the possible propeller conformations is formed, giving rise to the corresponding characteristic ECCD couplet. In this case, *S*-amino acids result in negative ECCD and *vice versa*.[4] This system works for chiral primary amines, β-aminoalcohols and N,N,dialkyl α-amino acids,[3,5] with appropriate derivatization.

More recently[6] in 2007, they reported a chiral tripodal ligand containing two monosubstituted tetraphenylporphyrin (TPP) moieties, (Figure 2-3) and used it for the

stereochemical determination of chiral amino alcohols and amino acids. The ligand incorporates the porphyrins as chromophores to enhance the CD amplitude.

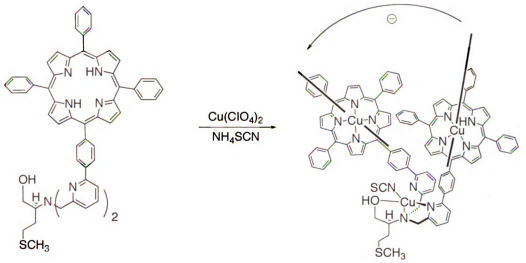

Figure 2-3. Tripodal ligand, derived from methioninol, incorporating TPP as chromophores

The tripodal system is flexible, and can adopt different conformations in solution, but once it complexes to the Cu(II), the ligand wraps around the metal, fixing the geometry of the chromophores in a way that positions the porphyrins such that the strong Soret electronic transitions couple to give ECCD. A strong negative CD spectrum was obtained for this system, which indicated a spatial orientation of the net transition dipole from the Soret bands in the porphyrins with a counterclockwise twist, corresponding to the *S* configuration of the chiral center.

In their systems however, the chirality is incorporated within one of the arms of the tripod, and the chiral amine to be studied requires derivatization into the tripopdal system, which may not always be feasible.

In 2001, a new methodology[7-9] was developed by Inuoe et al. for the assignment of the stereochemistry of monoamines and monoalcohols without the need for derivatization. As shown in Figure 2-4, their method calls for the use of a porphyrin tweezer with a very short linker. In this system, the achiral folded *syn* conformer of the ethane-bridged porphyrin switches to the corresponding chiral extended *anti* conformer upon ligand binding.

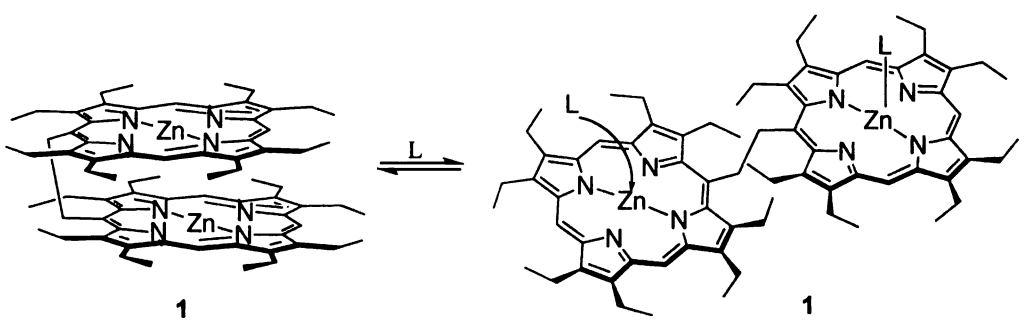

Figure 2-4. Porphyrin tweezer system used for stereochemical determination of chiral monoamines. For the second ligation step, the ligand approaches from the same face. (asymmetric approach)

The mechanism of the chiral induction is based on the chiral ligand binding to zinc, and subsequent formation of either right- or left-handed twist, due to steric interactions between the ethyl groups on the porphyrin ring, and the largest substituent on the asymmetric carbon on the ligand. The major drawback of this method is the requirement of an excess of the chiral molecule (mM concentration) and low amplitudes less than 50 $M^{-1}cm^{-1}$ observed for most substrates.

Our main interest is to develop non-tweezer host systems that can be used for the assignment of stereochemistry of compounds with only one site of attachement, without derivatization, and in μM concentration. This requires that the host system should have

the capability to bind chiral molecules that contain a single site of attachment, be sensitive to the chiral disposition of the substituents, and adopt an induced asymmetry that results in an observable ECCD signal. The readout would then correlate to the absolute stereochemistry of the bound chiral guest. Because porphyrins lead to high amplitudes, we wish to use porhyrins as the two required chromophores.

2-2. Design of Porphyrins for Aggregation

Supramolecular chirality[10-13,14] is a relatively new area of research that combines supramolecular chemistry and molecular chirality. The most important part of this field is supramolecular chirogenesis, which is "symmetry breaking" in intrinsically achiral multi or unimolecular systems and chirality amplification in supramolecular assemblies consisting of chiral components upon interaction with a chiral enviroment, via a chirality transfer mechanism.

Molecular self-assembly is the spontaneous association of molecules into stable, structurally well-defined aggregates by non-covalent interactions such as hydrogen bonding, π-π interactions, electrostatic interactions, *etecetra*. The first technological application of molecular assemblies was the *Langmuir-Blodgett technique* where layers of amphiphilic molecules are deposited onto a solid from the surface of a liquid. This is done by immersing the solid substrate into a liquid, adding a monolayer with each immersion step to form the *Langmuir-Blodgett films*.[15-17] Because of this, films with very accurate thickness can be formed. These films have been used in material science in optical and electronic devices.[18]

More recent applications of molecular assembly is in DNA nanotechnology.[19] The basic idea behind DNA nanotechnology is to use the unique molecular recogition properties of DNA to form target materials with predictable and controllable 3D structures. One interesting recent example is where Chichak and co-workers use DNA to prepare a molecular analogue of the Borromean rings.[20]

Molecular self-assembly is common in biological systems and underlies the formation of many complex biological processes[8] like protein folding and pairing of nucleotides. Molecular assemblies of chromophores in particular are important; for example the light harvesting complex employed for photosynthesis by green plants and purple bacteria,[11] as well as molecular assemblies in technological applications like sensors and nonlinear optics can be cited.[8,21,22] Currently the main problem faced during the application of molecular assemblies and aggregates is the difficulty in controlling the arrangement and orientation of the monomers in the aggregates.

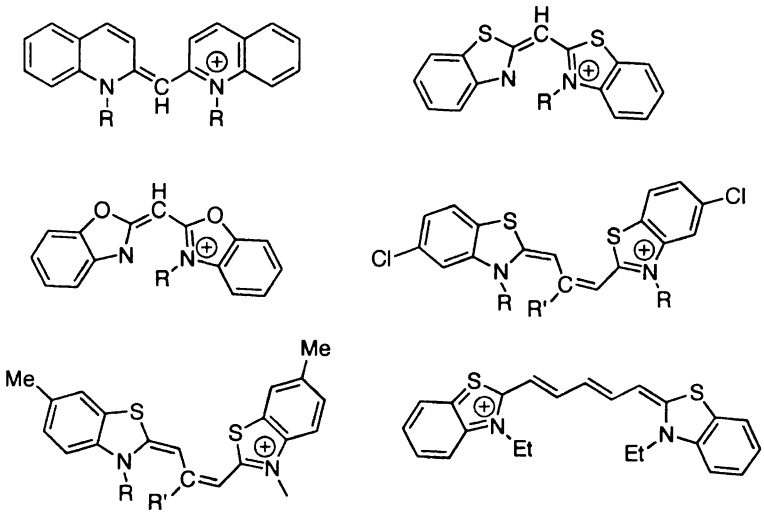

Figure 2-5. Structures of some cyanine dyes.

The chirality of supramolecular systems can be produced through direct synthetic modifications, and/or by asymmetric induction via self-assembly, axial ligation, or aggregation processes. Of these, aggregation processes have a

greater possibility for control of chirality induction.[7]

The monomeric units of the chromophores can be arranged in different ways in an aggregate structure due to π-stacking, which may or may not be ordered. These aggregates, if ordered, can form highly organized structures classified according to the orientation of the induced transition dipole of their constituent monomers.[23,24] The most studied aggregate system is that of the cyanine dyes, (Figure 2-5) that were first synthesized over a century ago.[25,26]

Cyanine dyes are characterized by two heterocyclic components joined by a polymethine chain that has an odd number of carbons. Cyanine dyes and their aggregates are one of the most important photofunctional materials used in photography,[27-31] information storage,[32] (CDs and DVD's) and nonlinear optical devices.[22]

Cyanine dyes are known to aggregate into J- and H-aggregates, in which the molecular arrangement is highly ordered.[25,26] The J-aggregate is one of the most important dye assemblies for photographic spectral

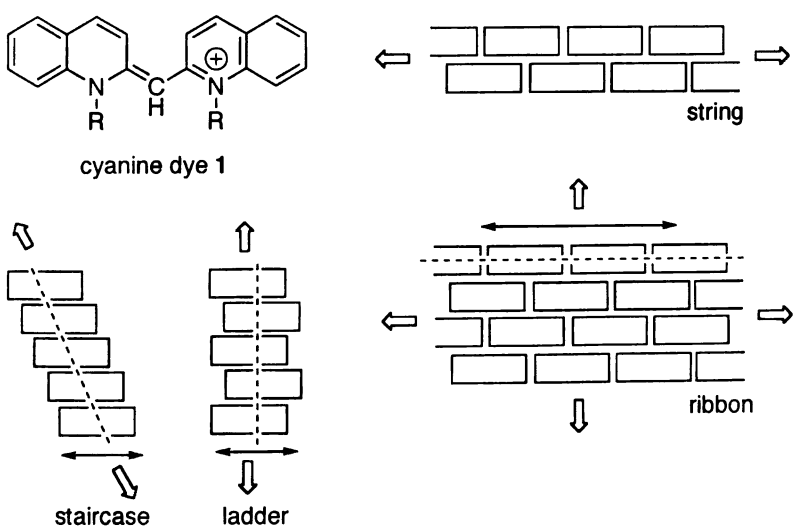

Figure 2-6. Arrangements proposed for J-aggregates of cyanine dye 1. ⟷: transition dipole moment, - - -: line connecting monomer centres and ⇨: direction of growth of aggregate.

sensitization.[27-31] The first independent observation of J-aggregates was in 1,1'-diethyl-2-2'cyanine chloride by Jelly[25] and Scheibe[26] in 1936. In these structures, the molecules are arranged in the "head–to-tail" manner such that the transition dipole moments of the monomers comprising the aggregate are parallel to the line connecting their centers. In the ideal case, the angle between the molecular centers is zero.[33]

There are several arrangements that have been proposed for J-aggregates, some of which are shown in Figure 2-6. From these models, the brickstone model (string and ribbon) is the most widely accepted model, because, as discussed above, the transition moment must be parallel to the long axis of the chromophore. The staircase and ladder models are not in agreement with this requirement since their transition moments are perpendicular to the lines connecting the centers of their monomers.

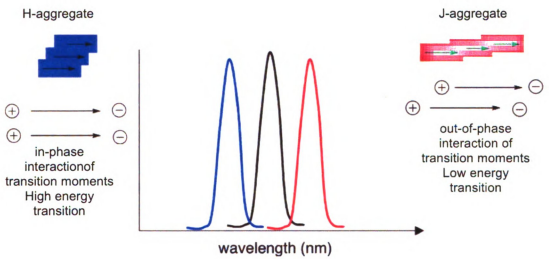

Figure 2-7. One dimensional aggregate structures. Sandwich structures (left) give a blue shifted H-aggregate whereas brickwork structures (right) are characterized by a red shift J-aggregate of the Soret band.

In the recent past, porphyrins have been shown to be well suited for studying the process of supramolecular chirality induction.[10,24,34-40] Porphyrins have an ease of self-assembly due to the facile π-π interactions, allowing for the formation of different types of dimeric and multi-molecular assemblies. They also have well-resolved and red-shifted intense Soret bands in the spectral region where most chiral molecules to be studied do not absorb.

The J-aggregate of porphyrins is characterized by an intense narrow absorption band (red curve) that is red shifted relative to the Soret band (black curve) of the monomer (Figure 2-7). This spectroscopic property is explained by the interaction between the transition dipole moments of the monomers arranged in the "head-to-tail" manner.[24,35,39]

On the other hand, H-aggregates are structures arranged in one dimension, in such a way that the transition dipole moments of the monomers are perpendicular to the line connecting their centers[24,35,39] (a "face-to-face" arrangement) resulting in a characteristic blue shift in the UV/vis (Figure 2-7).

There are many examples of aggregation of porphyrins in the literature, some of which study the self-aggregation of various neutral,[40] cationic,[35] or anionic[41] porphyrins in aqueous or organic solvents. Others have

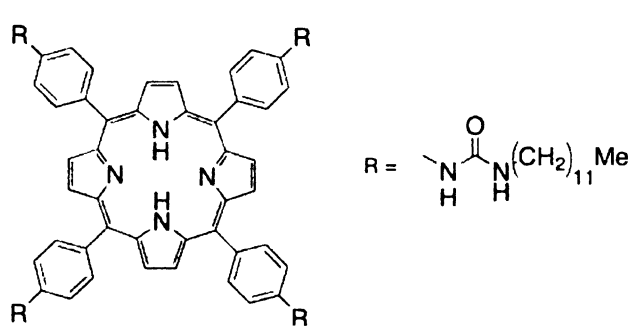

Figure 2-8. porphyrin with four urea groups at its periphery

studied the factors influencing these aggregations, be it π-π stacking, solvent effects, covalent or non-covalent interactions and temperature.[42-45] Of note however, are those that have formed porphyrin aggregates to study memory of chirality.

Small chiral molecules and biopolymers are often the choice for templates for induction of chirality. Shun-ichi et al. make use of four chiral urea derivatives on the periphery of the porphyrin, which cause the porphyrins to form fibrous aggregates by inducing a chiral twist (Figure 2-7).[38]

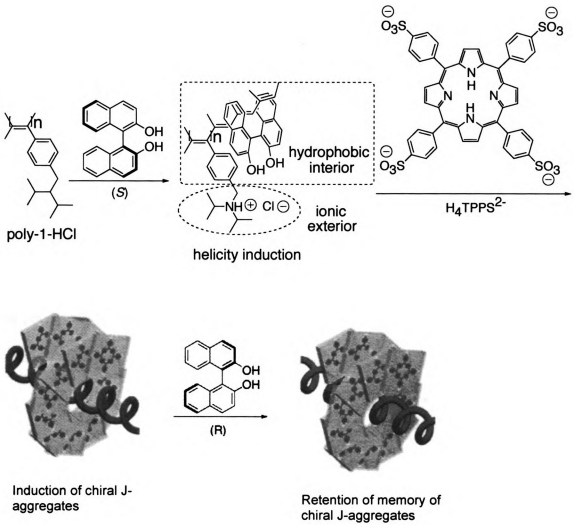

Figure 2-9. Induction of helicity in poly-1-HCl upon complexation with (*S*-BINOL) induces formation of chiral J-aggregates, and retention of memory after inversion of helicity of the poly-1-HCl by addition of excess (*R*)-BINOL.

Onouchi et al. demonstrated that a charged poly(phenylacetylene) could trap hydrophobic chiral guests (in its helical cavity), in water, which will then induce helicity within the poly(phenylacetylene), and this could then serve as a template for induction of supramolecular chirality in achiral porphyrins forming optically active *J*-aggregates.[37] Once the *J*-aggregates are formed, they are able to maintain the induced chirality without

further assistance from the template. By inversion of the helicity of the poly-**1**-HCl, it is expected that the helicity of the aggregate would be affected and change from J- to H-aggregate. (Inversion of the helicity of the poly-**1**-HCl is done by addition of excess (*R*) BINOL to the formed J-aggregates). However, retention of helicity of the J-agregate is observed (Figure 2-9). If there was no retention of chirality, the helicity of the aggregate should have changed from J- to H-aggregate. This suggests that the porphyrin assembly is able to retain the initial memory of chirality even after inversion of helicity of the poly-1-HCl.

Most recently, Monti et al. made use of electrostatic-templated heteroaggregation of porphyrin derivatives shown in Figure 2-10. In their system, they derivatize a chiral cationic functionality and a chiral anionic functionality into the porphyrins.[36] In this case, they use (L)-prolininium moieties which help steer the self-aggregation process towards the formation of large porphyrin aggregates with high supramolecular chirality.

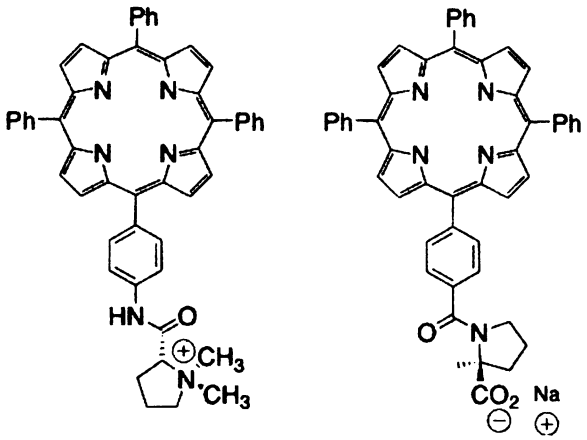

Figure 2-10. porphyrins with a) chiral cationic b) chiral anionic prolininium functionalities.

They co-aggregate the two porphyrins forming a template due to electrostatic forces between the positive and negative charges, giving rise to a negative ECCD spectrum. In this work, they have

the chirality incorporated into the porphyrin, which limits the scope of chiral molecules that can be used with the system.

As seen in Chapter One, the coordination of a chiral diamine to the bis-porphyrin system induces an asymmetric environment into the complex resulting in a helical arrangement of the chromophores. We envisioned that a similar approach might be taken for the formation of chiral aggregates in non-aqueous media. This would exclude the use of charged species, due to their poor solubility in organic solvents. Lack of charged species however, may affect the geometry of the porphyrin interaction, especially if electrostatic interactions between cationic and anionic porphyrins (as in the case of Monti et al.[36]) leads to the formation of the aggregate with specific geometry (mostly J-aggregates). Because spontaneous self-assembly triggered by π-stacking leads to the formation of a mixture of both H- and J-aggregates, by incorporating a coordination site (Zn metal) within the porphyrin, upon coordination of a guest molecule, this mixture of aggregates can then be transformed into a single superstructure, either H or J by induction of chirality. We also believe, as shown by Monti and co-workers, that the asymmetry of the bound guest can affect the handedness of the formed assembly and generate an optically active aggregate (Figure 2-10), the helicity of which can be identified through Exciton Coupled Circular Dichroism (ECCD). Detection of exciton coupling brings up the issue that must be considered for the ECCD method, that is a relative orientation of the transition moment of porphyrins in the assembly. Appearance of ECCD signal and correlation of its sign with the helicity of the aggregate is based on the relative orientation of the electric transition moments of porphyrins,[46] and thus depends on the existence of such transition. Defined orientation of electric transition moment (C_{15}-C_5 direction) can

be achieved by breaking the symmetry of the porphyrin through introduction of an electron withdrawing carboxylate group onto the *meso*-position of the porphyrin (Figure 2-10). The large electric transition moment in this porphyrin is oriented approximately collinearly with the long axis of the porphyrin ester and almost parallel to the direction of the C-O ester bond.

Another aspect to consider is that, unlike porphyrin tweezer complexes that have only two porphyrin molecules, porphyrin aggregates are able to incorporate an infinite number of molecules of the guest molecule. In this case, each of the complexes formed within the aggregate can give rise to a CD bisignate curve, and the overall spectrum should be interpreted as a summation of the signals of all chiral complexes.[47] The goal of this project is the formation of chiral porphyrin aggregates through an induction of chirality by chiral monoamines in non-chiral porphyrin assemblies. The ECCD method will be used to determine the absolute stereochemistry of the formed aggregates. In order to form the chiral ECCD active assemblies, the following conditions have to be met:

a) The porphyrin aggregate should be formed. This can be achieved by increasing the porphyrin concentration in the solution.

b) The two interacting porphyrins have to come close together so as to experience exciton coupling. This can be achieved with both the formation of the aggregate, and by the metal-substrate binding interaction.

c) There should be a fixed direction of the permanent dipole moment within the porphyrins. This can be controlled by the introduction of a group with different electronic properties at the meso-position of the porphyrin ring.

d) The alignment of the porphyrins in the aggregate has to be controlled, i.e. the permanent dipole moments of the porphyrins in the assembly have to be oriented in the same direction.

Conditions c) and d) can be achieved by the introduction of a hydrophilic tail that should enable intermolecular hydrophilic interaction with a similar part of the neighboring porphyrin rings (Figure 2-11a). Consequently, while spontaneous aggregation of hydrophobic porphyrin rings triggers the formation of a mixture of H- and J-type assemblies, hydrophilic interaction between oxygenated tails might stabilize the relative orientation of electric transition moments in the assemblies. A controlled orientation of the transition moments will also be helpful for the interpretation of the sign observed upon chiral induction.

For these reasons, the TPP porphyrin mono-tail shown in figure 2-11b, was proposed as the first system for investigation.

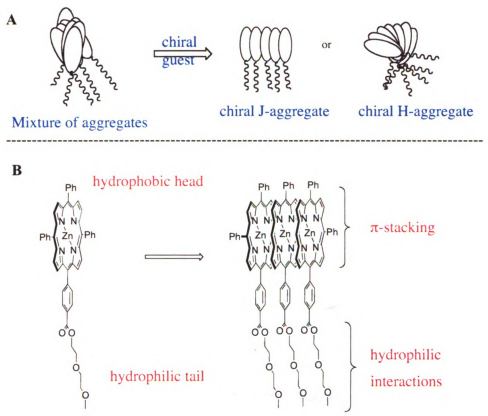

Figure 2-11: A) Triggered by π-stacking, aggregation of porphyrins results in formation of a mixture of H- and J-assemblies. B) Controlled by hydrophobic/hydrophilic interactions aggregation of porphyrins leads to fixed relative orientation of transition moment in the assembly and makes possible detection of chirality by ECCD and identification of relative orientations of porphyrins in the assembly.

Results and Discussion

ZnTPP mono-tail porphyrin shown in Figure 2-11b was synthesized[48] and used for initial aggregation studies. For the UV/vis studies, 1 mM porphyrin solution is added in 1 μL portions into a 1mm UV cell containing the solvent of choice (0.2 mL) and the UV spectrum obtained. This titration is repeated until the porphyrin starts to aggregate at 40 μM concentration (Figure 2-12, yellow curve). Increasing the concentration to 50 μM

concentration leads to splitting of the Soret band mixture into two geometrically different assemblies, the H- and J-aggregates.

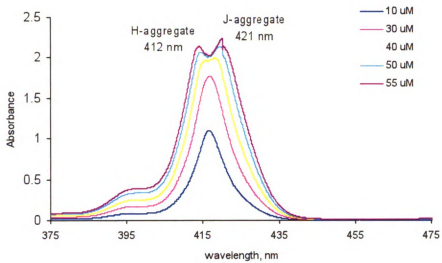

Figure 2-12: Aggregation of Zn-TPP-tail porphyrin in hexane starts at $3x10^{-5}$ M (broadening of the Soret band). Further increase of porphyrin concentration (40 μM and higher) results in a split of the Soret band.

Formation of a complex between the chiral amine and the aggregate system can be monitored by UV-vis spectroscopy. Taking (*S*)-1,2-diaminopropane, complexation studies were first performed in hexane. However, upon addition of the diamine to the porphyrin aggregate leads to formation of a precipitate.

Performing the same UV-vis titration studies in methylcyclohexane preceeds without precipitation and gives the porphyrin aggregate complexed with (*S*)-1,2-diaminopropane with absorption at 423 nm (Figure 2-13). CD studies were therefore done with 50 μM ZnTPP-tail solution in methylcyclohexane. Upon addition of (*S*)-1,2-

diaminopropane to the porphyrin aggregate, chiral induction is observed at porphyrin/substrate ration 1:0.2 as a positive ECCD curve (Figure 2-14).

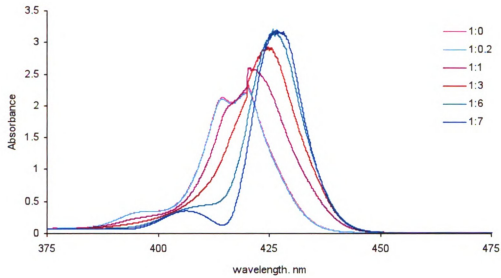

Figure 2-13. Addition of (*S*)-1,2-diaminopropane to the porphyrin aggregate in methylcyclohexane yields the formation of a single assembly (UV-vis spectra).

The UV/vis spectra of the (*S*)-1,2-diaminopropane complexes shows a red shift of both the H- and J-bands (414 nm and 420 nm respectively) to a single transition at 423 nm, which could indicate the formation of a new assembly (Figure 2-13).

Both L-ornithine methyl amide and L-lysine methyl ester cause a similar transformation of the J- and H-species into a single assembly absorbing at 423 nm when subjected to UV-vis spectroscopy. They also both induce negative helicity (Figure 2-15) of the porphyrin aggregate in CD spectroscopy, consistent with results obtained with zincated bis-tetraphenyl porphyrin tweezer (ZnTPP-tz).[49]

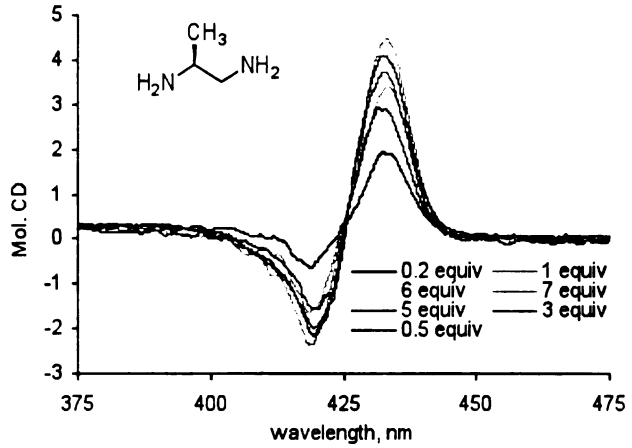

Figure 2-14. Induction of helicity into the porphyrin aggregate (50 μM) with (*S*)-2-diaminopropane yields a positive ECCD spectrum

Increase of diamine concentration leads to the gradual enhancement of ECCD amplitude that leveled off after addition of more than 5 equiv of diamine, probably due to saturation of the coordination sites of zinc.

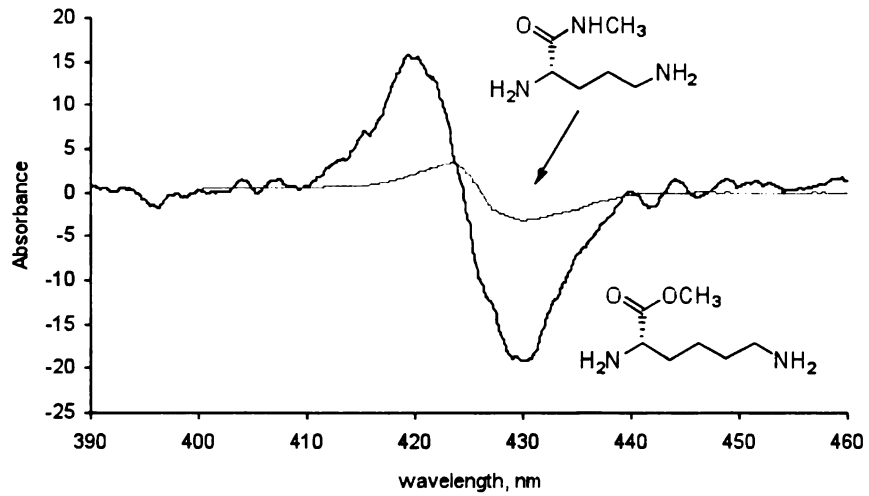

Figure 2-15. ECCD of ZnTPP-tail with: Magenta - L-Ornithine methyl amide; Blue - L-Lysine methyl ester at aggregate/substrate ratio 1:0.1.

This consistency in ECCD sign for both the aggregate system and the zincated bis-tetraphenyl porphyrin tweezer method suggests that the complexation in both systems occurs through an identical binding mode and similar ECCD active conformation of the substrate in the formed complex. In every case, the helicity of the chiral assembly can be retionalized on the basis of steric interaction taking place between the porphyrin and the two substituents at the asymmetric centre of the chiral substrate.[49] Reducing this steric strain in the complex with (*S*)-1,2-diaminopropane leads to a clockwise relative orientation of the porphyrins, and results in a positive ECCD signal. Similarly, the negative ECCD observed with L-ornithine methyl amide and L-lysine methyl ester is due to the counterclockwise orientation of the porphyrins induced by steric interaction between the porphyrin and the carbonyl group.[1]

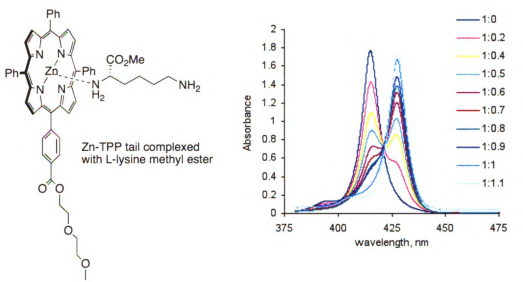

Figure 2-16. Complexation of porphyrin–tail monomer with L-lysine-methyl ester results in 12 nm red shift upon formation of 1:1 complex.

The next step was to look into the type of porphyrin aggregate being formed (H- or J-aggregate). Experiments to grow crystals of the complex for X-ray crystallography were unsuccessful, probably because of the flexibility of the oligomeric tail. However, it is possible to analyze the change in the absorption of monomeric complexes upon aggregation because, the absorption of the porphyrin-amine complex should be altered if porphyrin aggregates are formed. Formation of aggregate can either contribute positively to a shift of the Soret band of the complex (J-type) or negatively, i.e. induce a blue shift of the Soret band of the aggregate upon H-aggregation.

It is well known that coordination of an amine with a metalloporphyrin induces a red shift in the Soret band.[49] In addition, complexation of bis-porphyrin tweezer with diamines results in the formation of a 1:1 complex at equimolar ratio of diamine to porphyrin tweezer. For example, complexation of ZnTPP to a monoamine results in a 12 nm bathochromic shift of λ_{max}, indicating the formation of a 1:1 porphyrin:amine complex.

Addition of L-lysine methyl ester to the monomeric Zn-TPP tail (at 5 μM, no aggregate) leads to the formtion of new complexed species that absorbs at 427 nm, a 12 nm shift from the Soret band of the free porphyrin. This shift corresponds to the formation of a 1:1 porphyrin-amine complex (Figure 2-16).

Complexation of ZnTPP-tail aggregate with 0.1 equivalents of L-lysine methyl ester in methylcyclohexane gives rise to a single new transition at 421 nm and the disappearance of the blue shifted absorption absorption of the H-aggregate at 412 nm. The overall 9 nm shift of the H-transition is in agreement with formation of monomeric

porphyrin-diamine 2:1 complex reported for the bis-porphyrin systems.[1] Moreover, presence of a single band refers to equilibration of both H- and J-aggregates in one chiral superstructure that is blue shifted with respect to the monomeric complex. Since the formation of H-aggregates is accompanied by a blue shift in the Soret band, we can identify the geometry of the formed chiral aggregate as face-to-face H-aggregate. (Figure 2-17)

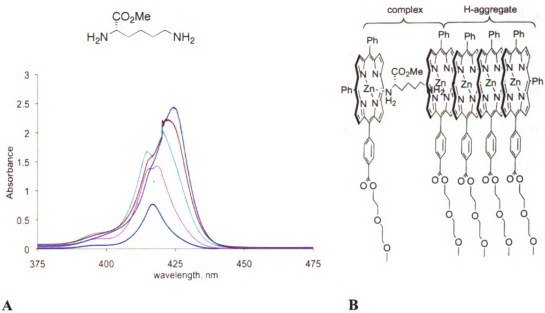

Figure 2-17. Complexation of the ZnTPP-tail aggregates (H- and J-) with L-lysine methyl ester in methylcyclohexane results in the equilibration of a single UV-vis transition A) Teal – porphyrin aggregate, Brown – aggregate with 0.2 equiv of diamine (421 nm); Blue – aggregate with 1 equiv of diamine (423 nm); B) Pictorial representation of the H-aggregate-diamine complex formed in solution.

However, when the Zn-TPP porphyrin system was applied to the study of monoamines, they were ECCD silent. This could be due to the porphyrin aggregate falling apart upon the amine binding to the metal and in the process, disrupting the π-π-

stacking interaction, and the hydrophilic interaction not being strong enough to keep the aggregate. In the case of diamines, the second amine can still coordinate to the zinc of the second porphyrin and maintain the bisporphyrin tweezer-like system.

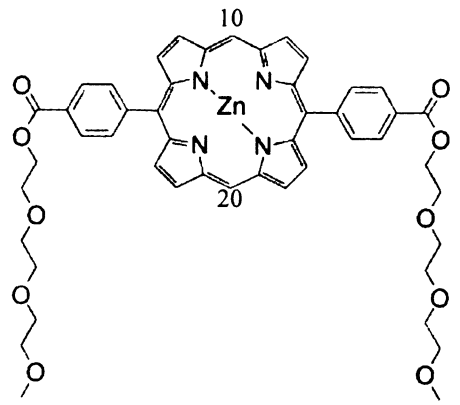

Figure 2-18. Zn-2H-bis-tail porphyrin

In order to solve this problem, bis-tail porphyrin (Figure 2-18) was proposed as a solution, where a second hydrophilic tail was introduced in order to keep the aggregate from falling apart. Absence of aromatic rings at positions 10 and 20 in the porphyrin will reduce the steric interaction between the plane of the porphyrin rings, thus strengthening the π-π stacking. The first approach to the synthesis of this porphyrin was that of acid catalyzed 2+2 condensation as shown in Scheme 2-1.

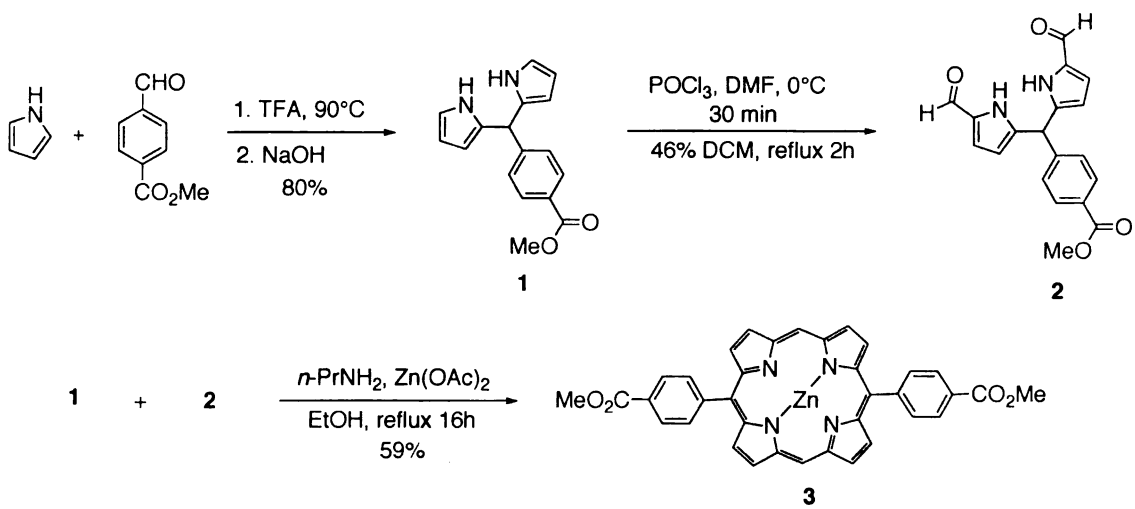

Scheme 2-1: Synthesis of porphyrin **3** via 2+2 condensation.

Condensation of terepthaldehydic acid methyl ester in neat excess pyrrole yielded dipyrromethane **1**. This was purified by column chromatography as a white solid. Vilsmeier-Haack formylation of this dipyrromethane with excess $POCl_3$/DMF in dichloromethane followed by hydrolysis with aqueous K_2CO_3 resulted in the diformyldipyrromethane **2** in 46% yield. A [2+2] condensation of **1** and **2** with propyl amine, in the presence of zinc acetate yielded dimethylester-porphyrin **3**, which was isolated using column chromatograhy as a purple solid in 59% yield. This was then hydrolyzed to the di-carboxylic acid under basic conditions. After the reaction mixture was refluxed overnight in NaOH solution, it was acidified with 6N hydrochloric acid and extracted with methylene chloride. Unfortunately at this stage, the di-acid was extremely soluble in water and it was impossible to extract it from the aqueous phase.

In order to circumvent this issue, we decided to put on the oxygenated tail first to avoid the hydrolysis step. This was done as described below.

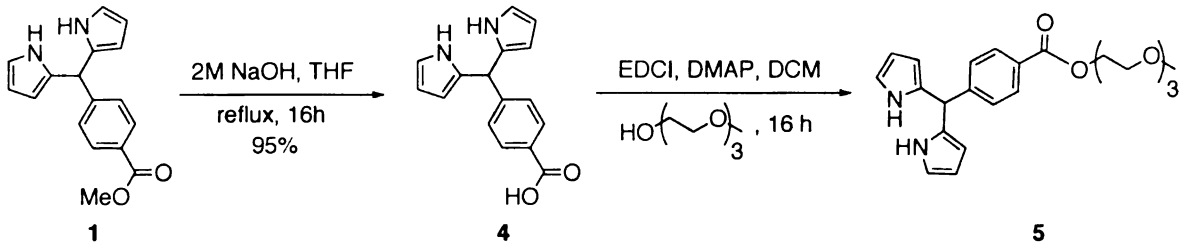

1 **4** **5**

Scheme 2-2. Synthesis of dipyrromethane ester **5**

Dipyrromethane **1** was hydrolyzed to carboxylic acid **4** under basic conditions. After the reaction mixture was refluxed overnight, it was acidified with 6N hydrochloric acid and extracted with methylene chloride as a brown oil. The oxygenated tail was then

introduced by EDCI coupling of the carboxylic acid with triethylene glycol to give the triethylene glycol dipyrromethane ester **5**.

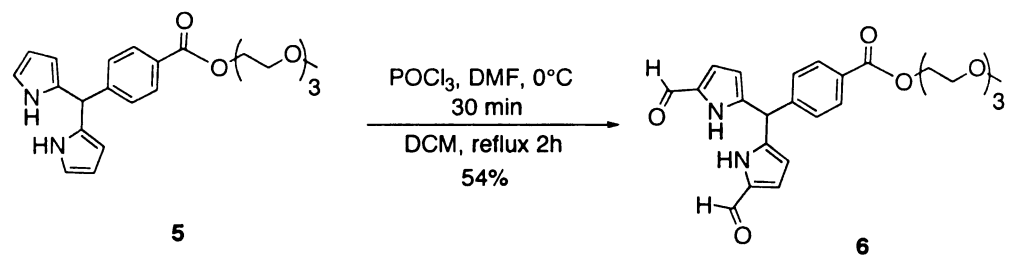

5 **6**

Scheme 2-3. Vilesemeier –Hack formylation of dipyrromethane **5** to diformyldipyrromethane ester **6**

Vilsmeier-Haack reaction with excess $POCl_3$/DMF was then employed to introduce the di-aldehydes, forming the diformyldipyrromethane ester **6**. This was then coupled with **5** in a 2+2 coupling reaction to give the bis-tail porphyrin **7**.

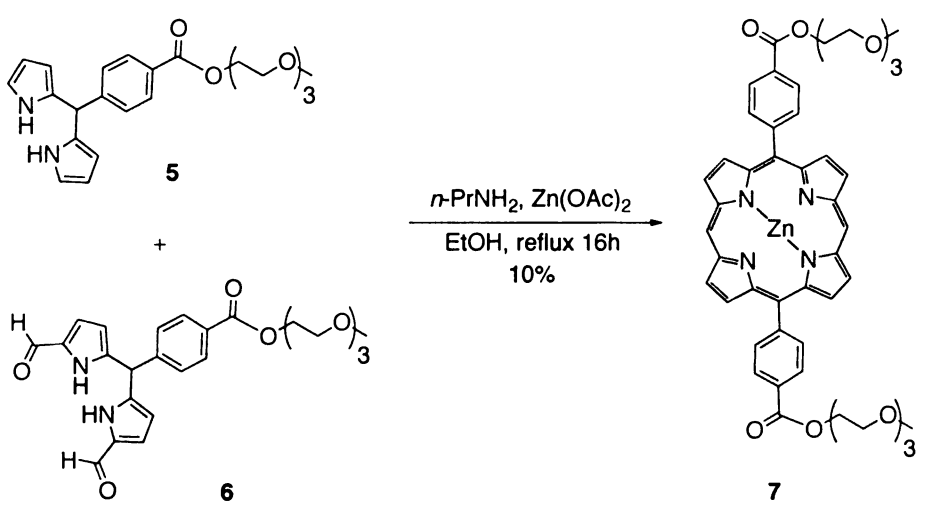

5 + **6** **7**

Scheme 2-4. 2+2 condensation of **5** and **6** to give bis-tail porphyrin **7**.

Porphyrin **7** was isolated from a mixture of several side products as a purple solid using column chromatography, and was used for UV/Vis and CD studies.

UV/Vis and CD studies

We first carried out a solvent study to identify the best solvent suitable for aggregation of the porphyrin. Titration of the porphyrin was done at room temperature using various HPLC grade solvents (CH_2Cl_2, hexanes, methylcyclohexane), in a 1 mm UV cell. At lower temperatures, the porphyrin precipitates out of solution. For detection of the aggregation process, 1 mM porphyrin solution is added in 1 μL portions into a 1 mm UV cell containg the solvent of choice. After addition of the first portion (C = 5 x 10^{-6} M), the λ_{max} of the Soret band of the monomeric porphyrin is measured as follows: dichloromethane: λ_{max} = 408 nm, methylcyclohexane λ_{max} = 408 nm, hexane: λ_{max} = 408 nm. Addition of the porphyrin is continued until aggregation is observed.

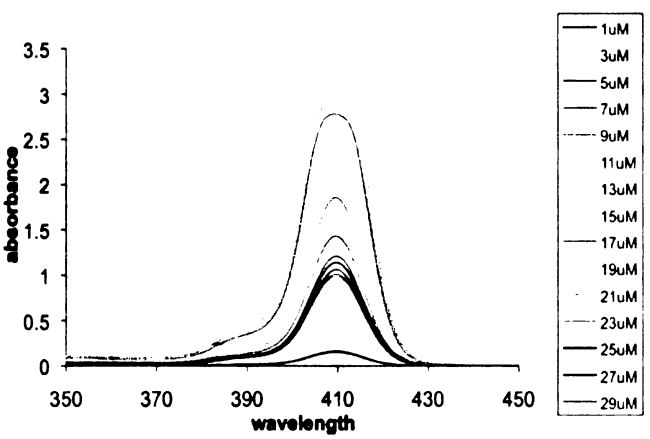

Figure 2-19. UV/Vis of porphyrin **7** in dichloromethane at room temperature. Aggregation of porphyrin starts at 25 μM (dark blue curve).

Dichloromethane was found to be the best solvent for the aggregation of the porphyrin (Figure 2-19). It is a well-documented fact[50,34,51] that aggregation of porphyrins is typically accompanied by the splitting, hypochromicity, and broadening of the soret band. As can be seen from the UV titration curve (Figure 2-19), the porpyrin begins to aggregate at around 27 μM concentration, to form a mixture of both H- and J- aggregates

(lack of a significant blue or red shift in the soret band). Increasing the concentration leads to a split in the Soret band (Figure 2-22, yellow curve).

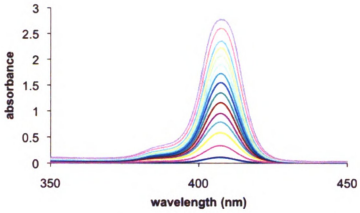

Figure 2-20. UV/Vis of porphyrin **7** in hexane. Titration from 1 μM (blue curve) until 65 μM (pink curve). Increasing the concentration beyond 65 μM does not result in aggregation.

In the case of hexane, aggregation is not observed even at high porphyrin concentration (Figure 2-20). Methylcylohexane behaves in a similar manner to hexane, failing to promote aggregation.

After identifying the concentration at which aggregation is achieved, the next thing to do was a binding study of amines. We first studies chiral diamines in order to investigate their behaviour with the aggregate system.

For the UV-vis studies, a 30 μM porphyrin solution in dichloromethane is added into a 1 mM UV cell. Upon addition of the first two equivalents of (1*R*, 2*R*)-cyclohexyldiamine, both the H- and J-aggregates get transformed into one assembly with transition at 417 nm (Figure 2-21).

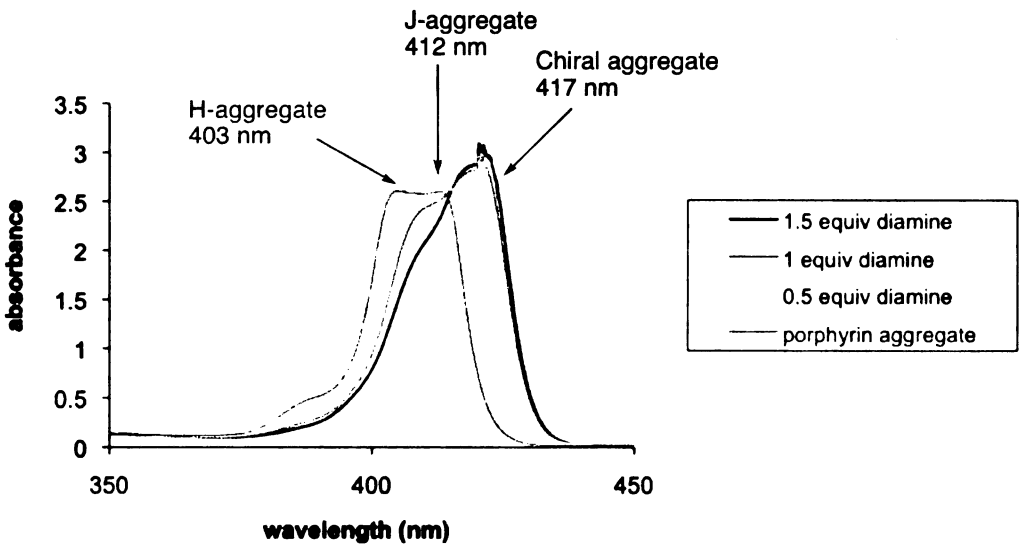

Figure 21. UV-vis titration of porphyrin aggregate **7** (light blue curve) with (1*R*, 2*R*)-cyclohexyldiamine. Addition of 1 equiv of amine in dichloromethane results in formation of red-shifted complex with absorption at 420 nm (30 μM, pink curve).

ECCD studies were therefore done with 30 μM ZnTPP-bis tail solution in dichloromethane. Upon addition of (1*R*, 2*R*)-cyclohexyldiamine to the preformed aggregate of porphyrin **7**, chiral induction is observed at porphyrin/substrate ratio 1:0.5 as a negativECCD curve (Figure 2-22).

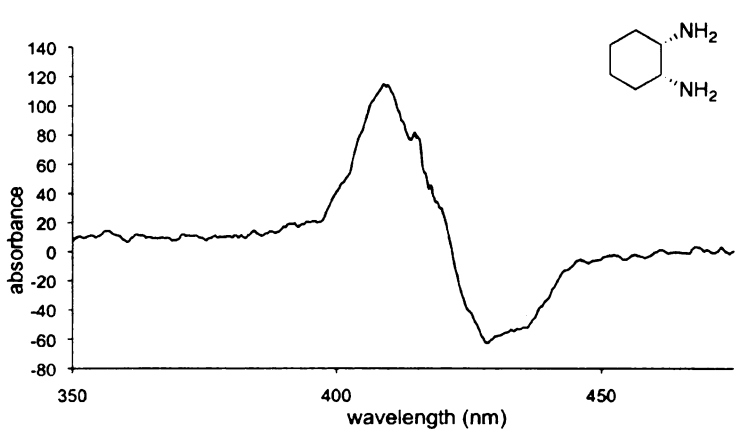

Figure 2-22. ECCD of ZnTPP-bistail with (1R,2R)-cyclohexyldiamine at aggregate/substrate ratio 1:0.5

Both L-Lysine methyl ester and (*R*)-2-diaminopropane cause a similar transformation of the J- and H-species into a single assembly absorbing at 419 nm when subjected to UV-vis spectroscopy. They also induce a negative helicity of the porphyrin aggregate in CD spectroscopy.

Binding studies for chiral monoamines was done by titrating (*S*)-1-cyclohexylpropan-1-amine (Figure 2-23) as well as (*S*)-Methyl-benzylamine (Figure 2-24), against the aggregate (29 μM). Both amines are able to bind to the aggregate system, inducing a red shift in the Soret band.

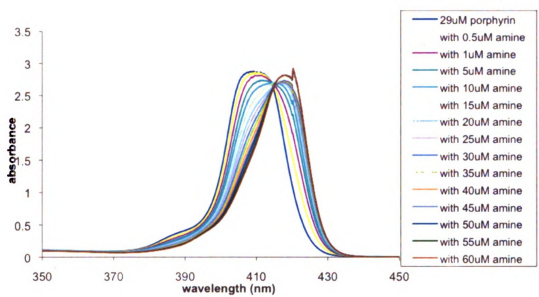

Figure 2-23. UV-vis titration of porphyrin aggregate **7** with (S)-cyclohexylpropane-1-amine in dichloromethane. Addition of amine to the aggregate results in formation of red-shifted complex.

It is clear from Figure 2-24 that upon addition of amine, both H- and J-aggregates get transformed into one assembly with transition at 417 nm This could indicate the formation of a new assembly.

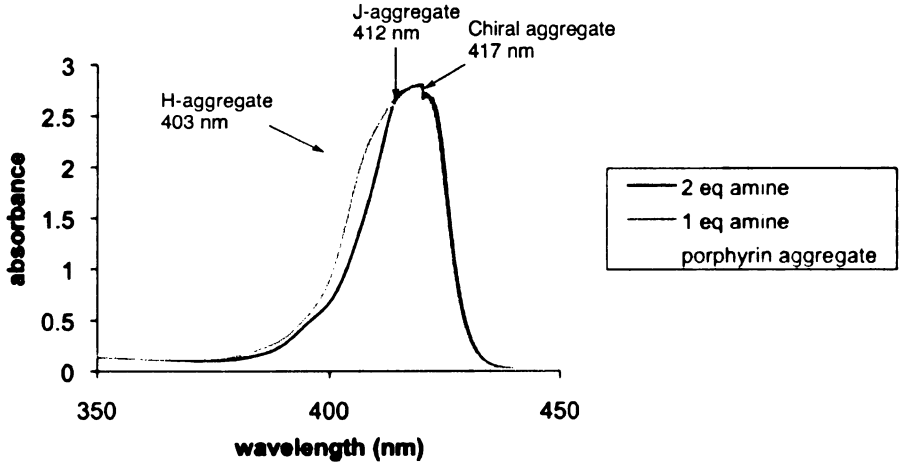

Figure 2-24. UV-vis titration of porphyrin aggregate **7** (yellow curve) with (S)-Methyl-benzylamine. Addition of 1 equiv of amine in dichloromethane results in formation of red-shifted complex with absorption at 419 nm (30 μM, pink curve).

Table 2-1. ECCD study of chiral monoamines with porphyrin **7**

entry	amine	amplitude
1	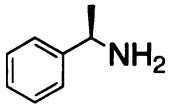	+5
2	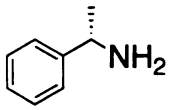	-6
3	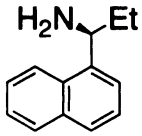	-50
4	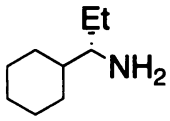	-5
5	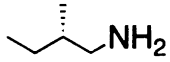	-3
6	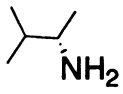	-4

Data obtained in dichloromethane at 29 μM porphyrin concentration, at 25°C. Data reported for porphyrin:substrate ratio 1:2

Table 2-1 shows the ECCD results obtained with a number of monoamines. This was done at room temperature, for reasons discussed above, using dichloromethane at 29 μM porphyrin concentration. The titration of the amines was done starting at 1:1 equivalent of porphyrin to amine, and increasing the concentration of amine, until the concentration where the aggregate was disassembled, as evident by UV-vis spectroscopy.

The monoamines follow a trend where (*S*) enantiomers result in a negative ECCD. However, it is noteworthy that all of the ECCD signals obtained are not the typical smooth ECCD bisignate curves as shown in a representative spectrum for (S)-1-amino-2-ethylnaphthalene. (Figure 2-25)

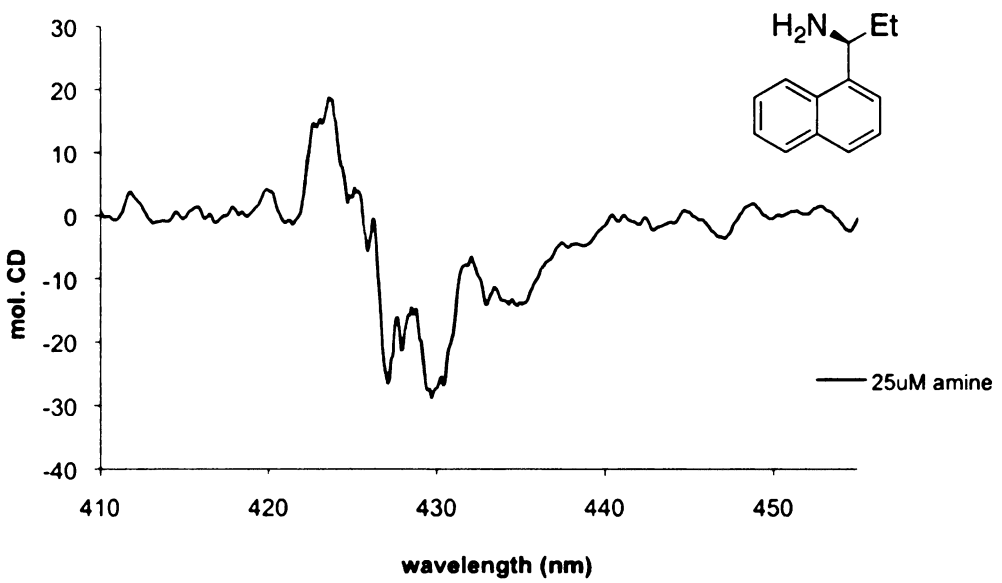

Figure 2-25. ECCD spectrum of (S)-1-amino-2-ethylnaphthalene with porphyrin **7**. Negative signal is obtained at porphyrin:substrate ratio of 1:1.

This could be due to the different possible conformations in solution upon binding of the amines due to the free rotation about the coordination Zn-N (N of bound amine) bond (Figure 2-26).

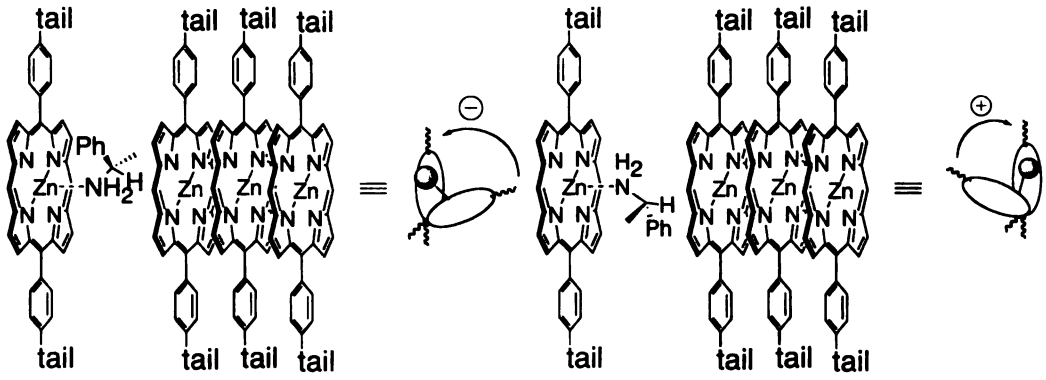

Figure 2-26. Possible different conformations upon binding of the amines to the porphyrins. **A)** sliding of the aggregate towards the smaller group (H), results in a negative ECCD signal. **B)** sliding of the aggregate towards the largd group (phenyl) results in a clockwise orientation of the dipole moments, resulting in a positive ECCD signal.

For ECCD to be observed in the porphyrin tweezer method, steric interaction takes place between the porphyrin facing the chiral carbon and the two substituents at the asymmetric centre. In order to alleviate this strain the porphyrin slides away from the larger substituent towards the smaller substituent. The helical twist thus induced leads to ECCD signal.

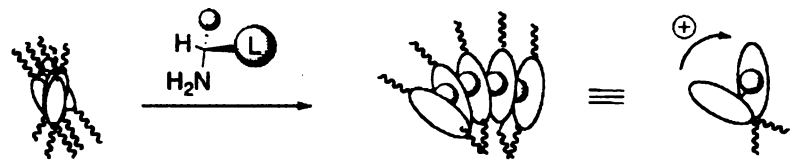

Figure 2-27. Induction of chiral twist by R enantiomer inducing a clockwise chiral twist

For example, in order to obtain the positive ECCD spectra for the (*R*)-enantiomers, once the amine binds to one of the porphyrins, the neighbouring porphyrin will twist away from the large group towards the small group inducing a chiral twist (Figure 2-27) resulting in the observed positive ECCD spectrum.

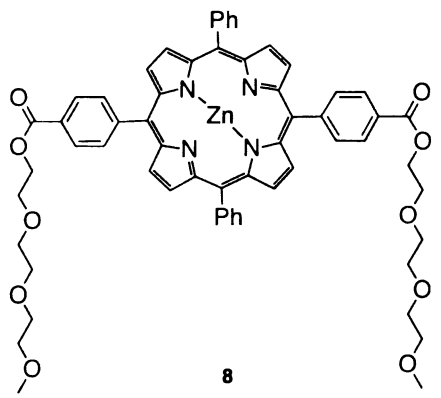

8

Figure 2-28. ZnTPP-bis tail porphyrin

In an attempt to further investigate this, porphyrin **8** was proposed as the next chromophoric host for aggregation studies. Here, phenyl groups are introduced at positions 10 and 20 of the porphyrin that could serve to increase steric differentiation, but even more important, because of increased π-π interactions between the introduced phenyl rings, this could lead to increased ability of the porphyrin to aggregate, which could help stabilize one conformation over the other, hence improve the quality of the ECCD signals obtained.

The condensation of an aldehyde with a dipyrromethane that has a sterically unhindered aryl substituent at the 5-position usually results in very low yield and a mixture of porphyrin products as a result of scrambling. Rao et al. published a procedure for the efficient synthesis of monoacyl dipyrromethanes and used them to prepare sterically unhindered *trans*-porphyrins (Scheme 2-5).[52] The initial approach was to use this procedure towards the synthesis of porphyrin **8**.

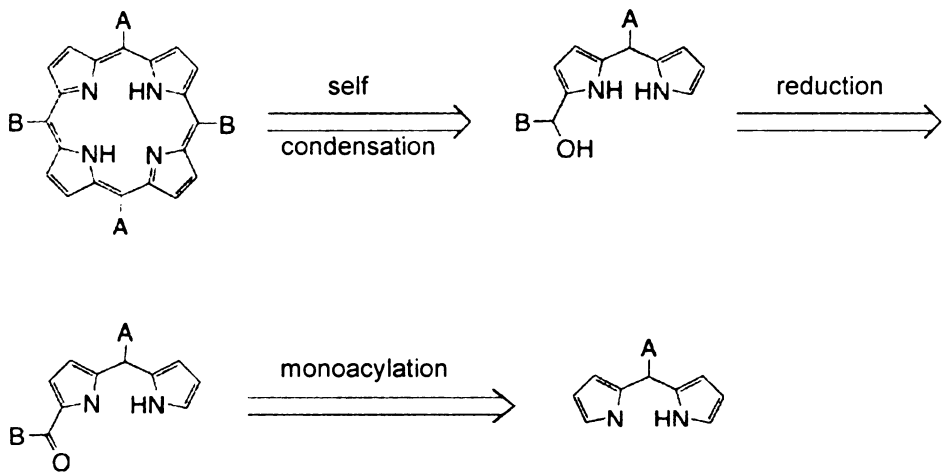

Scheme 2-5. Retro-synthesis of monoacyl dipyrromethanes

Thioester **9** was readily prepared in high yield by condensation of benzoyl chloride with 2-mercaptopyridine. Treatment of dipyrromethane **5** at 1M with 2.5 eq EtMgBr was followed by addition of thioester in THF. This resulted in a product mixture that composed primarily of monoacyl dipyrromethane **10**, and unreacted dipyrromethane **5**. The product was eluted from a silica column with CH_2Cl_2/EtOAc, 25:1, as a brown oil. The dipyrromethane was then subjected to reduction conditions using $NaBH_4$ (dashed box), in a mixture of methanol and THF. However, instead of obtaining the desired carbinol, decomposition products were obtained, and these could not be separated for characterization.

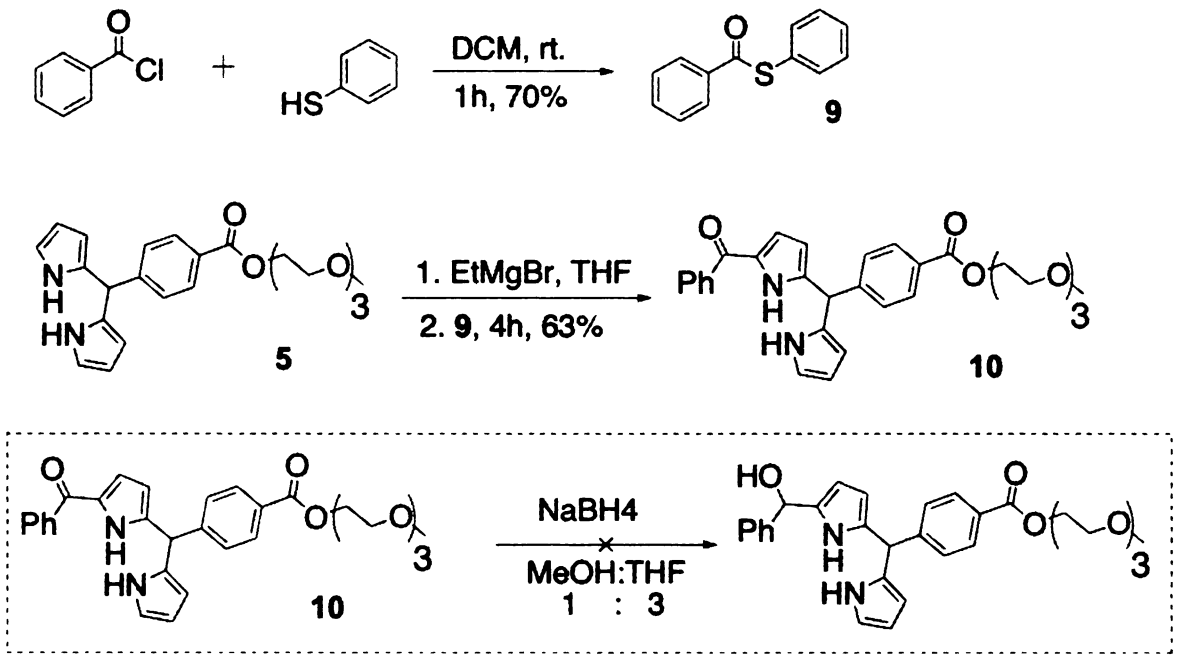

Scheme 2-6. Synthesis of monoacyl dipyrromethane **10**

As a result, this route was abandoned and instead, the condensation procedure was applied (Scheme 2-7).

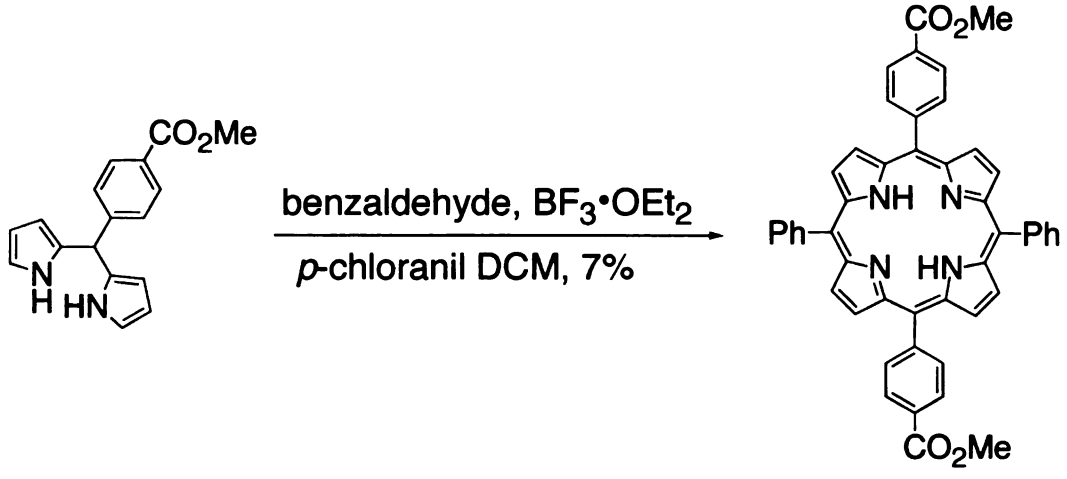

Scheme 2-7. Synthesis of bis-methyl ester porphyrin **11**

Condensation of dipyrromethane **5** and benzaldehyde was carried out in CH_2Cl_2, catalyzed by $BF_3 \bullet OEt_2$, and dimethylester porphyrin **11** was isolated using column chromatography as a purple solid (Scheme 2-7). This was then hydrolyzed to the di-acid **12** under basic conditions, which was then subjected to EDCI coupling with triethylene glycol to yield the desired bis-tail porphyrin **13** (Scheme 2-8).

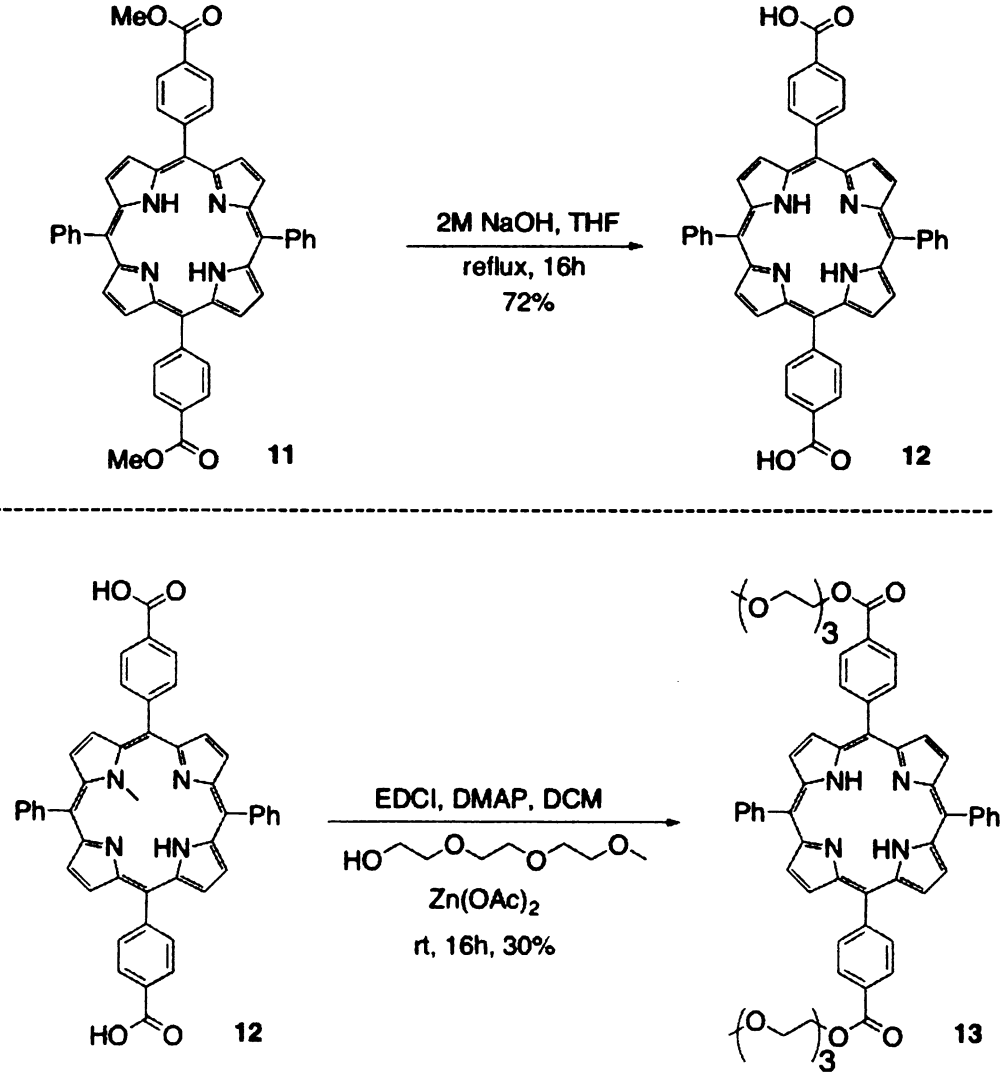

Scheme 2-8. Synthesis of bis-tail porphyrin **13**

UV/Vis and CD studies

As with porphyrin **7**, we first carried out a solvent study to identify the best solvent suitable for aggregation of the porphyrin. The titration of the porphyrin was done at room temperature in various HPLC grade solvents (CH_2Cl_2, hexane, methyl cyclohexane), in a 1 mm UV cell. At lower temperatures, the porphyrin precipitates out of solution. The best solvent for aggregation of this porphyrin was found to be hexane. As can be seen from the UV-vis titration curve, (Figure 2-29) the porphyrin is aggregated at μM concentrations, and also forms a mixture of both H- and J-aggregates with λ_{max} 425 and 432 respectively. It is worth noting that the monomeric porphyrin corresponding to non-aggregated porphyrin is not observed even at concentrations less than 3 μM. This is because of the presence of the incorporated phenyl rings, which help to improve the π-π interactions, hence improve the porphyrins' aggregation properties.

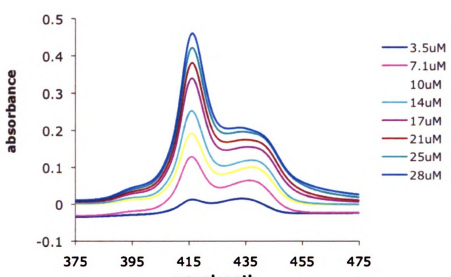

Figure 2-29. UV/Vis titration curve of porphyrin **13**

Binding studies for ECCD analysis were then carried out using (*S*)-amino-2-methyl-phenyl amine. As was the case for porphyrin **7**, the chiral amine was able to bind with the aggregate of porphyrin **13**. Having verified the binding of the amine, CD studies were then carried out in hexane, and at room temperature. The CD studies were carried out on the same substrates as those in Table 2-1. However, only one substrate (*S*-1-amino-2-ethylnaphthalene) showed an ECCD signal with amplitude, A = + 40.

The fact that this porphyrin works worse than porphyrin **7** could be attributed to the presence of the phenyl groups at positions 10 and 20. These phenyls could be increasing the π-π stacking of the porphyrin, making it aggregate much more as evidenced by the UV-vis data. Because of this, it is harder for the monoamines to disrupt this aggregation to induce helicity. It is possible that in the case of entry 3, the naphthalene is able to have π-π interactions with the porphyrin, hence compensate for the disruption of the π-π stacking. However, this compensation is still not sufficient and can be seen in the drop in amplitude.

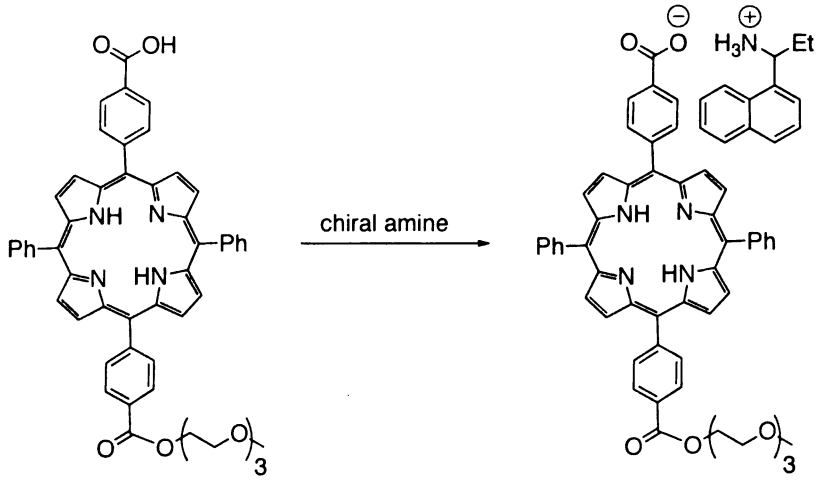

14

Scheme 2-9. Formation of chiral salt upon addition of (*S*)-1-amino-2-ethylnaphthalene to porphyrin **14**.

In order to solve these problems, we wanted to use a different approach in generating the helical aggregates.

This approach is to induce the asymmetry from a point external to the face of the porphyrin ring. With this idea in mind, porphyrin **14** was designed, where upon addition of a chiral amine should result in the formation of a chiral salt at the periphery of the aggregate, and hence, it should not interfere with the aggregate assembly (Scheme 2-9). Prediction of the ECCD spectra for this assembly is more difficult, and testing of the system with a variety of chiral amines should lead to a better understanding of the important elements in the induction of helicity within the aggregate.

The synthesis of this porphyrin started from di-carboxylic acid **12**, which was encountered during synthesis of porphyrin **13**. EDCI coupling with 1.2 equivalents of triethylene glycol resulted in formation of both the bis-tail porphyrin **13**, as well as the desired mono-tail porphyrin **14**. These were separated by column chromatography.

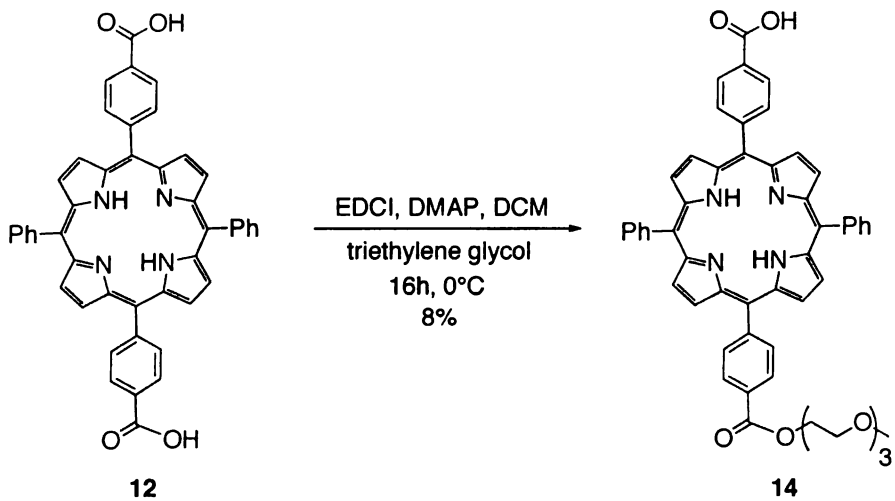

12 **14**

Scheme 2-10. Synthesis of mono-tail porphyrin **14.**

Aggregation studies were done in various HPLC grade solvents including CH_2Cl_2, hexane, ethanol, ethanol:water at various ratios, water, toluene, petroleum ether and acetonitrile. However, there was no aggregation or amine binding observed in these

solvents. As expected, no ECCD spectrum was observed with any amine when the porphyrin was subjected to CD studies (due to a lack of aggregation).

Unfortunately, it appears that when the chiral salt is formed upon addition of the amines, there is electrostatic repulsion between the charged species that would be brought close together by aggregation, as seen by the lack of aggregation detected in UV-vis. In order to avoid this scenario, we then decided to introduce a covalent bond. This would require derivatization of the amines onto the porphyrin, forming either an imine (Scheme 2-11), or an amide bond (Scheme 2-13).

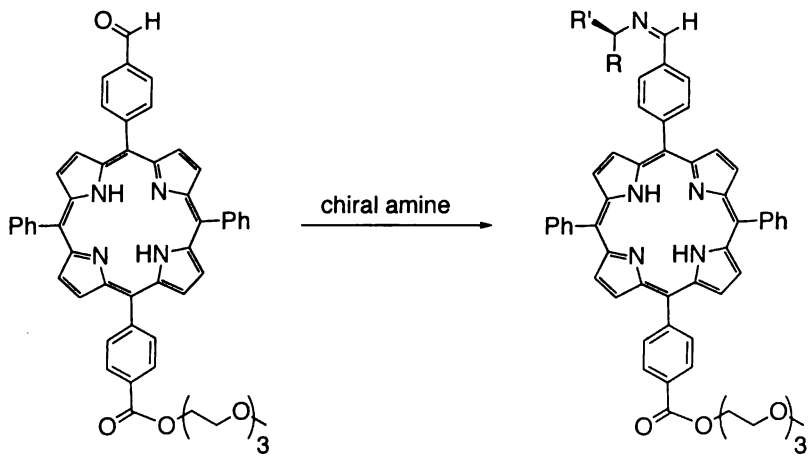

Scheme 2-11. Proposed structure of chiral amide porhyrin

Synthesis of the porphyrin for derivatization begun with the DIBAL reduction of methyl ester **1** to alcohol **15** (Scheme 2-12). This resulted in formation of the desired product as well as recovery of the starting ester. The alcohol was isolated from column chromatography as a brown oil. This was then reacted with di-aldehyde **6** to give porphyrin **16**, which was purifed using column chromatography and obtained as a purple solid. However, attempts to carry out PCC oxidation of **16**, led to a decomposition of the

starting alcohol to unidenfiable products, and without any recovery of starting material. To avoid using oxidation, we went back to a porphyrin that we had encountered before, porphyrin **14**. We decided to do an EDCI mediated coupling of this porphyrin with the amine, to form the amide. This was not the original method of choice because it requires coupling of every amide with the porphyrin, which is extra chemistry and wasteful of the porphyrin, but in order to investigate whether the system would be ECCD active, we tried it nonetheless with one chiral amine. This is shown in Scheme 2-13.

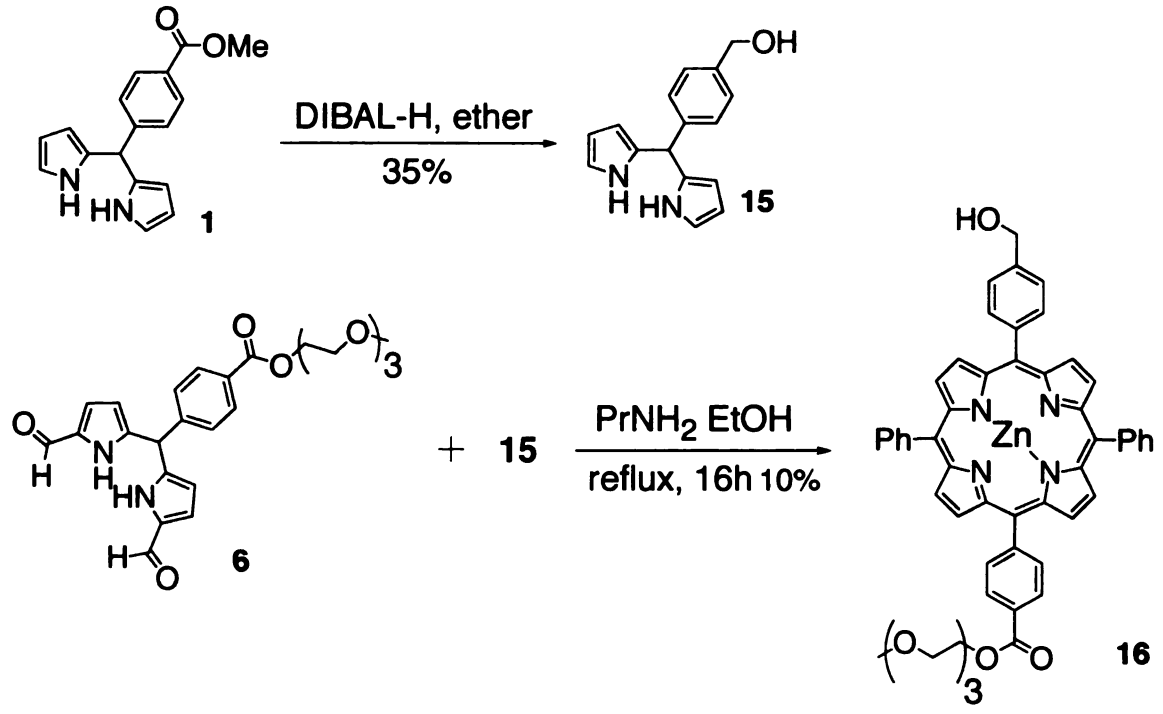

Scheme 2-12. Synthesis of porphyrin **16**.

EDCI coupling was carried out using **14**, and (*S*)-1-amino-2-methylnaphthalene, resulting in **17**, in moderate yield.

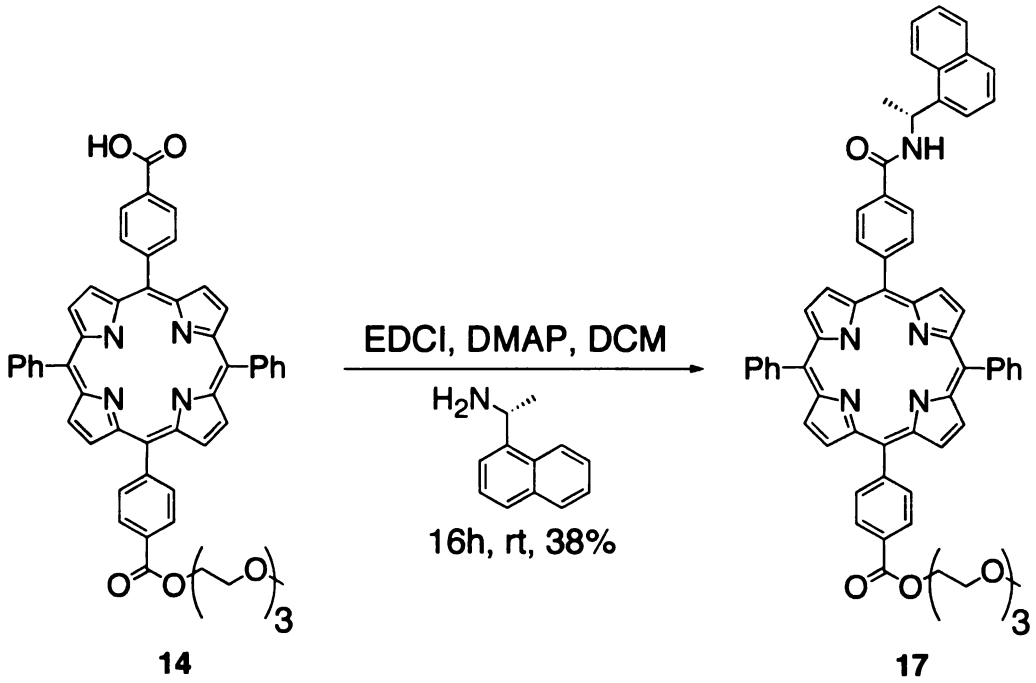

Scheme 2-13. EDCI coupling of (*S*)-1-amino-2-methylnaphthalene with porphyrin **14**.

Aggregation studies were done in various HPLC grade solvents including dicloromethane, hexane and methylcyclohexane. Unfortunately, there was no aggregation observed for this system in all the solvents, and when it was subjected to CD studies, it was also ECCD silent.

From these studies, it seems that having the chiral groups at the periphery is not aiding with the aggregation process, and might even be interfering with it. So we should revert back to binding at the zinc in the porphyrin, but with some improvements in the porphyrin design. For example, since it seems that having phenyl groups in the system seems to interfere with induction of helicity, we can design a new porphyrin without any phenyl groups like that shown in Figure 2-30. This should improve its ability for induction of chirality due to decreased π-π stacking.

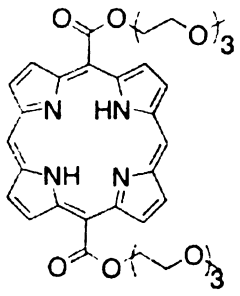

Figure 2-30. Proposed porphyrin structure for aggregation.

However, due to lack of time, efforts to use porphyrin aggregates as reporters of chirality were stopped. However, considering the interesting and promising results obtained, perhaps more time spent on this idea is worthwhile.

References

(1) Huang, X. F.; Borhan, B.; Berova, N.; Nakanishi, K. "UV-vis spectral changes in the binding of acyclic diamines with a zinc porphyrin tweezer" *Journal of the Indian Chemical Society* **1998**, *75*, 725-728.

(2) Yang, Q.; Olmsted, C.; Borham, B. "Absolute stereochemical determination of chiral carboxylic acids" *Organic Letters* **2002**, *4*, 3423-3426.

(3) Holmes, A. E.; Simpson, S. A.; Canary, J. W. "Stereodynamic coordination complexes. Dependence of exciton coupled circular dichroism spectra on molecular conformation and shape" *Monatshefte Fur Chemie* **2005**, *136*, 461-475.

(4) Xu, X. D.; Maresca, K. J.; Das, D.; Zahn, S.; Zubieta, J.; Canary, J. W. "Crystal-driven distortion of ligands in copper coordination complexes: Conformational pseudo-enantiomers" *Chemistry-a European Journal* **2002**, *8*, 5679-5683.

(5) Zahn, S.; Canary, J. W. "Absolute configurations of N,N-dialkyl alpha-amino acids and beta-amino alcohols from exciton-coupled circular dichroism spectra of Cu(II) complexes" *Organic Letters* **1999**, *1*, 861-864.

(6) Holmes, A. E.; Das, D.; Canary, J. W. "Chelation-enhanced circular dichroism of tripodal bisporphyrin ligands" *Journal of the American Chemical Society* **2007**, *129*, 1506-+.

(7) Borovkov, V. V.; Lintuluoto, J. M.; Fujiki, M.; Inoue, Y. "Temperature effect on supramolecular chirality induction in bis(zinc porphyrin)" *Journal of the American Chemical Society* **2000**, *122*, 4403-4407.

(8) Borovkov, V. V.; Lintuluoto, J. M.; Inoue, Y. "Supramolecular chirogenesis in zinc porphyrins: Mechanism, role of guest structure, and application for the absolute configuration determination" *Journal of the American Chemical Society* **2001**, *123*, 2979-2989.

(9) Borovkov, V. V.; Yamamoto, N.; Lintuluoto, J. M.; Tanaka, T.; Inoue, Y. "Supramolecular chirality induction in bis(zinc porphyrin) by amino acid derivatives: Rationalization and applications of the ligand bulkiness effect" *Chirality* **2001**, *13*, 329-335.

(10) Balaban, T. S.; Bhise, A. D.; Fischer, M.; Linke-Schaetzel, M.; Roussel, C.; Vanthuyne, N. "Controlling chirality and optical properties of artificial antenna systems with self-assembling porphyrins" *Angewandte Chemie-International Edition* **2003**, *42*, 2140-2144.

(11) Elemans, J.; Van Hameren, R.; Nolte, R. J. M.; Rowan, A. E. "Molecular materials by self-assembly of porphyrins, phthalocyanines, and perylenes" *Advanced Materials* **2006**, *18*, 1251-1266.

(12) Lehn, J. M. "Toward complex matter: Supramolecular chemistry and self-organization" *Proceedings of the National Academy of Sciences of the United States of America* **2002**, *99*, 4763-4768.

(13) Whitesides, G. M.; Mathias, J. P.; Seto, C. T. "MOLECULAR SELF-ASSEMBLY AND NANOCHEMISTRY - A CHEMICAL STRATEGY FOR THE SYNTHESIS OF NANOSTRUCTURES" *Science* **1991**, *254*, 1312-1319.

(14) Stupp, S. I.; LeBonheur, V.; Walker, K.; Li, L. S.; Huggins, K. E.; Keser, M.; Amstutz, A. "Supramolecular materials: Self-organized nanostructures" *Science* **1997**, *276*, 384-389.

(15) Roberts, G. G. "LANGMUIR-BLODGETT FILMS" *Contemporary Physics* **1984**, *25*, 109-128.

(16) Roberts, G. G. "Langmuir-blodgett films" *Plenum, New York* **1990**.

(17) Zasadzinski, J. A.; Viswanathan, R.; Madsen, L.; Garnaes, J.; Schwartz, D. K. "LANGMUIR-BLODGETT-FILMS" *Science* **1994**, *263*, 1726-1733.

(18) Roberts, G. G. "MOLECULAR ELECTRONICS USING LANGMUIR-BLODGETT FILMS" *Advances in Chemistry Series* **1988**, 225-270.

(19) Seeman, N. C. "At the crossroads of chemistry, biology, and materials: Structural DNA nanotechnology" *Chemistry & Biology* **2003**, *10*, 1151-1159.

(20) Chichak, K. S.; Cantrill, S. J.; Pease, A. R.; Chiu, S. H.; Cave, G. W. V.; Atwood, J. L.; Stoddart, J. F. "Molecular Borromean rings" *Science* **2004**, *304*, 1308-1312.

(21) Czarnik, A. W. S. "Chemosensors for Ion and Molecular Recognition" *Kluwer, Dordrecht, The Netherlands* **1997**.

(22) Verbiest, T.; Van Elshocht, S.; Kauranen, M.; Hellemans, L.; Snauwaert, J.; Nuckolls, C.; Katz, T. J.; Persoons, A. "Strong enhancement of nonlinear optical properties through supramolecular chirality" *Science* **1998**, *282*, 913-915.

(23) al, K. T. C. I. Y. H. e. "Photophysical Property and Photostability of J-aggregate Thin Films of Thiacyanine Dyes Prepared by the Spin-Coating Method" *Journal of Physical Chemistry. B* **2008**, *112*, 836 - 844.

(24) Maiti, N. C.; Mazumdar, S.; Periasamy, N. "J- and H-aggregates of porphyrin-surfactant complexes: Time-resolved fluorescence and other spectroscopic studies" *Journal of Physical Chemistry B* **1998**, *102*, 1528-1538.

(25) Jelly, E. E. *Nature* **1936**, *138*, 1009.

(26) Scheibe, G. *Angewandthe Chemie* **1936**, *49*, 563.

(27) Brooker, L. W. e. a. *Photogr. Sci.* **1953**, *1*, 173.

(28) Daehne, S. *Photogr. Sci.* **1979**, *23*, 219.

(29) Kemnitz, K. Y. T., K. *J. Phys. Chem.* **1990**, *94*, 3099.

(30) Saunders, V. I. L. *Photogr. Sci.* **1980**, *24*, 171.

(31) Tani, T. S. e. a. *J. Phys. Chem.* **1992**, *96*, 2778.

(32) Yabushiata, A. F. T. K., T. "Nonlinear propagation of ultrashort pulses in cyanine dye solution investigated by SHG FROG" *Chem. Phys. Lett.* **2004**, *398*, 495.

(33) Kuhn, H. K. K., T. "J-Aggregates" *Chapter 1* **1996**.

(34) Balaz, M.; De Napoli, M.; Holmes, A. E.; Mammana, A.; Nakanishi, K.; Berova, N.; Purrello, R. "A cationic zinc porphyrin as a chiroptical probe for Z-DNA" *Angewandte Chemie-International Edition* **2005**, *44*, 4006-4009.

(35) Kubat, P.; Lang, K.; Prochakova, K.; Anzenbacher, P. "Self-aggregates of cationic meso-tetratolylporphyrins in aqueous solutions" *Langmuir* **2003**, *19*, 422-428.

(36) Monti, D.; Venanzi, M.; Stefanelli, M.; Sorrenti, A.; Mancini, G.; Di Natale, C.; Paolesse, R. "Chiral amplification of chiral porphyrin derivatives by templated heteroaggregation" *Journal of the American Chemical Society* **2007**, *129*, 6688-+.

(37) Onouchi, H.; Miyagawa, T.; Morino, K.; Yashima, E. "Assisted formation of chiral porphyrin homoaggregates by an induced helical poly(phenylacetylene) template and their chiral memory" *Angewandte Chemie-International Edition* **2006**, *45*, 2381-2384.

(38) Tamaru, S.; Uchino, S.; Takeuchi, M.; Ikeda, M.; Hatano, T.; Shinkai, S. "A porphyrin-based gelator assembly which is reinforced by peripheral urea groups and chirally twisted by chiral urea additives" *Tetrahedron Letters* **2002**, *43*, 3751-3755.

(39) Wang, Y. T.; Jin, W. J. "H-aggregation of cationic palladium-porphyrin as a function of anionic surfactant studied using phosphorescence, absorption and RLS spectra" *Spectrochimica Acta Part a-Molecular and Biomolecular Spectroscopy* **2008**, *70*, 871-877.

(40) Yu, W.; Li, Z. S.; Wang, T. Y.; Liu, M. H. "Aggregation and supramolecular chirality of achiral amphiphilic metalloporphyrins" *Journal of Colloid and Interface Science* **2008**, *326*, 460-464.

(41) Koti, A. S. R.; Periasamy, N. "Cyanine induced aggregation in meso-tetrakis(4-sulfonatophenyl)porphyrin anions" *Journal of Materials Chemistry* **2002**, *12*, 2312-2317.

(42) Kano, K.; Fukuda, K.; Wakami, H.; Nishiyabu, R.; Pasternack, R. F. "Factors influencing self-aggregation tendencies of cationic porphyrins in aqueous solution" *Journal of the American Chemical Society* **2000**, *122*, 7494-7502.

(43) Kano, K.; Minamizono, H.; Kitae, T.; Negi, S. "Self-aggregation of cationic porphyrins in water. Can pi-pi stacking interaction overcome electrostatic repulsive force?" *Journal of Physical Chemistry A* **1997**, *101*, 6118-6124.

(44) Takeuchi, M.; Tanaka, S.; Shinkai, S. "On the influence of porphyrin pi-pi stacking on supramolecular chirality created in the porphyrin-based twisted tape structure" *Chemical Communications* **2005**, 5539-5541.

(45) Yin, C. X.; Tan, X. L.; Mullen, K.; Stryker, J. M.; Gray, M. R. "Associative pi-pi interactions of condensed aromatic compounds with vanadyl or nickel porphyrin complexes are not observed in the organic phase" *Energy & Fuels* **2008**, *22*, 2465-2469.

(46) Nakanishi, K. B. W., R. W. "*Circular Dichroism, Principles and Application*" *New-York* **1994**.

(47) Zhou, P.; Zhao, N.; Rele, D. N.; Berova, N.; Nakanishi, K. "A CHIROPTICAL CHEMICAL STRATEGY FOR CONFIGURATIONAL ASSIGNMENTS OF ACYCLIC 1,3-SKIPPED POLYOLS - MODEL 1,2,4,6-TETROLS" *Journal of the American Chemical Society* **1993**, *115*, 9313-9314.

(48) Tanasova, M. *PhD Thesis* **2008**.

(49) Huang, X. F.; Rickman, B. H.; Borhan, B.; Berova, N.; Nakanishi, K. "Zinc porphyrin tweezer in host-guest complexation: Determination of absolute configurations of diamines, amino acids, and amino alcohols by circular dichroism" *Journal of the American Chemical Society* **1998**, *120*, 6185-6186.

(50) Kuhn, H. K., C.; Kobayashi, T., "J-Aggregates" **1996**, Chapter 1.

(51) Mosinger, J.; Janoskova, M.; Lang, K.; Kubat, P. "Light-induced aggregation of cationic porphyrins" *Journal of Photochemistry and Photobiology a-Chemistry* **2006**, *181*, 283-289.

(52) Rao, P. D.; Littler, B. J.; Geier, G. R.; Lindsey, J. S. "Efficient synthesis of monoacyl dipyrromethanes and their use in the preparation of sterically unhindered trans-porphyrins" *Journal of Organic Chemistry* **2000**, *65*, 1084-1092.

Materials and Methods

A. General Procedures

Anhydrous CH_2Cl_2 was dried over CaH_2 and distilled. The solvents used for CD and UV measurements were purchased from Aldrich and were spectra grade. Column chromatography was performed using silica gel (230-400 mesh). ^{1}HNMR spectra were obtained on Varian Inova 300 MHz or 500 MHz instruments and are reported in parts per million (ppm) relative to the solvent resonances (d), with coupling constants (*J*) in Hertz (Hz). UV/Vis spectra were recorded on a Perkin-Elmer Lambda 40 spectrophotometer, and are reported as λ_{max} [nm]. CD spectra were recorded on a Jasco J-810 spectropolarimeter, equipped with a temperature controller (Neslab 111) for temperature studies, and is reported as λ [nm] ($\Delta\varepsilon_{max}$ [mol^{-1} cm^{-1}]).

General procedure for UV-vis and CD measurement: All the UV-vis and CD spectra were taken with μM solution of porphyrin tweezer in methylcyclohexane, hexane or methylene chloride. The UV-vis and CD spectra were carried out in 1 mm cells of 240 μL. The CD spectra were measured in millidegrees and normalized to $\Delta\varepsilon/\lambda$ [nm] units.

B. Synthesis of Compounds

1. Synthesis of **3**

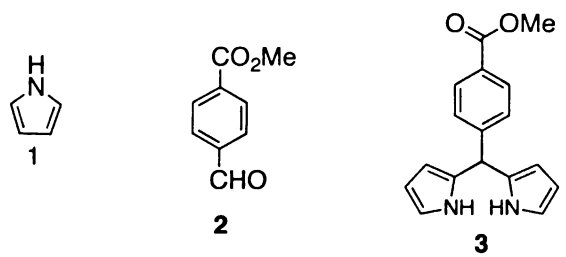

Terephthalaldehydic acid methyl ester **2** (4g, 0.0244 mol) was dissolved in pyrrole **1** (72 mL) and heated to 50°C after which the heating source was removed and TFA (0.6 mL, 1 mmol) was added. The temperature of the mixture increased to 80°C. This was left stirring for 15 min, then cooled to room temperature and quenched with 2M NaOH, (10 mL) and EtOAc (200 mL). The organic layer was extracted with ethyl acetate, washed with water, and dried with anhydrous Na_2SO_4. The solvent was removed under reduced pressure after which the residue was transferred into a silica gel column and eluted with a solution of CH_2Cl_2/Hexanes 4:1 to give the desired product **3** as a white solid in 62% yield.

R_f (CH_2Cl_2/Hex 4:1) = 2.4; m.p.= 155°C

^{1}H NMR ($CDCl_3$, 300 MHz,): δ 4.03 (s, 3H), 5.51 (s, 1H), 5.87-5.86 (m, 2H), 6.14 (m, 2H) 6.71-6.69 (m, 2H), 7.26 (d, 2H, J=8.1 Hz), 7.96 (d, 2H, *J* = 8.1 Hz), 7.97-7.94 (s, br, 2H (NH). ^{13}C NMR ($CDCl_3$): δ 44.4, 52.4, 107.7, 108.8, 117.8, 128.7, 129.1, 130.2, 131.8, 147.5, 167.1

GC/MS: M^+ = 280 (obs), 280 (calc)

2. Synthesis of **4**

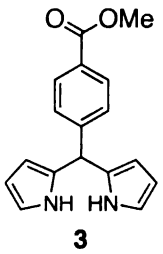

3

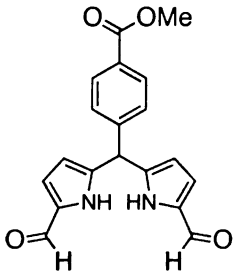

4

Freshly distilled $POCl_3$ (1.27 g, 0.054 mmol) was added dropwise to DMF (15 mL) in a 250 mL three necked flask at 0°C, under nitrogen. This was stirred for 30 min before adding methyl 4-(di(1 *H*-pyrrol-2-yl)methyl)benzoate **3** (2.2 g, 8.8 mmol) dissolved in CH_2Cl_2 (150 mL). The ice bath was removed and the mixture was refluxed for 2 h after which it was poured into water, followed by slow addition of K_2CO_3 until a pH > 11 was reached. After 1 h, additional K_2CO_3 (10 mL) was added and the mixture was left stirring overnight. The organic phase was separated, and the aqueous phase was extracted twice with CH_2Cl_2. The combined organic phases were washed several times with water, dried and evarporated to dryness. After flash silica gel chromatography, the product was isolated as a brown oil.

R_f (40% Et_2OH/Hex) = 0.5; ^1H NMR ($CDCl_3$, 300 MHz,): δ 3.88 (s, 3H), 5.61 (s, 1H), 6.00-6.01 (m, 2H), 6.83-6.85 (m, 2H), 7.35 (d, 2H, *J* = 8.4 Hz), 7.98 (d, 2H, *J* = 8.1 Hz), 9.14 (s, 1H), 10.57 (s, br, 2H). ^{13}C NMR ($CDCl_3$): δ 44.61, 52.4, 112.0, 112.4, 128.8, 129.8, 130.5, 133.0, 140.9, 144.4, 166.8, 179.3

GC/MS: M^+ = 336 (obs), 336 (calc)

3. Synthesis of **5**

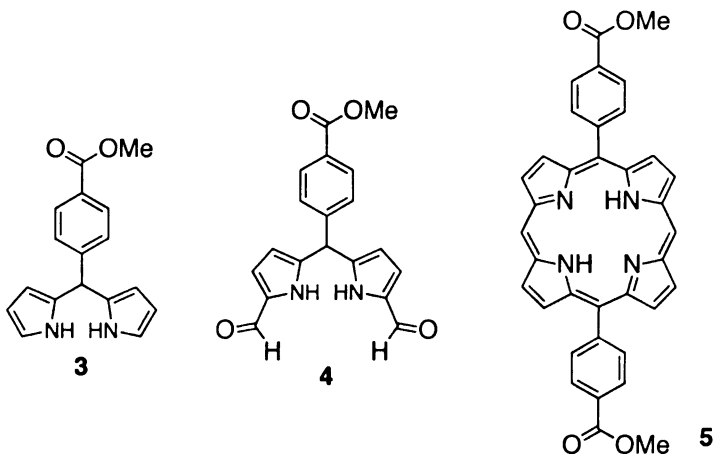

Methyl 4-(di(1 *H*-pyrrol-2-yl)methyl)benzoate **3** (833 mg, 2.97 mmol) was added to a stirred mixture of methyl 4-(bis(5-formyl-1*H*-pyrrol-2-yl)methyl)benzoate (1 g, 2.9 mmol) and $^{n}PrNH_2$ (0.35 g, 6 mmol) in EtOH (29.7 mL). $Zn(OAc)_2$ (1.9 g, 8.9 mmol) was added in and the reaction was refluxed for 24 h. The reaction mixture was then cooled, treated twice with THF (100 mL), and stirred vigorously for 20 min at room temperature and then filtered through a Buchner funnel. The filtrate was concentrated, dissolved in ether (300 mL), washed first with water and then brine, and dried with anhydrous $NaSO_4$, and concentrated. After flash silica gel chromatography (50% CH_2Cl_2/Hex), the product was isolated as a purple solid in 59% yield.

R_f (CH_2Cl_2) = 0.46; ^1H NMR ($CDCl_3$, 300 MHz,): δ 4.10 (s, 6H), 8.32 (d, 4H, J = 8.0 Hz), 8.45 (d, 4H, J = 7.7 Hz), 9.0 (d, 4H, J = 4.5 Hz), 9.43 (d, 4H, J = 4.5 Hz), 10.32 (s, 2H).

GC/MS: M^+ = 578(obs), 578(calc)

4. Synthesis of **6**

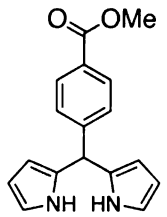

3

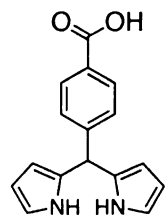

6

Methyl 4-(di(1 *H*-pyrrol-2-yl)methyl)benzoate **3** (6.9 g, 0.02 mol) was refluxed in 2M NaOH solution (50 mL). The reaction was monitored by TLC, and upon complete consumption of starting material (5 h), the THF was removed under reduced pressure. The remaining solution was acidified with 10% HCl solution, and the product extracted with CH_2Cl_2. The organic phase was concentrated to give 4-(di(1*H*-pyrrol-2-yl)methyl)benzoic acid **6** as a white solid in quantitative yield.

m.p.= 160°C;

^{1}H NMR ($CDCl_3$, 300 MHz,): δ 5.70 (s, 1H), 6.04– 6.06 (m, 1H), 6.31–6.32 (m, 1H), 6.87–6.88 (m, 1H), 7.47 (d, 2H, *J* = 8.1 Hz), 8.19 (s, br, 2H), 8.20 (d, 2H, *J* = 8.4 Hz).

^{13}C NMR ($CDCl_3$): δ 44.3, 107.8, 108.9, 117.8, 127.6, 128.8, 130.8, 131.6, 148.5, 171.3

GC/MS: M^+ = 266 (obs), 266 (calc)

5. Synthesis of **7**

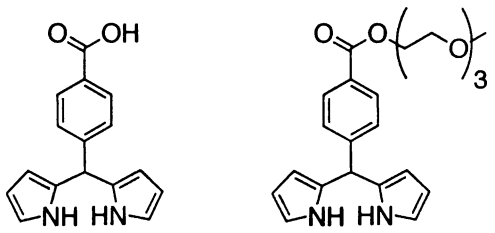

6 **7**

EDCI (0.31 mL, 2.25 mmol), DMAP (305 mg, 2.5 mmol), and triethylene glycol (0.63 mL, 3.7 mmol) were added to a 100 mL flame dried flask containing 4-(di(1*H*-pyrrol-2-yl)methyl)benzoic acid **6** (500 mg, 1.9 mmol) in freshly distilled CH_2Cl_2 (50 mL). This reaction mixture was stirred at room temperature while monitoring by TLC. Upon completion of the reaction (24 h), the solvent was concentrated under reduced pressure. 2-methoxyethyl 4-(di(1*H*-pyrrol-2-yl)methyl)benzoate **7** was collected as a dark brown oil from a silica gel column (20% EtOAc/Hex), in 58% yield.

R_f (20% EtOAc/Hex) = 0.4;

^{1}H NMR ($CDCl_3$, 300 MHz,): δ 3.32 (s, 3H), 3.48–3.50 (m 2H), 3.60-3.64 (m, 4H), 3.67–3.68 (m, 2H), 3.78–3.80 (m, 2H), 4.42–4.44 (m, 2H), 5.49 (s, 1H), 5.86 (m, 2H), 6.13 (q, 2H J = 2.5 Hz), 6.67– 6.69 (m, 2H), 7.25 (d, 2H J = 8.0 Hz), 7.96 (d, 2H J = 8.0 Hz), 7.99 s, br, 2H). ^{13}C NMR ($CDCl_3$): δ 44.2, 59.2, 64.3, 69.4, 70.8, 70.8, 70.9, 72.1, 107.7, 108.7, 117.7, 128.6, 129.0, 130.2, 131.8, 147.7, 166.5

GC/MS: M^+ = 412 (obs), 412 (calc)

6. Synthesis of **8**

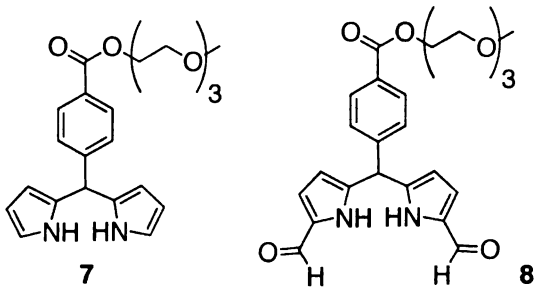

Freshly distilled $POCl_3$ (194 mg, 0.63 mmol) was added dropwise to DMF (92 g) in a 250 mL three necked flask at 0°C, under nitrogen. This was stirred for 30 min before adding 2-methoxyethyl 4-(di(1*H*-pyrrol-2-yl)methyl)benzoate **7** (200 mg, 0.4 mmol) dissolved in CH_2Cl_2 (150 mL). The ice bath was removed and the mixture was refluxed for 2 h. The reaction mixture was poured into water, followed by slow addition of K_2CO_3 until a pH > 11 was reached. After 1 h, additional K_2CO_3 was added and the mixture was left stirring overnight. The organic phase was separated, and the aqueous phase was extracted twice with CH_2Cl_2. The combined organic phases were washed several times with water, dried with anhydrous $NaSO_4$ and evarporated to dryness. After flash silica gel chromatography (30% CH_2Cl_2/EtOAc), 2-methoxyethyl 4-(bis(5-formyl-1*H*-pyrrol-2-yl)methyl)benzoate **8** was isolated as a brown oil in 54% yield.

R_f (30% CH_2Cl_2/EtOAc) = 0.4; ^1H NMR ($CDCl_3$, 300 MHz,): δ 3.32 (s, 3H), 3.48–3.51 (m, 2H), 3.60–3.68 (m, 8H), 3.78-3.81 (m, 2H), 4.42–4.46 (m, 2H), 5.60 (s, 1H), 5.98–6.66 (m, 2H), 6.82–6.84 (m, 2H), 7.37 (d, 2H, J = 8.1 Hz), 8.01 (d, 2H, J = 8.4 Hz), 9.13 (s, 2H), 10.77 (s, br, 2H).

GC/MS: M^+ =

7. Synthesis of **9**

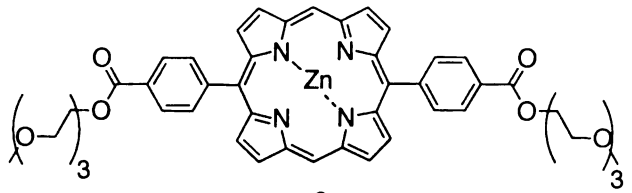

9

2-Methoxyethyl 4-(di(1*H*-pyrrol-2-yl)methyl)benzoate **7** (0.44 g, 1.06 mmol) was added to a stirred mixture of before adding 2-methoxyethyl 4-(bis(5-formyl-1*H*-pyrrol-2-yl)methyl)benzoate **8** (0.5 g, 1.06 mmol) and $^{n}PrNH_2$(0.2 mL, 2.13 mmol) in EtOH (10.7 mL). $Zn(OAc)_2$ (0.7g, 3.2 mmol) was added in and the reaction was refluxed for 24 h. The reaction mixture was then cooled, treated twice with THF (100 mL), and stirred vigorously for 20 min at room temperature and then filtered through a Buchner funnel. The filtrate was concentrated, dissolved in ether (300 mL), washed first with water and then brine, and dried with anhydrous $NaSO_4$, and concentrated. After flash silica gel chromatography (EtOAc), the product was isolated as a purple solid in 10% yield.

R_f (EtOAc) = 0.44;

^1H NMR ($CDCl_3$, 300 MHz,): δ 3.30, (s, 6H), 3.47–3.49 (m, 4H), 3.61–3.63 (m, 4H), 3.67–3.69 (m, 4H), 3.76-3.78 (m, 4H), 3.93-3.95 (m, 4H), 4.61–4.63 (m, 4H), 8.31 (dd, 4H *J* = 2 Hz, 8 Hz), 8.45 (dd, 4H *J* = 3 Hz, 8 Hz), 9.06 (t, 4H *J* = 4 Hz), 9.43 (d, 4H *J* = 4.5 Hz), 10.31 (s, 2H).

GC/MS: M^+ = 906 (obs), 906 (calc)

8. Synthesis of **11**

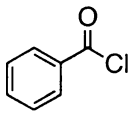

12

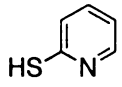

13

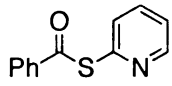

11

A solution of benzoyl chloride (5.6 g, 40 mmol) in CH_2Cl_2 (100 mL) was added over 10 min to a stirred solution of 2-mercaptopyridine (4.44 g, 40 mmol) in CH_2Cl_2 (250 mL). after 1 h, 2M NaOH was added. The organic phase was isolated, washed with water, and then dried with anhydrous $NaSO_4$ and the solvent removed to afford a yellow oil. This was dissolved in a minimum amount of EtOAc and precipitated with hexane. Filtration afforded *S*-2-pyridyl-4-benzothioate **11** as colorless crystals in 75% yield. Spectral data of **11** were identical to those reported.[43]

9. Synthesis of **14**

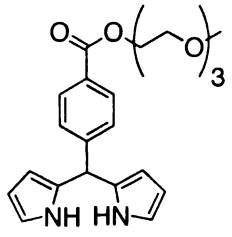

7

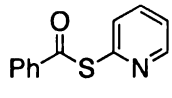

11

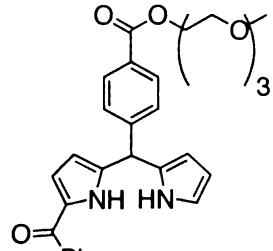

14

A solution of EtMgBr in THF (2.5 mL of 3M solution in ether) was carefully added via syringe to a stirred solution of **7** in THF (3.4 mL) under nitrogen. This was stirred at room temperature for 10 min and then cooled to -78 °C. A solution of **11** (0.643 g) in THF (3.4 mL) was then added over 1 min. The reaction was maintained at -

78 °C for 10 min and then the cooling bath was removed. TLC showed complete consumption of **11** after 4 h. The reaction was quenched with saturated NH_4Cl (15 mL), and poured into CH_2Cl_2. The organic phase was washed with water, dried with anhydrous $NaSO_4$ and concentrated. After flash silica gel chromatography (CH_2Cl_2 to CH_2Cl_2/Hex; 25:1), **14** was isolated as a viscous dark brown oil in 62% yield.

R_f (EtOAc) = 0.4;

^1H NMR ($CDCl_3$, 300 MHz,): δ 3.32 (s, 3H), 3.49-3.51 (m, 2H), 3.59–3.68 (m, 6H), 3.78–3.81 (m, 2H), 4.42–4.45 (m, 2H), 5.59 (s, 1H), 5.85 (s, 1H), 5.93 (s, 1H), 6.02–6.04 (m, 1H), 6.11–6.14 (m, 1H), 6.68–6.70 (m, 2H), 6.77–6.79 (m, 1H), 7.25 (d, 3H J = 7.8 Hz), 7.43 (t, 2H J = 7.5 Hz), 7.51 (d, 1H J = 7.2 Hz), 7.78 (d, 1H J = 7.0 Hz), 7.93–7.97 (m, 2H), 8.29, (br, s, 1H), 9.86, (br, s, 1H)

GC/MS: M^+ = 516.2 (obs), 516 (calc)

10. Synthesis of **16**

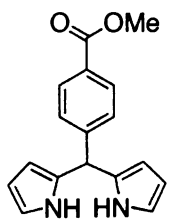

3

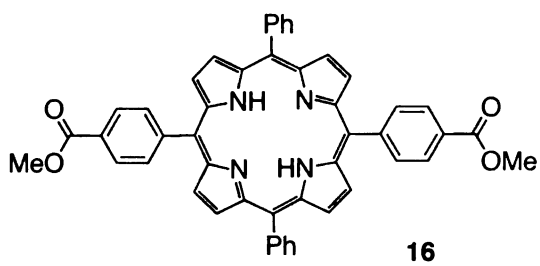

16

Methyl 4-(di(1 *H*-pyrrol-2-yl)methyl)benzoate **3** (4 g, 14 mmol), benzaldehyde (1.6 mL, 14 mmol), and BF_3•OEt_2 (0.45 mL) were stirred in freshly distilled CH_2Cl_2 (1.5 L) for 1 h. *p*-Chloranil (5.4 g, 14 mmol) was then added in and the reaction was stirred

for an additional 1 h at room temperature, after which the solvent was removed under reduced pressure. After flash silica gel chromatography (50% CH_2Cl_2/Hex to CH_2Cl_2), **16** was isolated as a purple solid in 7% yield.

R_f (CH_2Cl_2) = 0.5;

^{1}H NMR ($CDCl_3$, 300 MHz,): δ -2.72 (s, br, 2H), 4.12 (s, 6H), 7.75–7.77 (m, 6H), 8.23 (d, 4H J = 8.1 Hz), 8.32 (d, 4H J = 8.0 Hz), 8.46 (d, 4H J = 8.1 Hz), 8.83 (d, 4H J = 8.0 Hz), 8.91 (d, 4H J = 8.0 Hz)

GC/MS: M^+ = 730.1(obs), 730(calc)

11. Synthesis of **17**

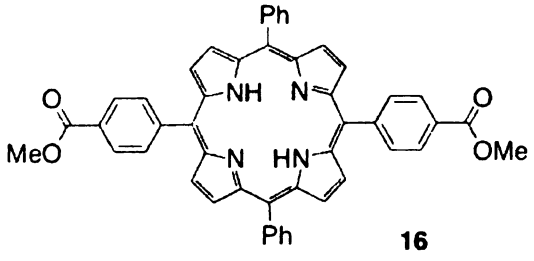

16

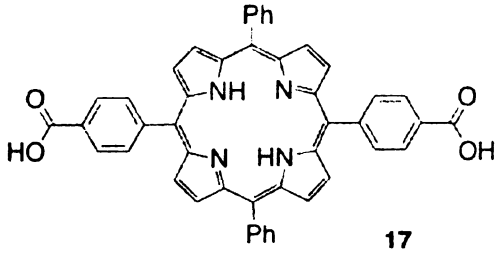

17

Dimethyl ester porphyrin **16** (9.0 g) was refluxed in 2M NaOH solution (60 mL). Upon complete consumption of the starting material, THF was removed under reduced pressure and the remaining solution was acidified with 10% HCl solution. The product was extracted with CH_2Cl_2, and the organic phase was concentrated to give di-acid porphyrin **17** as a purple solid in quantitative yield.

^{1}H NMR (DMSO, 300 MHz,): δ -2.93 (br, s, 2H), 7.85–7.87 (m, 6H), 8.41 (d, 4H J = 8.0 Hz), 8.36 (d, 8H J = 8.1 Hz), 8.86 (s, 8H)

GC/MS: M^+ = 702.1 (obs), 702(calc)

12. Synthesis of **19**

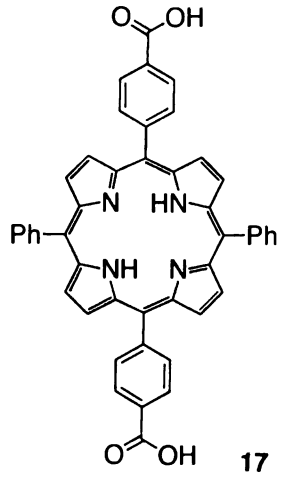

17

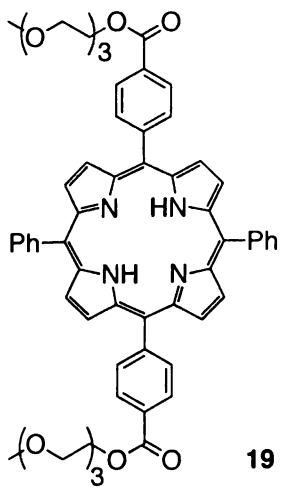

19

EDCI (0.62 mL, 4.50 mmol), DMAP (610 mg, 5.0 mmol), and triethylene glycol (1.26 mL, 7.4 mmol) were added to a 250 mL flame dried flask containing di-acid porphyrin **17** (1.0 g, 3.9 mmol) in freshly distilled CH_2Cl_2 (100 mL) and stirred at room temperature. The reaction was monitored by TLC, and upon completion (24 h), the solvent was removed under reduced pressure. After flash silica gel chromatography (20-30% EtOAc/Hex), bis-tail **19** was collected as a purple solid from a mixture of monoalkylated product **20** (10% yield), and starting material in 30% yield.

19: R_f (20% EtOAc/Hex) = 0.4;

^{1}H NMR ($CDCl_3$, 300 MHz,): δ -2.72 (br, s, 2H), 3.43 (s, 6H), 3.56–3.58 (m, 4H), 3.69–3.76 (m, 12H), 3.80–3.82 (m, 4H), 3.96–3.99 (m, 4H), 4.65–4.68 (m, 4H), 7.80–7.84 (m, 6H), 8.27 (dd, 4H *J* = 2.4 Hz, 7.8 Hz), 8.36 (d, 2H *J* = 8.4 Hz), 8.52 (d, 2H *J* = 8.7 Hz), 8.87 (ddd, 8H *J* = 4.8Hz, 12.3Hz, 8.4 Hz).

GC/MS: M^+ = 995.2(obs) , 995(calc)

20: R_f (50% EtOAc/Hex) = 0.2,

^{1}H NMR ($CDCl_3$, 300 MHz,): δ -0.06 (s, br, 2H), 3.37 (s, 3H), 3.53–3.76 (m, 6H), 3.82 (m, 2H), 3.97 (t, 2H), 4.66 (t, 2H), 7.72–7.78 (m, 6H), 8.21 (d, 4H), 8.30 (d, 2H), 8.39 (d, 2H), 8.45 (d, 2H), 8.61 (d, 2H), 8.78–8.89 (m, 8H).

GC/MS: M^+ = 849 (obs), 848 (calc)

13. Synthesis of **21**

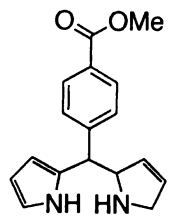

3

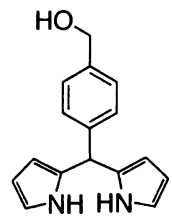

21

Dibal (1.1 mL, 3.7 mmol) was carefully added via syringe to a cooled solution of methyl 4-(di(1 *H*-pyrrol-2-yl)methyl)benzoate **3** (2.5 g, 1.85 mmol) in ether (40 mL) and left to stir at room temperature for 3 h. After complete consumption of starting material (from TLC), the reaction was quenched with Roschell's salt (4 mL) and left to stir until two distinct layers formed. The organic layer was separated and the remaining aqueous layer was extracted using ether (2 x 10 mL). The combined organic layers were washed once with water after which the solvent removed under reduced pressure. After flash

silica gel chromatography (20% EtOAc/Hex), 4-(di(1*H*-pyrrol-2-yl)methyl)phenyl)methanol **21** was isolated as a brown oil in 35% yield.

R_f (CH_2Cl_2) = ; ^{1}H NMR ($CDCl_3$, 300 MHz,): δ 1.77 (br, s, 1H), 4.82 (s, 2H), 5.62 (s, 1H), 6.04-6.07 (m, 2H), 6.02–6.32 (m, 2H), 6.83–6.85 (m, 2H), 7.35 (d, 2H), 7.45 (d, 2H), 8.11 (br, s, 2H). ^{13}C NMR ($CDCl_3$): δ 43.9, 65.2, 107.4, 108.6, 117.5, 127.5, 128.8, 132.6, 139.7, 141.9

GC/MS: M^+ = 252 (obs), 252 (calc)

14. Synthesis of **23**

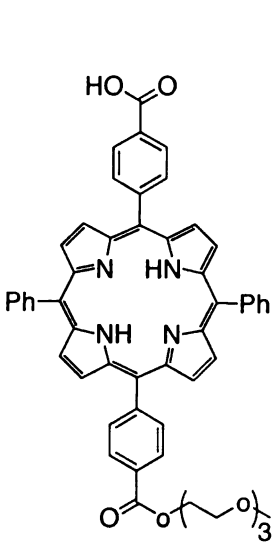

20

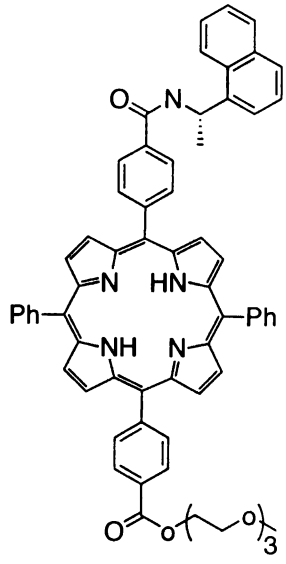

23

EDCI (3.8 μL, 28 μmol), DMAP (3.45 mg, 5.0 28 μmol), and (S)-1-amino-2-methylnaphthalene (1.26 mL, 7.4 mmol) were added to a 250 mL flame dried flask containing mono-acid porphyrin **20** (8.1 mg, 47 28 μmol) in freshly distilled CH_2Cl_2 (10

mL). This reaction mixture was stirred at room temperature for 24 h, after which the solvent was concentrated. After flash silica gel chromatography (20% EtOAc/Hex to 50% EtOAc/Hex), amide porphyrin **23** was collected as a purple solid, in 38% yield.

R_f (50% EtOAc/Hex) = 0.4;

^{1}H NMR ($CDCl_3$, 300 MHz,): δ -2.78 (br, s, 2H), 1.99 (d, 3H), 3.41 (s, 3H), 3.60–3.63 (m, 2H), 3.73–3.81 (m, 4H), 3.84–3.88 (m, 2H), 4.02 (t, 2H), 4.70, (t, 2H), 6.37 (p, 1H), 6.70 (d, 1H), 7.5–7.63 (m, 2H), 7.70 (dt, 1H), 7.76–7.82 (m, 7H), 7.95 (dd, 2H), 8.16 (d, 2H), 8.21–8.34 (m, 8H), 8.39 (d, 1H), 8.48 (d, 2H), 8.80 (t, 4H), 8.89 (t, 4H)

GC/MS: M^+ = 1001.0 (obs), 1001.4 (calc)